May 2013

Vacua and Inflation in String Theory and Supergravity

Dissertation

zur Erlangung des Doktorgrades

des Departments Physik

der Universität Hamburg

vorgelegt von

Markus Rummel

aus Brilon

Hamburg

2013

Gutachter der Dissertation:	Prof. Dr. Jan Louis Dr. Alexander Westphal
Gutachter der Disputation:	Prof. Dr. Jan Louis Prof. Dr. Wilfried Buchmüller
Datum der Disputation:	3. Juli 2013
Vorsitzender des Prüfungsausschusses:	Prof. Dr. Günter Sigl
Vorsitzender des Promotionsausschusses:	Prof. Dr. Peter H. Hauschildt
Dekan der Fakultät für Mathematik, Informatik und Naturwissenschaften:	Prof. Dr. Heinrich Graener

Abstract

We study the connection between the early and late accelerated expansion of the universe and string theory. In Part I of this thesis, the observational degeneracy between single field models of inflation with canonical kinetic terms and non-canonical kinetic terms, in particular string theory inspired models, is discussed. The 2-point function observables of a given non-canonical theory and its canonical transform that is obtained by matching the inflationary trajectories in phase space are found to match in the case of Dirac-Born-Infeld (DBI) inflation. At the level of the 3-point function observables (non-Gaussianities), we find degeneracy between non-canonical inflation and canonical inflation with a potential that includes a sum of modulated terms. In Part II, we present explicit examples for de Sitter vacua in type IIB string theory. After deriving a sufficient condition for de Sitter vacua in the Kähler uplifting scenario, we show that a globally consistent de Sitter model can be realized on a certain Calabi-Yau manifold. All geometric moduli are stabilized and all known consistency constraints are fulfilled. The complex structure moduli stabilization by fluxes is studied explicitly for a small number of cycles. Extrapolating to a larger number of flux carrying cycles, we verify statistical studies in the literature which show that, in principle, the string landscape can account for a universe with an extremely small cosmological constant.

Zusammenfassung

Diese Arbeit untersucht den Ursprung von früher und heutiger beschleunigter Expansion des Universums im Kontext von Stringtheorie. Teil I widmet sich den Observablen von inflationären Theorien, die durch ein einzelnes skalares Feld mit kanonischen oder nicht-kanonischen kinetischen Termen beschrieben werden. Einer nicht-kanonischen Theorie wird durch Übereinstimmug der Phasenraumtrajektorie der inflationären Lösungen eine kanonische Theorie zugeordnet dessen 2-Punkt-Funktions Observablen im Fall von DBI Inflation mit denen der nicht-kanonischen Theorie übereinstimmen. Diese Entartung existiert auch im Fall der 3-Punkt-Funktions Observablen wenn dem Potential der kanonischen Theorie modulierte Terme hinzugefügt werden. In Teil II präsentieren wir explizite Beispiele für de Sitter Vakua in Typ IIB Stringtheorie. Wir leiten zunächst eine hinreichende Bedingung für de Sitter Vakua im 'Kähler uplifting' Szenario her und geben dann ein Beispiel für eine solche Konstruktion auf einer bestimmten Calabi-Yau Mannigfaltigkeit an. Dabei werden alle geometrischen Moduli stabilisiert und alle bekannten Konsistenzbedingungen erfüllt. Die Komplexe-Struktur-Moduli werden für eine kleine Zahl and Zykeln explizit stabilisiert. Wir extrapolieren unsere Ergebnisse zu Fällen mit einer größeren Anzahl von Zykeln. Wir können so statistische Studien verifizieren, die vorhersagen das Stringtheorie ein Universum mit einer extrem kleinen kosmologischen Konstante beschreiben kann.

Contents

Chapter 1

Introduction

In recent years, experimental cosmology has provided us with deep new insights into the history of the universe: 1) the observation of the late-time accelerated expansion of the universe (dark energy) and 2) strong hints towards a much faster accelerated expansion of the universe (inflation) before the universe entered its thermal big bang phase. Dark energy was first observed by studying the brightness-redshift relation of supernovae [1, 2] and was later also detected in the cosmic microwave background (CMB) radiation [3, 4]. Strong hints for an inflationary epoch in the early universe originate from the observation of the CMB temperature field. The CMB has been found with the empirical properties to show an average mean temperature which is the same in all directions while having an almost scale invariant spectrum of tiny $\mathcal{O}(10^{-5})$ perturbations, and pointing to a spatially flat universe at the $\mathcal{O}(10^{-3})$ level [3–7].

On the theoretical side, string theory is a very promising candidate for a consistent theory of quantum gravity that has the potential to unify gravity and the known interactions of the standard model of particle physics in a common framework. At low energies, it reduces to the well know and tested theories of general relativity and potentially the standard model of particle physics. [1] General relativity governs the dynamics of the standard model of cosmology, the ΛCDM concordance model, in which the late time evolution of the universe is dominated by dark energy ('Λ') and cold dark matter ('CDM'), with traces of baryonic matter and radiation. However, in earlier times the universe had been much hotter, at the very least ~ 10 MeV during big bang nucleosynthesis (BBN), when nuclei heavier than the lightest isotope of hydrogen were formed. Furthermore, the energy scale

[1] String theory in principle provides all the necessary ingredients to realize the gauge group and matter content of the standard model of particle physics but to this day a fully explicit realization has not been established.

of many models of inflation is the GUT scale ($\sim 10^{16}$ GeV) which is only a few orders of magnitude smaller than the Planck scale ($M_{\rm P} \simeq 1.22 \cdot 10^{19}$ GeV), the natural energy scale of quantum gravity. Hence, signatures of an UV complete theory of gravity might show up in the observables of inflation, e.g., in the CMB. As a different motivation, when extrapolating the observed expansion backwards in time, at very high energies of $\mathcal{O}(M_{\rm P})$, quantum gravity significantly affects the general relativity description, rendering it inaccurate. Ignoring quantum gravity effects, the backwards extrapolated expansion leads to the famous big-bang singularity.[2] To understand what actually happens at energy scales above $M_{\rm P}$, a UV complete theory of gravity is necessary. For these reasons, it is sensible to connect questions of early universe cosmology and quantum gravity, in particular string theory since it is our best candidate for such a theory to date. The field of research is often referred to as string cosmology. After all, observational cosmology might be our best chance to confront string theory with experimental data since no terrestrial experiment can come close to the energy densities available in the early universe.

Let us first comment on the connection between inflation and string theory. The dynamics of inflation can effectively be modeled by one or more scalar fields, minimally coupled to gravity, so-called inflaton(s). An important class of models is given by Lagrangians of a canonically normalized scalar field ϕ, i.e., the kinetic term is given as $(\partial_\mu \phi)^2$. Then, the crucial feature is an almost flat potential, in order for inflation to last long enough to realize the observed homogeneity and flatness of the CMB. Most phenomenological features, for instance the calculation of the quantum fluctuations that source the temperature fluctuations of the CMB, do not depend on the UV completion of these effective field theories. However, the almost flatness of the potential is often an ad-hoc assumption as generically there should be corrections from $M_{\rm P}$ suppressed operators, especially when the range the field travels during inflation is (super-)Planckian. The compactification of $D > 4$ dimensional string theories to 4D, generically leads to a large number of gravitationally coupled scalar fields that parametrize the shape and size of the curled up extra dimensions, the so-called moduli fields. In simple compactifications, there is no potential for these moduli. However, for phenomenological reasons, e.g., the non-observation of fifth-forces on solar system scales and also cosmological constraints, these moduli have to be stabilized at a rather high scale of at least ~ 10 TeV. The potential for the moduli fields is generated by considering more complicated compactifications. An interesting question is, if one or more of these moduli

[2] However, it is not clear if a singularity remains when an inflationary epoch has preceded the hot big bang phase.

might have played the role of the inflaton(s). In this context, an attempt can be made to actually compute the $M_{\rm P}$ suppressed operators, constructing an effective field theory of D3-brane inflation that is UV completed by string theory [8–10]. An effective field theory of the inflationary quantum fluctuations in the spirit of the pion Lagrangian can be written largely UV-independent [11]. Furthermore, string theory can be useful in leading to signals that cannot arise in the framework of effective field theories, and inspire the discovery of these potential signals in effective field theories.

In Part I of this thesis, we study the scenario in which the dynamics of inflation are governed by a single scalar field ϕ. Most generally, the kinetic term in the effective 4D Lagrangian of this inflaton is intrinsically non-canonical, i.e., cannot be transformed to $(\partial_\mu\phi)^2$ via a field redefinition. For instance, such non-canonical kinetic terms frequently arise in the 4D effective action of compactified string theories. Our limitation to single field inflation is for simplicity since a single field is sufficient to construct inflationary models that are in agreement with the data. In particular, multi-field inflation generically predicts a detectable non-Gaussian signal in the CMB temperature fluctuations. However, the CMB temperature spectrum follows, to a very large extent, a Gaussian distribution. The constraints on non-Gaussianity have been improved by the recent Planck data [4], such that many multi-field models are observationally disfavored.

The main point of interest in Part I is the observational degeneracy between non-canonical and canonical models of single field inflation. More precisely, we want to answer the following question: if and under which conditions can a canonical model that agrees with a given non-canonical model at the level of the observational consequences be constructed? We begin with a review (Chapter 2) where we provide a brief summary of the ΛCDM concordance model, the concept of inflation and its dynamics in terms of a (non-) canonically normalized scalar field. In what follows, we focus on the inflationary observables. These are calculated as n-point functions of the quantum fluctuations of ϕ and the metric degrees of freedom. In Chapter 3 we give a summary of our work [12]. We describe a procedure to construct a canonical theory from a non-canonical theory which, under certain specified conditions, agrees with the original non-canonical theory at the level of the 2-point function observables. The matching at the level of the 3-point function observables, i.e., non-Gaussianities, is discussed in Chapter 4, summarizing our work [13]. The 2-point function observables are matched by constructing a canonical theory whose inflationary phase space trajectory is identical to that of a non-canonical theory. Matching of the 3-point function observables proceeds via a summation of periodic non-Gaussianities such that the non-Gaussianity that is

characteristic for non-canonical theories, is resembled in a Fourier series of these periodic contributions. Hence, we are ultimately able to show that we can construct a canonical inflationary theory that agrees with a given non-canonical theory at the level of the 2- and 3-point function observables.

In Part II of this thesis, we turn to the connection of the late phase of accelerated expansion of the universe (dark energy) and string theory. We study explicit models for dark energy in the context of the string theory landscape. As is consistent with current experimental data, dark energy is assumed to arise as vacuum energy, i.e., an effective cosmological constant of the theory of quantum gravity which we consider to be string theory. This effective cosmological constant depends on the value of the effective potential of the scalar fields of the theory, in particular the moduli, at a (local) minimum in field space.[3] String theory, in principle, contains an extremely high number of such vacuum configurations, i.e., a whole landscape of string vacua [14–19]. This is useful in addressing a very serious fine-tuning problem: the extreme smallness of the observed value of the cosmological constant today in terms of the natural scale of quantum gravity, the Planck scale. The enormous number of vacua found in string theory tells us that in principle there should also be a vacuum with an extremely small cosmological constant which is selected on anthropic grounds, as not even galaxies would have been possible to form in a universe with a large cosmological constant [20].

The goal in Part II is to construct explicit vacua in string theory that allow for fine-tuning of the cosmological constant to the extremely small observed value. The motivation for this task is proof of existence: a fully explicit string compactification with a small positive cosmological constant, i.e., a de Sitter (dS) vacuum, that fulfills all mathematical consistency constraints would indicate that string theory can in fact describe our world. Conversely, if string theory could not describe such a state, this would indicate the need to look for alternative explanations of dark energy or even a different theory of quantum gravity altogether. Note that the extreme tuning necessary to obtain a cosmological constant that is extremely small is a highly non-trivial and very restrictive constraint.

We work in type IIB string theory since in this corner of the string theory landscape, moduli stabilization is arguably best understood and hence most suitable for explicit constructions of de Sitter vacua. In a review (Chapter 5), we first motivate the quest for de Sitter vacua in string theory in more detail and also review moduli stabilization in type IIB supergravity, which is the low energy limit

[3] In case of a global minimum the vacuum is stable, while it is meta-stable in the case of a local minimum, decaying via quantum tunneling to the true vacuum state of the theory.

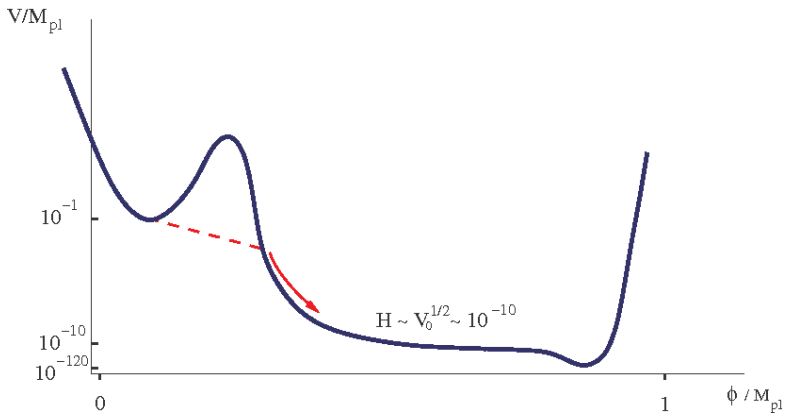

Figure 1.1: This figure schematically shows a possible realization of the history of our universe in the string theory landscape in terms of a one dimensional potential $V(\phi)$ with a scalar field ϕ representing the moduli fields. H is the Hubble rate which characterizes the energy scale of inflation. Figure taken from [27].

of type IIB string theory. In Chapter 6, we present the results of our work [21], where a sufficient condition for de Sitter vacua which depends on the compactification parameters is derived. Chapter 7 is dedicated to an explicit construction of a de Sitter vacuum that fulfills all known mathematical consistency conditions on a specific compactification manifold, stabilizing all moduli. The construction is along the lines of the sufficient condition found in [21] and was first presented in [22]. Finally, in Chapter 8, we discuss to what extent the vacua allow for tuning of the cosmological constant. Statistical studies of the string theory landscape predict that a large amount of fine-tuning for the cosmological constant is available [17, 23, 24]. Based on explicitly constructing the full solution space of a three moduli example, we confirm that there is indeed, in principle, a sufficiently large number of vacua for compactifications with $\mathcal{O}(10-100)$ moduli fields to tune the cosmological constant to its observed small value. The results presented in this chapter were first published in [25] and [26].

In summary, this thesis deepens the study of the connection between string theory and the two known phases of accelerated expansion in the history of the universe: inflation and dark energy. The dynamics and vacuum configurations of scalar moduli fields originating from the compactification of string theory effectively model these two phases. Moduli stabilization is therefore the crucial factor in obtaining a better understanding of accelerated expansion in the framework of string theory. In Figure 1.1, we sketch a potential realization of the history of our universe in the context of the string theory landscape: The universe starts at a meta-stable vacuum state with a rather high energy of order of the Planck scale

and then tunnels to a region where the scalar potential is flat enough to support an inflationary expansion. Next, the field "rolls down" this flat region of the potential and ends up in another minimum with an extremely small vacuum energy which is the vacuum state we observe today.

Part I

Non-canonical inflation

Chapter 2

The inflationary paradigm

In this chapter, we provide background information for Chapter 3 and Chapter 4. We start with a review of the ΛCDM concordance model in Section 2.1 which finishes with a discussion of its shortcomings at the end of this section. A solution to these in the framework of the inflationary paradigm is presented in Section 2.2, where we explain the physical concept of inflation. In Section 2.3, we give a more detailed explanation of the inflationary mechanism in terms of a single scalar field minimally coupled to gravity with a canonical or non-canonical kinetic term. We end this chapter with a motivation and outline for the comparison of inflationary observables in canonical and non-canonical theories of inflation.

2.1 The ΛCDM concordance model

The ΛCDM concordance model of cosmology [1] very successfully explains the history of the universe at least until BBN, i.e., up to temperatures of $\sim$ 1 MeV. Assuming homogeneity and isotropy on the largest scales of the universe, the space-time of the universe can be described by a Friedmann-Lemaître-Robertson-Walker (FLRW) metric

$$ds^2 = -dt^2 + a(t)d\boldsymbol{x}^2\,, \tag{2.1}$$

where t is the cosmological time coordinate, $\boldsymbol{x}$ represents the three spatial coordinates and $a(t)$ is the scale factor which completely determines the evolution of the homogeneous universe. The expansion rate is characterized by the Hubble parameter

$$H = \frac{\dot{a}}{a}\,, \tag{2.2}$$

[1] For books covering cosmology and in particular inflation see e.g., [28–30]. For reviews on inflation, see e.g., [31–33].

which is positive for an expanding universe and negative for a collapsing universe.

The dynamics of the homogeneous and isotropic universe are described by the Einstein equations

$$\mathcal{R}_{\mu\nu} - \frac{1}{2} g_{\mu\nu}\mathcal{R} + \Lambda g_{\mu\nu} = T_{\mu\nu}\,, \tag{2.3}$$

where $\mathcal{R}_{\mu\nu}$ is the Ricci curvature tensor, $\mathcal{R}$ the Ricci scalar, Λ the cosmological constant and $T_{\mu\nu}$ the energy-momentum tensor. We have set the reduced Planck mass $M_{\rm P}/\sqrt{8\pi} \equiv 1$ in eq. (2.3) and will continue to use this convention in the following unless demonstrating suppression of certain quantities by $M_{\rm P}$. Furthermore, we use the signature $(-1, 1, 1, 1)$ for the metric in Minkowski space and use natural units $c = \hbar = 1$. The energy-momentum tensor is that of a perfect fluid with energy density ρ and pressure p which in is given as

$$T_{\mu\nu} = \begin{pmatrix} \rho & 0 & 0 & 0 \\ 0 & p & 0 & 0 \\ 0 & 0 & p & 0 \\ 0 & 0 & 0 & p \end{pmatrix}\,, \tag{2.4}$$

in the fluid rest frame. For the ansatz eq. (2.1), the Einstein eq's (2.3) become the Friedmann equations

$$H^2 = \left(\frac{\dot{a}}{a}\right)^2 = \frac{1}{3}\rho - \frac{k}{a^2}\,, \tag{2.5}$$

$$\dot{H} + H^2 = \frac{\ddot{a}}{a} = -\frac{1}{6}(\rho + 3p)\,, \tag{2.6}$$

where k characterizes the spatial curvature of the universe, i.e., $k = \pm 1$ for positively/negatively curved and $k = 0$ for flat space like hypersurfaces. Eq. (2.5) and eq. (2.6) can be combined into the continuity equation

$$\frac{d\rho}{dt} + 3H(\rho + p) = 0 \qquad \Leftrightarrow \qquad \frac{d\ln\rho}{d\ln a} = -3(1 + w)\,, \tag{2.7}$$

with the equation of state parameter $w \equiv p/\rho$ which is given as $w = 0$ for non-relativistic matter and $w = 1/3$ for radiation or relativistic matter. For a cosmological constant the equation of state is $w = -1$ which can be seen directly from the Einstein eq's (2.3). In a local free-fall frame with no matter, i.e., $g_{\mu\nu} = \eta_{\mu\nu}$ the Minkowski metric and the RHS in eq. (2.3) is zero and the energy-momentum tensor is given as

$$T^{\Lambda}_{\mu\nu} = \begin{pmatrix} \rho_\Lambda & 0 & 0 & 0 \\ 0 & -\rho_\Lambda & 0 & 0 \\ 0 & 0 & -\rho_\Lambda & 0 \\ 0 & 0 & 0 & -\rho_\Lambda \end{pmatrix}\,, \tag{2.8}$$

with $\rho_\Lambda = \Lambda$. Hence, $p_\Lambda = -\rho_\Lambda$.

The continuity eq. (2.7) is solved by

$$\rho_i \propto a^{-3(1+w_i)}\,, \tag{2.9}$$

where the index 'i' characterizes the different species that contribute to the energy density of the universe, i.e., baryons ('b'), dark matter ('dm'), photons ('γ'), neutrinos ('n'), dark energy/a cosmological constant ('Λ'). With

$$\rho \equiv \sum_i \rho_i \qquad \text{and} \qquad p \equiv \sum_i p_i\,, \tag{2.10}$$

and defining the present energy density relative to the critical energy density $\rho_{\rm crit} = 3H_0^2$ as

$$\Omega_i \equiv \frac{\rho_0^i}{\rho_{\rm crit}}\,, \tag{2.11}$$

eq. (2.5) can be expressed as

$$\left(\frac{H}{H_0}\right)^2 = \sum_i \Omega_i\, a^{-3(1+w_i)} + \Omega_k a^{-2}\,. \tag{2.12}$$

The index '0' refers to evaluation of a cosmological parameter at present time t_0 and we have normalized the scale factor such that $a_0 \equiv a(t_0) = 1$. Furthermore, $\Omega_k \equiv -k/a_0^2H_0^2$ parametrizes the curvature dependent term in the Friedmann equation eq. (2.5). At $t = t_0$, eq. (2.12) implies the consistency relation

$$\sum_i \Omega_i + \Omega_k = 1\,. \tag{2.13}$$

Observations of the CMB [4], baryon acoustic oscillations (BAO) [34] and supernovae (SNe) [1, 2] can determine the contribution of the different species to the current energy density of the universe to be

$$\Omega_b \simeq 0.05\,, \quad \Omega_{\rm dm} \simeq 0.27\,, \quad \Omega_\Lambda \simeq 0.68\,, \quad |\Omega_k| \leq 10^{-3}\,. \tag{2.14}$$

Despite the notable successes of the hot big bang model it has the following severe shortcomings with respect to initial conditions:

- *The horizon problem:* The horizon is defined as the maximum distance light can travel after the big bang

$$\tau \equiv \int_0^t \frac{dt'}{a(t')} = \int_0^a \frac{da}{H\,a^2} = \int_0^a d\ln a \left(\frac{1}{aH}\right)\,, \tag{2.15}$$

where $(aH)^{-1}$ is the comoving Hubble radius. If the universe is dominated by one species, i.e., $\Omega_i \simeq 1$ with equation of state w, eq. (2.12) can be solved by

$$\frac{1}{aH} = \frac{1}{H_0} a^{\frac{1}{2}(1+3w)} , \tag{2.16}$$

which implies

$$\tau = \int_0^a \frac{da}{H\, a^2} \propto a^{\frac{1}{2}(1+3w)} . \tag{2.17}$$

During the hot big bang the universe is either dominated by radiation ($w = 1/3$) or matter ($w = 0$) such that the horizon is monotonically increasing with time.

The CMB is homogeneous up to relative fluctuations of $\sim 10^{-5}$. However, in the hot big bang model only regions within an angle of less than 1° have been in causal contact, i.e., their particle horizons during recombination, which is the time at which protons and electrons formed neutral hydrogen for the first time, intersect. In fact, the CMB consists of roughly 10^5 patches that have never been in causal contact in the hot big bang but yet are in thermal equilibrium. This immense fine-tuning of spatial initial conditions is dubbed the horizon problem.

- *The flatness problem:* Defining [2]

$$\Omega(a) \equiv \frac{\rho(a)}{\rho_{\text{crit}}(a)} \qquad \text{with} \qquad \rho_{\text{crit}} \equiv 3H(a)^2 , \tag{2.18}$$

we can write eq. (2.5) as

$$1 - \Omega(a) = \frac{-k}{(aH)^2} = \frac{-k}{H_0^2}\, a^{1+3w} , \tag{2.19}$$

using eq. (2.16). Hence, during matter or radiation domination the deviation of $\Omega(a)$ from one grows as the universe evolves. To explain the smallness of $|\Omega_k| = |1 - \Omega(a_0)| \leq 10^{-3}$ today, $\Omega(a)$ must have been even closer to one in the past, e.g., $|1 - \Omega(a_{\text{BBN}})| \leq 10^{-16}$ during BBN.[3] Since $1 - \Omega(a)$ can be expressed as the difference between the average potential energy and the average kinetic energy over a region of space, one can interpret its smallness as a fine-tuning of initial velocities.

[2] Note that the density $\Omega(a)$ is time-dependent while $\Omega = \Omega(a_0)$ in eq. (2.11) is a constant.

[3] An obvious solution to the flatness problem is that the universe has always been exactly flat, i.e., $k = 0$. In this sense, the flatness problem does not necessarily involve a high degree of tuning in terms of digits and can hence be considered less severe than the horizon problem.

- *The defect problem:* This problem is less severe than the two previously mentioned or might even be absent since it depends on the kind of physics that describe the universe if one extrapolates the hot big bang to much earlier times, i.e., higher energies than BBN. If this kind of physics implies that the universe passed through phase transitions that produce large abundances of topological defects such as very massive particles carrying magnetic charges, cosmic strings or domain walls, these effects can spoil for instance homogeneity or successful predictions of the hot big bang such as BBN.

2.2 The concept of inflation

Whereas the hot big bang model cannot explain the very special initial conditions described in the above problems, the framework of inflation [35–37] can give a natural explanation to these conditions. A crucial input in deriving both the horizon and flatness problems was the monotonic growth of the comoving Hubble radius $(aH)^{-1}$ during the hot big bang. The simple idea of inflation is to introduce a period that precedes the hot big bang where $(aH)^{-1}$ is *decreasing*, or conversely, where $\ddot{a} > 0$, i.e., the expansion accelerates.[4]

This solves the horizon problem by enlarging the particle horizon τ at recombination compared to the hot big bang theory, see eq. (2.15). In other words, regions of the universe that have never been in causal contact during the hot big bang phase have been in causal contact during the inflationary epoch. The flatness problem is solved since during an inflationary period where $(aH)^{-1}$ is decreasing, $\Omega(a) = 1$ is an attractor as can be seen from eq. (2.19). The defect problem is solved since relics such as magnetic monopoles are exponentially diluted during an inflationary period. This explains their absence in the following hot big bang phase. Finally, density perturbations and their scale dependence observed in the CMB and in BAO are generated from quantum fluctuations during inflation. These quantum fluctuations are generated on subhorizon scales, exit when the comoving Hubble radius becomes smaller than their comoving wavelength and hence become classical superhorizon density perturbations.

The defining property of inflation, i.e., the shrinking of $(aH)^{-1}$, can be formulated as the following equivalent conditions on the dynamics of the inflationary

[4] For alternative ideas to inflation see e.g., the pre-big bang [38] or cyclic universe [39] scenarios. However, a major drawback for these models is the difficulty to predict the observed density perturbation spectrum also at the level of polarizations of the CMB whereas this is not a problem in the case of inflation.

epoch:

- *Accelerated expansion:*

$$\frac{d}{dt}\left(\frac{1}{aH}\right) < 0 \quad \Leftrightarrow \quad \ddot{a} > 0\,, \tag{2.20}$$

  whereas in the hot big bang phase $d^2a/dt^2 < 0$ for matter fulfilling the strong energy condition $\rho + 3p \geq 0$, as can be seen from eq. (2.6). The second time derivative of a can be related to the first time derivative of $H = \dot{a}/a$ via

$$\frac{\ddot{a}}{a} = H^2(1-\epsilon)\,, \qquad \text{with} \qquad \epsilon \equiv -\frac{\dot{H}}{H^2}\,, \tag{2.21}$$

  such that $\ddot{a} > 0$ implies $\epsilon < 1$ during inflation.

- *Negative pressure:* In return, $d^2a/dt^2 > 0$ requires

$$p < -\frac{1}{3}\rho\,, \tag{2.22}$$

  i.e., negative pressure or a violation of the strong energy condition. This condition can also be validated from the dependence of $(aH)^{-1}$ on w, i.e., eq. (2.16) implies $w < -1/3$.

To solve the horizon, flatness and defect problem, inflation has to stretch physical scales sufficiently. A convenient way to measure the growth of the scale factor from the beginning a_i to the end a_e of inflation is the number of efolds

$$N_e \equiv \ln\frac{a_e}{a_i} = \int_{t_i}^{t_e} H\, dt\,. \tag{2.23}$$

Depending on the energy scale of reheating, i.e., the transition of the inflationary phase to the hot big bang phase, 50-60 efolds are necessary to solve the horizon and flatness problem. This also implies a very strong dilution of defects if these would have been produced in an epoch preceding inflation.

As can be seen from eq. (2.6), during inflation $\dot{H} < 0$ which implies that if $|\dot{H}| \lesssim 1$, inflation will not last long enough to generate 50-60 efolds. To generate enough efolds, we have to demand that $|\dot{H}|, |\ddot{H}| \ll 1$. Demanding that H is almost constant during inflation we can expand

$$H = H_{(0)} - H_{(1)}t - \frac{1}{2}H_{(2)}t^2 - \mathcal{O}(t^3)\,, \tag{2.24}$$

with $H_{(i)} > 0$. Defining

$$\eta \equiv \frac{\dot{\epsilon}}{H\epsilon} = \frac{\ddot{H}}{\dot{H}\,H} - 2\frac{\dot{H}}{H^2}\,, \tag{2.25}$$

and using the definition of ϵ in eq. (2.21), we can write

$$\begin{aligned} N_e &= H_{(0)}(t_e - t_i) - \frac{1}{2} H_{(1)}(t_e^2 - t_i^2) - \frac{1}{6} H_{(2)}(t_e^3 - t_i^3) - \mathcal{O}(t^4) \,, \\ &\simeq H_{(0)}(t_e - t_i) - \frac{1}{2} \epsilon H_{(0)}^2(t_e^2 - t_i^2) - \frac{1}{6} \epsilon(\eta + 2\epsilon) H_{(0)}^3(t_e^3 - t_i^3) - \mathcal{O}(t^4) \,. \end{aligned} \tag{2.26}$$

Hence, assuming $H_{(0)}(t_e - t_i) \sim 50 - 60$ we have to demand $\epsilon, |\eta| \lesssim \mathcal{O}(10^{-2})$ in order to generate enough efolds. The fact that $H \simeq H_{(0)}$ is almost constant during inflation implies an exponential growth of the scale factor $a \propto e^{H_{(0)}t}$.

2.3 Canonical vs. non-canonical dynamics

In this section, we will discuss which physical theory can realize an inflationary epoch. Let us study a single scalar field ϕ minimally coupled to gravity via

$$S = \int d^4x \sqrt{g} \left[\frac{M_{\rm P}^2}{2} \mathcal{R} + p(X, \phi) \right] \,, \tag{2.27}$$

with 4D Ricci scalar $\mathcal{R}$ and $X \equiv -(\partial_\mu \phi)^2/2 \simeq \dot{\phi}^2/2$ since spatial derivatives are rapidly washed out during inflation. Even though this is obviously not the most general ansatz (we could consider multiple scalar fields or non-minimal coupling to gravity [5]) it is the most economic ansatz since it can provide an inflationary model that is consistent with the current CMB data as we will see below. Furthermore, the motivation to consider only one scalar field is strengthened by the fact that multi scalar field inflation is observationally disfavored due to the non-observation of non-Gaussianities in the CMB until this day [4]. Fermions are not useful for inflationary model building since a background field value different from zero would break Lorentz invariance. Massive vector bosons, on the other hand, could provide viable inflatons. However, the come at the price of a certain spatial anisotropy of the universe after inflation [42] that has so far evaded detection.

The most general form of $p(X, \phi)$ for which the equations of motion derived from eq. (2.27) are second-order in the field ϕ, in order to avoid propagating ghosts or extra degrees of freedom, is the Hordenski action [43–45]. From an effective field theory point of view, we expect the function $p(X, \phi)$ to have the form

$$p(X, \phi) = \sum_{n \geq 0} c_n(\phi) \frac{X^{n+1}}{\Lambda^{4n}} - V(\phi) = \Lambda^4 S(X, \phi) - V(\phi) \,, \tag{2.28}$$

[5] In the case of $f(\mathcal{R})$ theories [40], this can be transformed to a minimally coupled Lagrangian of the form eq. (2.27) via a Weyl transformation of the metric. The Higgs boson may be a valid candidate for the inflaton if it is non-minimally coupled to gravity [41].

with some cutoff scale Λ that characterizes where the effective field theory description breaks down. In this work, we will restrict ourselves for practical reasons to the case where the coefficients c_n are not field dependent, i.e., $c_n(\phi) = c_n$, such that $p(X, \phi)$ is separable, i.e.,

$$p(X, \phi) = \Lambda^4 S(X) - V(\phi)\,. \tag{2.29}$$

A theory is intrinsically non-canonical if the higher order kinetic terms X^n with $n > 1$ play a significant role in the dynamics. Note that this is qualitatively different from theories with non-canonical kinetic terms e.g.,

$$\mathcal{L} = -\frac{1}{2\phi^2}(\partial_\mu \phi)^2 - V(\phi)\,, \tag{2.30}$$

where one can, at least in principle, find a field redefinition. In this case, $\psi = \ln \phi$ transforms eq. (2.30) to a canonical theory in ψ.

The inflationary dynamics and observables are described in terms of the generalized slow-roll parameters ϵ and η defined in eq. (2.21) and (2.25), the speed of sound and its time derivation [46, 47]

$$c_s^2 \equiv \left(1 + 2X\frac{\partial^2 p/\partial X^2}{\partial p/\partial X}\right)^{-1}\,, \quad \kappa \equiv \frac{\dot{c}_s}{H\, c_s}\,. \tag{2.31}$$

In the canonical case $p(X, \phi) = X - V(\phi)$ these reduce to

$$\epsilon = \epsilon_V \equiv \frac{1}{2}\left(\frac{V'}{V}\right)^2\,, \quad \eta = 4\epsilon_V - 2\eta_V\,, \quad \eta_V \equiv \frac{V''}{V}\,, \quad c_s^2 = 1\,, \quad \kappa = 0\,. \tag{2.32}$$

The equations of motion derived from eq. (2.27) with pressure $p = p(X, \phi)$ and energy density

$$\rho = 2X\frac{\partial p}{\partial X} - p\,. \tag{2.33}$$

are

$$\begin{aligned} p &= -\rho\,(1 - \frac{2}{3}\epsilon)\,, \\ \dot{\rho} &= -3H\,(\rho + p) = -6H\,X\,\frac{\partial p}{\partial X}\,. \end{aligned} \tag{2.34}$$

Since during inflation $\epsilon \ll 1$ and hence $p \simeq -\rho$ we can write the second equation in eq. (2.34) as

$$-\sqrt{2X}\,\frac{\partial p}{\partial X} \simeq \frac{1}{3H}\frac{\partial p}{\partial \phi}\,. \tag{2.35}$$

In the canonical limit $p(X, \phi) = X - V(\phi)$ the equations of motion turn into the slow-roll equations

$$\ddot{\phi} + 3H\dot{\phi} + V'(\phi) = 0 \qquad \text{and} \qquad H^2 = \frac{1}{3}\left(\frac{1}{2}\dot{\phi}^2 + V(\phi)\right)\,. \tag{2.36}$$

The equation of state becomes

$$w = \frac{\frac{1}{2}\dot{\phi}^2 - V(\phi)}{\frac{1}{2}\dot{\phi}^2 + V(\phi)}\,, \tag{2.37}$$

so we have to demand $\frac{1}{2}\dot{\phi}^2 \ll V(\phi)$ for inflation and hence $H^2 \simeq \frac{1}{3}V(\phi)$.

For general separable $p(X,\phi)$ given in eq. (2.29), inflationary solutions can be found as algebraic solutions $X_{inf} = X(A)$ to the equation [48]

$$\sqrt{2X}\,\Lambda^2\,\frac{\partial S(X)}{\partial X} = A\,, \tag{2.38}$$

with the 'non-canonicalness' parameter

$$A(\phi) = \frac{V'}{3\,H\,\Lambda^2}\,. \tag{2.39}$$

$A \ll 1$ is equivalent to the canonical limit of the theory, since

$$A(\phi) = \left(\frac{2}{3}\epsilon_V \frac{V}{\Lambda^4}\right)^{1/2}\,, \tag{2.40}$$

and $\epsilon_V \ll 1$. On the other hand, for $A \gg 1$ the theory shows its non-canonical nature, i.e., the terms X^n with $n > 1$ dominate the Lagrangian and we can have $\epsilon_V > 1$ but still $\epsilon \ll 1$.

For theories with a finite convergence radius $X/\Lambda^4 < R$ of $S(X)$, it was shown that a truly non-canonical inflationary solution of eq. (2.38) with $A \gg 1$ exists under the following conditions [48]:

- The derivative $\partial_X S(X)$ diverges at the radius of convergence R.
- The potential is large in units of the cutoff scale, i.e., $V \gg \Lambda^4$ such that the energy density of the potential always dominates that of the kinetic terms.[6]

Note that a finite radius of convergence implies a speed limit $X < R\Lambda^4$. Theories without a speed limit with a $p(X,\phi)$ monotonically increasing in X might loose validity for $X > \Lambda$ as an effective field theory. Furthermore, it has been shown that that inflationary solutions act as an attractor in phase space, i.e., for general initial conditions $(\phi, X)_{in}$ the phase space trajectory flows towards the inflationary solution [48].

The two central questions that we will discuss in the following two chapters are:

[6] Note that the effective field theory description is valid as long as $H < \Lambda$. This generally allows large values of the potential in terms of the cutoff scale since $\frac{H}{\Lambda} \simeq \left(\frac{V}{\Lambda^4}\right)^{1/2} \frac{\Lambda}{M_P}$.

- *Can an inflationary solution of a non-canonical theory be transfered to a canonical theory?*
- *If yes, under which condition do the phenomenologies of the original non-canonical theory and the transformed canonical theory agree?*

It is hard to transform the complete theory, i.e., to find a field transformation $\phi \to \chi$ that transforms a general function $p(X, \phi)$ to a canonical Lagrangian $\tilde{p}(X, \chi) = X - V(\chi)$. On the other hand, finding a transformation that relates only the inflationary solution of a general $p(X, \phi)$ to an inflationary solution of a canonical theory is straightforward, as shown in Section 3.1. We will refer to this kind of transformation as *on-shell* since it relates only special solutions to the equations of motion to each other instead of a transformation of the full Lagrangian.

As far as phenomenology is concerned, the inflationary observables arise as quantum fluctuations of the field ϕ and the metric degrees of freedom around the classical background inflationary solution given in eq. (2.38). By transforming a non-canonical theory to a canonical theory via an on-shell transformation these background solutions are in agreement but it is not clear if the fluctuations around these solutions are as well. The inflationary observables are related to n-point functions of scalar and tensor fluctuations. These are the comoving curvature perturbations $\mathcal{R}$ which are a gauge invariant mixture of the fluctuations of ϕ and the scalar degrees of freedom of the metric, and the two polarization modes h of the tensor fluctuations h_{ij} of the metric. In perturbation theory, CMB observables such as temperature fluctuations are qualitatively a series expansion in the n-point functions with the expansion parameter being the relative amplitude of the fluctuations $sim10^{-5}$.

In Chapter 3, we first discuss how to match the inflationary background solution of a non-canonical theory to a canonical inflationary theory in Section 3.1 and then move on to the potential matching of the inflationary observables of the two theories at the level of the 2-point function. In Section 3.2, we discuss a condition on the speed of sound $c_s(A)$ as a function of the non-canonicalness parameter A for the matching of the 2-point function observables. DBI inflation [49, 50] as an example of non-canonical inflation that matches these conditions is discussed in more detail in Section 3.3. This Chapter summarizes the results of [12].

In Chapter 4, we discuss the matching of 3-point function observables, i.e., non-Gaussianities. There is generally a large amplitude of non-Gaussianities in non-canonical inflation [47], while in canonical slow-roll inflation non-Gaussianities tend to be small [51]. However, resonant features in the potential $V(\phi)$ of a canon-

ical theory can generate large non-Gaussianities [52–54]. These can be superimposed to generate similar non-Gaussianities to those generated in non-canonical inflation [13],[7] hence indicating a possible matching of canonical and non-canonical inflationary observables at the level of the 3-point function. After briefly introducing non-Gaussianities in the beginning of Chapter 4, we explain the summation of resonant non-Gaussianities in Section 4.1. The degeneracy with non-Gaussianities from non-canonical inflation is demonstrated in Section 4.2. Finally, we give some concluding remarks on Part I.

[7]Note that this degeneracy can also arise via a different mechanism, as in [55, 56]. Here, equilateral non-Gaussianity is induced by inflaton fluctuations sourced by gauge quanta via the pseudoscalar coupling $\phi F\tilde{F}$ to some gauge field F. However, the non-Gaussianity we consider in Chapter 4 has a different origin, coming only from the potential for ϕ.

Chapter 3

Comparison of 2-point function observables

Before we discuss the observational degeneracy of canonical and non-canonical inflationary theories at the level of the 2-point function, let us introduce the 2-point function observables. In momentum space, the power spectra $\Delta_s^2 \equiv \Delta_{\mathcal{R}}^2$ of the scalar modes $\mathcal{R}$ and $\Delta_t^2 \equiv 2\Delta_h^2$ of the tensor modes h are given by

$$\begin{aligned} \langle\, \mathcal{R}(\mathbf{k})\mathcal{R}(\mathbf{k}')\,\rangle &= (2\pi)^3\, \delta(\mathbf{k}+\mathbf{k}')\, \frac{2\pi^2}{k^3}\, \Delta_s^2(k)\,, \\ \langle\, h(\mathbf{k})h(\mathbf{k}')\,\rangle &= (2\pi)^3\, \delta(\mathbf{k}+\mathbf{k}')\, \frac{\pi^2}{k^3}\, \Delta_t^2(k)\,, \end{aligned} \tag{3.1}$$

with $k = |\boldsymbol{k}| = |\boldsymbol{k}'|$ and $\langle \dots \rangle$ is the ensemble average of the fluctuations. The scale dependence of the power spectra is defined by the scalar spectral indices/tilts

$$n_s(k) - 1 \equiv \frac{d\ln \Delta_s^2(k)}{d\ln k} \qquad \text{and} \qquad n_t(k) \equiv \frac{d\ln \Delta_t^2(k)}{d\ln k}\,. \tag{3.2}$$

The inflationary observables, i.e., the scalar power spectrum Δ_s^2, the tensor power spectrum Δ_t^2, the scalar spectral index n_s and the tensor spectral index n_t can then be calculated via [46, 47]

$$\begin{aligned} \Delta_s^2(k) &= \left.\frac{1}{8\pi^2}\frac{H^2}{M_p^2}\frac{1}{c_s\epsilon}\right|_{c_s k = aH}\,, \\ \Delta_t^2(k) &= \left.\frac{2}{\pi^2}\frac{H^2}{M_p^2}\right|_{k=aH}\,, \\ n_s(k) - 1 &= \left.-2\epsilon - \eta - \kappa\right|_{c_s k = aH}\,, \\ n_t(k) &= \left.-2\epsilon\right|_{k=aH}\,. \end{aligned} \tag{3.3}$$

The observables have to be evaluated at the time of horizon crossing aH. Note that scalar fluctuations travel with speed of sound c_s while tensor perturbations

travel with speed of light $c = 1$. In the canonical case, eq. (3.3) reduces to

$$\begin{aligned} \Delta_s^2(k) &= \frac{1}{8\pi^2}\frac{H^2}{M_p^2}\frac{1}{\epsilon}\bigg|_{k=aH} , \\ \Delta_t^2(k) &= \frac{2}{\pi^2}\frac{H^2}{M_p^2}\bigg|_{k=aH} , \\ n_s(k) - 1 &= -2\epsilon - \eta|_{k=aH} , \\ n_t(k) &= -2\epsilon|_{k=aH} , \end{aligned} \tag{3.4}$$

where we have used $c_s = 1$.

3.1 On-shell transformation of inflationary solutions

In any theory, canonical or non-canonical with scalar field χ, the inflationary solution can be expressed as a function in phase space $X_{inf}(\chi)$. We want to obtain the solution $X_{inf}(\phi)$ from a canonically normalized Lagrangian with scalar field ϕ and potential $V_{can}(\phi)$. In the following we describe how to construct $V_{can}(\phi)$.

In a canonically normalized theory that allows slow-roll inflation, the equations of motion eq. (2.36) are approximately

$$\dot{\phi} \simeq -\frac{V'_{can}(\phi)}{3H(\phi)} , \qquad H^2(\phi) \simeq \frac{V_{can}(\phi)}{3} , \tag{3.5}$$

where $'$ denotes the derivative with respect to ϕ. Using $\dot{\phi} = -\sqrt{2X}$ we obtain

$$\sqrt{6X}\, d\phi = \frac{1}{\sqrt{V_{can}}}\, dV_{can} . \tag{3.6}$$

Now, going on-shell $X = X_{inf}(\chi)$ and using $d\phi = d\chi$ we can integrate both sides of eq. (3.6) to solve for V_{can}:

$$\begin{aligned} \int_{\phi_0}^{\phi} \sqrt{6X_{inf}(\chi)}\, d\chi &= \int_{V_{0can}}^{V} \frac{dV_{can}}{\sqrt{V_{can}}} , \\ \Rightarrow \quad V_{can}(\phi) &= \left(\sqrt{V_{0can}} + \int_{\phi_0}^{\phi} \sqrt{\frac{3}{2}\, X_{inf}(\chi)}\, d\chi \right)^2 , \end{aligned} \tag{3.7}$$

with $V_{0can} = V_{can}(\phi_0)$. Eq. (3.7) can be seen as an on-shell transformation of the originally possibly non-canonical theory to a canonical theory. It gives us the potential V_{can}, whose dynamics described in eq. (3.5) give exactly the same trajectory in phase space as in the original theory. In other words, given an

inflationary trajectory in a theory with general kinetic term, we have derived the form of the potential in a theory with canonical kinetic term which will give rise to the same inflationary trajectory. We assume that the kinetic term is canonical and $X = X_{inf}^{can} = X_{inf}^{noncan} = X_{inf}$, and find the corresponding V_{can}. This is not a field transformation, since we simply match the inflationary trajectory in two different theories. Hence, for any properties regarding the inflationary background solution, the fields χ and ϕ are the same while their general dynamics governed respectively by their non-canonical and canonical Lagrangians are different.

If the original theory is canonical with potential $V(\chi)$, the inflationary trajectory is given by [48]

$$X_{inf}^{can} = \frac{(V')^2}{6\,V}\,, \tag{3.8}$$

such that $V_{can}(\phi) = V(\chi)$.

3.2 Conditions on the agreement of observables

In this section, we compare the number of efolds N_e, the scalar power spectrum Δ_s^2, the tensor power spectrum Δ_t^2 and the scalar spectral index n_s of non-canonical and canonical inflation. We discuss under what conditions these observables will match for a non-canonical theory and a canonical theory whose potential is obtained via eq. (3.7) such that it describes the same dynamics as the non-canonical theory.

The natural time measure during inflation is the number of efolds N_e that inflation produces in the time interval $[t_i, t_f]$. According to eq. (2.23), it is defined as

$$N_e = \int_{t_i}^{t_f} H(t)\,dt = \int_{\phi_{N_e}}^{\phi_{end}} \frac{H(\phi)}{\dot\phi}\,d\phi = \int_{\phi_{end}}^{\phi_{N_e}} \left(\frac{V(\phi)}{6\,X_{inf}(\phi)}\right)^{1/2} d\phi\,, \tag{3.9}$$

where in the last equation we have used $H^2 \simeq V/3$ and $\dot\phi = -\sqrt{2X}$ on the inflationary trajectory in phase space and ϕ_{end} is the field value when inflation ends. In the case of a canonically normalized Lagrangian, this reduces to

$$N_e = \int_{\phi_{end}}^{\phi_{N_e}} \frac{V(\phi)}{V'(\phi)}\,d\phi = \int_{\phi_{end}}^{\phi_{N_e}} \frac{1}{\sqrt{2\epsilon}}\,d\phi\,. \tag{3.10}$$

The observables are evaluated as functions of the comoving momentum k. Due to the fact that the sound speed c_s is generically different from one, the time of horizon crossing for scalar modes is different from the time of horizon crossing for tensor modes. In terms of efolds N_e, the different times of horizon crossing are

determined via

$$\begin{aligned} &\text{scalar modes:} \qquad c_s k = aH \quad \Leftrightarrow \ln k = (N_e - \ln c_s) + \ln H \,, \\ &\text{tensor modes:} \qquad k = aH \quad \Leftrightarrow \ln k = N_e + \ln H \,. \end{aligned} \tag{3.11}$$

Hence, the moment of horizon crossing of the scalar modes is earlier than that of the tensor modes and the correction is logarithmic in c_s with $\ln c_s < 0$ due to $c_s < 1$. The speed of sound is constrained from the non-observation of non-Gaussianities of the equilateral type to be $c_s \gtrsim 0.1$ such that the correction to horizon crossing is of the order of one efold. We will ignore this correction in the remainder of this section but will discuss its significance in Section 3.3.2. It will turn out that the correction is negligible for Δ_s^2 and Δ_t^2 while it is significant for n_s.

3.2.1 Theories with a speed limit

Let us examine under which conditions the observables of non-canonical inflation and canonical inflation obtained as a function of N_e, as discussed in Section 3.1, will agree. Let us make two assumptions:

- The non-canonical theory has a canonical branch, i.e., a region in phase space where $p \simeq X - V$, and hence $V_{can} \simeq V$ in this region.
- The non-canonical theory has a speed limit R such that $X_{inf} \simeq \Lambda^4 R$ for $A \gg 1$.

We can perform the integration in eq. (3.7) analytically and obtain

$$V_{can}(\phi) = \frac{3}{2} R \, \Lambda^4 (\phi - C)^2 \,, \tag{3.12}$$

with a constant C for the canonical potential in the limit for $A \gg 1$. This implies

$$\epsilon_{can} = \frac{1}{2} \left(\frac{V'_{can}}{V_{can}} \right)^2 = \frac{3R\Lambda^4}{V_{can}(\phi)} \,. \tag{3.13}$$

It was shown in [48] that the first slow-roll parameter becomes

$$\epsilon = \sqrt{2R} \, \frac{\epsilon_V}{A} \tag{3.14}$$

for $A \gg 1$. Using the definition of A, eq. (2.39), and eq. (3.13), the agreement of Δ_s^2 and Δ_t^2 as a function of ϕ can be phrased as conditions on the potentials and the speed of sound, i.e.,

$$V_{can} \simeq V \qquad \text{and} \qquad c_s = \frac{\sqrt{2R}}{A} \qquad \text{for } A \gg 1 \,. \tag{3.15}$$

Note that the first condition in eq. (3.15) is trivially satisfied in the canonical limit $A \ll 1$. In the non-canonical limit $A \gg 1$, the derivative V' will generically have large values while V'_{can} has to be small in order to support slow-roll inflation. Thus, at some value A^* in the $A \gg 1$ limit, V and V_{can} will no longer agree. However, there can be an intermediate regime $A \in [1, A^*]$ with $V_{can} \simeq V$ and $V'_{can} \ll V'$. This intermediate regime can even serve to describe the complete phenomenologically interesting region if $c_s(A^*) < 0.1$, such that only the region $A > A^*$ is excluded due to non-observation of equilateral non-Gaussianities.

The first condition in eq. (3.15) implies an agreement as a function of N_e as well since according to eq. (3.9)

$$\begin{aligned} &\text{canonical:} \qquad N_e = \int_{\phi_{end}}^{\phi_{N_e}} \frac{1}{\sqrt{2\epsilon_{can}}}\, d\phi = \int_{\phi_{end}}^{\phi_{N_e}} \left(\frac{V_{can}(\phi)}{6R\Lambda^4}\right)^{1/2} d\phi\,, \\ &\text{non-canonical:} \qquad N_e = \int_{\phi_{end}}^{\phi_{N_e}} \left(\frac{V(\phi)}{6\,X_{inf}(\phi)}\right)^{1/2} d\phi = \int_{\phi_{end}}^{\phi_{N_e}} \left(\frac{V(\phi)}{6R\Lambda^4}\right)^{1/2} d\phi\,. \end{aligned} \tag{3.16}$$

As far as the spectral indices n_s and n_t are concerned we do not find agreement in the limit $A \gg 1$ since

$$\begin{aligned} &\text{canonical:} \qquad n_s - 1 = -6\epsilon_{can} + 2\eta_{can} = -\frac{12R\Lambda^4}{V_{can}}\,, \\ &\qquad\qquad\quad\; n_t = -2\epsilon_{can} = -\frac{6R\Lambda^4}{V_{can}}\,, \\ &\text{non-canonical:} \qquad n_s - 1 = -2\epsilon - \eta - \kappa = \frac{\sqrt{2R}}{A}(-6\epsilon_V + 2\eta_V) - \kappa\,, \\ &\qquad\qquad\quad\; n_t = -2\epsilon = -\frac{2\sqrt{2R}}{A}\epsilon_V\,, \end{aligned} \tag{3.17}$$

using $\eta = \sqrt{2R}/A(4\epsilon_V - 2\eta_V)$ as was shown in [48]. However, this does not exclude an agreement in an intermediate region $A \gtrsim 1$. Furthermore, the scalar spectral index n_s receives significant corrections from the fact that $c_s < 1$ in non-canonical theories. This can improve the agreement, as we will summarize in Section 3.3.2. For n_t we cannot expect such an improvement but this observable is phenomenologically much less relevant since at present not even Δ_t^2 has been measured.

Let us now investigate with some examples when the second condition in eq. (3.15) on the speed of sound c_s can be fulfilled. First, we note that using eq. (2.38) the speed of sound can be expressed as

$$c_s^2(A) = \frac{A\,\partial X_{inf}/\partial A}{2X_{inf}}\,. \tag{3.18}$$

Hence, we need to know the functional dependence $X_{inf}(A)$ in order to decide whether the observables Δ_s^2 and Δ_t^2 of the canonical and non-canonical theory agree. For $p(X,\phi) = \Lambda^4 S(X) - V(\phi)$ as defined in eq. (2.28) this dependence is determined by the identity

$$2\frac{X}{\Lambda^4}\left(\sum_{n\geq 0}(n+1)\,c_n\left(\frac{X}{\Lambda^4}\right)^n\right)^2 = A^2\,, \tag{3.19}$$

using the algebraic equation for the inflationary solution, eq. (2.38). To obtain $X_{inf}(A)$ we have to invert eq. (3.19), which is impossible for generic coefficients c_n. However, we will discuss some closed form expressions for $p(X,\phi)$ in the following.

Consider the class of non-canonical Lagrangians defined by

$$p(X,\phi) = \Lambda^4\left[1 - \left(1 - \frac{1}{a}\frac{X}{\Lambda^4}\right)^a\right] - V(\phi)\,, \tag{3.20}$$

with $0 < a < 1$ such that $\partial p/\partial X$ diverges at the radius of convergence $R_a = a$. This class of non-canonical Lagrangians includes the DBI action which is defined via the case $a = 1/2$, i.e.,

$$p(X,\phi) = \Lambda^4\left[1 - \left(1 - 2\frac{X}{\Lambda^4}\right)^{1/2}\right] - V(\phi)\,. \tag{3.21}$$

In this case, the inflationary solution, solving eq. (2.38), is given as

$$X_{inf} = \frac{\Lambda^4}{2}\frac{A^2}{1+A^2}\,. \tag{3.22}$$

It is discussed in Section 4.1 of [12], that $c_s^2 \simeq A^{-2}$ for $A \gg 1$, fulfilling the second condition in eq. (3.15), only for $a = 1/2$. There are of course plenty of other models apart from those defined by eq. (3.20) that fulfill the conditions of a canonical branch and a speed limit. The question of whether there could be examples other than DBI where the conditions on the potential and speed of sound eq. (3.15) for an agreement of Δ_s^2 and Δ_t^2 are fulfilled is hard to answer in full generality but no other cases were found in [12]. Due to the lack of other working examples where the agreement conditions eq. (3.15) are matched, we suspect that the description in terms of a canonical theory may be special to the DBI case. We will study this case more explicitly in the following section. We note at this point that the matching of the background equation of motion does not necessarily mean that fluctuations around this background in the two different theories should match. One should thus not expect agreement of the inflationary observables in general, even if the inflationary trajectory is the same. This makes the agreement in the DBI case all the more remarkable.

3.3 DBI inflation with an inflection point potential

We now want to give an example of our general considerations in Section 3.2.1. We consider the DBI action together with an inflection point potential:

$$p(X,\phi) = -\frac{1}{f(\phi)}\left(\sqrt{1-2f(\phi)X}-1\right) - V(\phi)\,, \tag{3.23}$$

with

$$V(\phi) = V_0 + \lambda(\phi-\phi_0) + \beta(\phi-\phi_0)^3\,. \tag{3.24}$$

To study a numerical example, we fix the parameters of this theory to be

$$V_0 = 3.7{\cdot}10^{-16}\,, \quad \lambda = 1.13{\cdot}10^{-20}\,, \quad \beta = 1.09{\cdot}10^{-15}\,, \quad \phi_0 = 0.01\,, \quad f = 1.6{\cdot}10^{21}\,. \tag{3.25}$$

These are the values that were considered in [48]. In particular, the field-dependent warp factor has been set to a constant $f = \Lambda^{-4}$ which is justified if the range of field values that ϕ travels during inflation is small. The parameters in eq. (3.25) have been chosen such that for a canonical kinetic term $p(X,\phi) = X - V$ the amplitude of the scalar fluctuations and the spectral index agree with observations, i.e., $\Delta_s^2 = 2.41 \cdot 10^{-9}$ and $n_s = 0.961$.

Let us first see when eq. (3.23) is in the non-canonical regime by evaluating the 'non-canonicalness' parameter A. We find that for $\phi \lesssim 0.025$ we are in the canonical regime $A \leq 1$, while for $\phi \gtrsim 0.025$ we enter the non-canonical regime $A > 1$. The phase space trajectory $X_{inf}(\phi)$ for eq. (3.23) is determined by eq. (3.22). This determines the potential $V_{can}(\phi)$ that resembles the trajectory from a canonical kinetic term via eq. (3.7). We perform the integration numerically and show $V_{can}(\phi)$ compared to the original inflection point potential $V(\phi)$ in Figure 3.1. We see that, as expected, V_{can} agrees with V in the canonical regime while it is flatter than V in the non-canonical regime. To see that V_{can} actually supports slow-roll inflation we check ϵ_{can} and η_{can} as functions of ϕ, finding that these parameters are $\ll 1$ in the canonical as well as in the non-canonical regime.

3.3.1 Comparison of observables

We compare the observables of the canonical and non-canonical theory in Figure 3.2, exemplarily for Δ_s^2. The agreement in Δ_s and Δ_t at the level of $\sim 1\%$ is up to values $\phi < 0.2$ which is roughly one order of magnitude more than the value of ϕ where the non-canonical regime begins. So as discussed following eq. (3.15) there

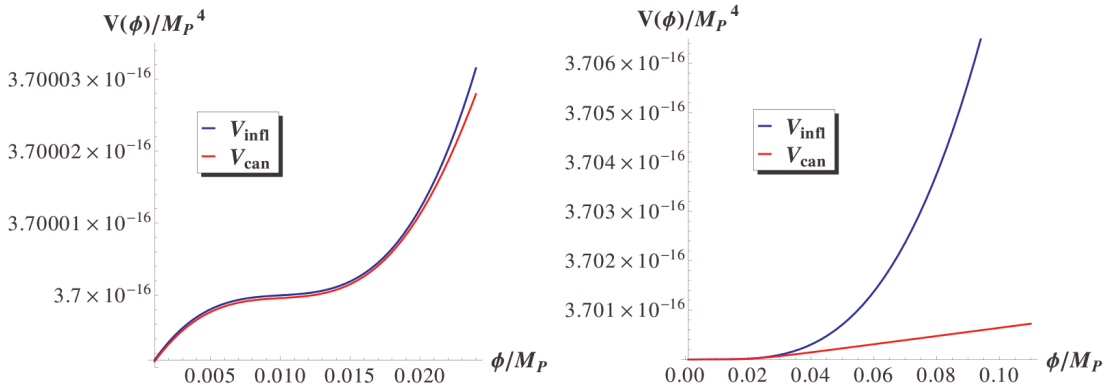

Figure 3.1: Comparison of the inflection point potential $V \equiv V_{infl}$ of eq. (3.24) and the potential of the canonical theory $V_{can}(\phi)$ obtained via eq. (3.7) for $\phi \in [0, 0.025]$ (left) and $\phi \in [0, 0.12]$ (right).

is indeed an intermediate regime where the observables agree even though V_{can} is much flatter than V. Furthermore, since $c_s < 0.1$ for $\phi > 0.06$, the phenomenologically viable region is included in this intermediate regime. The agreement of $n_s - 1$ of the two theories as functions of N_e holds only up to $\phi \leq 0.05$. However, there are important corrections to $n_s - 1$ induced by the fact that the speed of sound c_s in the non-canonical theory is smaller than one. We will discuss these corrections in Section 3.3.2.

Note that there is an additional upper bound on c_s which has to be fulfilled in order to treat the inflationary quantum fluctuations perturbatively [11, 57, 58]. If the speed of sound becomes too small, the perturbations become strongly coupled and in particular the expressions for the inflationary observables eq. (3.3) are not valid. For DBI this can be expressed as a bound on the 'non-canonicalness' parameter [48]

$$A < \left(\frac{3\,\epsilon}{V}\right)^{1/5} . \tag{3.26}$$

For our numerical example, this implies $A < \mathcal{O}(100)$ and hence $\phi \lesssim 0.2$. Note that this is exactly the region where we find agreement between the non-canonical and transformed canonical theory. A proof for the agreement of the observables Δ_s^2 and Δ_t^2 in the whole intermediate region (note that in Section 3.2.1 this was shown only in the limit $A \gg 1$) can be found in Section 4.2 of [12].

The agreement works out as well for the DBI action with a Coulomb type potential

$$V(\phi) = V_0 - \frac{T}{(\phi + \phi_0)^n} , \tag{3.27}$$

instead of an inflection point potential. The non-canonical regime is accessed for $\phi < \phi_0$ while the canonical regime is given by $\phi > \phi_0$. Hence, the agreement with

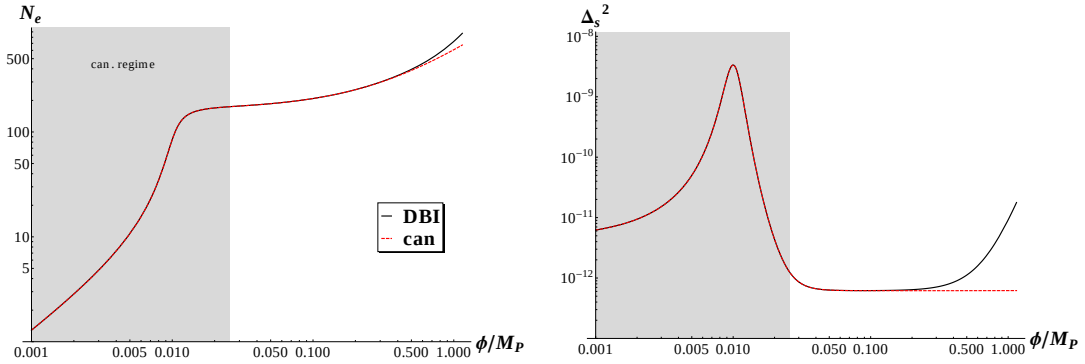

Figure 3.2: Comparison of the observables Δ_s^2 (right) of the non-canonical DBI and the transformed canonical theory. Since the number of efolds (left) of the two theories agrees as a function of ϕ, the agreement of the observables as a function of ϕ can be read as an agreement as a function of N_e.

the transformed canonical theory is trivially found for $\phi < \phi_0$ and extends to the non-canonical regime until the condition $V \simeq V_{can}$ is violated.

3.3.2 Corrections from $c_s < 1$

As we discussed in eq. (3.11), the observables have to be evaluated as functions of the comoving momentum k which implies different times of horizon crossing for scalar and tensor modes respectively. Under the condition $H_{can} \simeq H_{non-can}$ which follows from $V_{can} \simeq V$, an agreement of tensor observables T as functions of $\ln k$ is equivalent to $T_{can}(N_e) = T_{non-can}(N_e)$ having used $N_e = \ln k - \ln H$.

For scalar observables S however, we have to take into account that $N_e - \ln c_s = \ln k - \ln H$ in the non-canonical theory while $N_e = \ln k - \ln H$ in the canonical theory. Hence, we have to check for the equality $S_{can}(N_e) = S_{non-can}(N_e - \ln c_s)$. Since the non-observation of equilateral non-Gaussianities implies $|\ln c_s| \ll N_e^t$, it is sufficient to expand $S_{non-can}$ to first order in $\ln c_s$, i.e.,

$$S_{non-can}(N_e - \ln c_s) \simeq S_{non-can}(N_e) - S'_{non-can}(N_e)\, \ln c_s\,. \tag{3.28}$$

In Section 5 of [12], we perform this expansion for the scalar power spectrum Δ_s^2 and the scalar spectral index n_s. We find that the corrections to Δ_s^2 are of the order of the slow-roll parameters while the corrections to n_s can be sizable. We find that the regime where $n_s - 1$ of the canonical and non-canonical theory agree at the level of 1% is increased from $\phi \leq 0.05$ to $\phi \leq 0.08$. Consequently, the phenomenologically interesting region where $c_s > 0.1$ given by $\phi \leq 0.06$ is included due to the inclusion of this correction.

Chapter 4

Comparison of 3-point function observables/non-Gaussianities

So far CMB observations tell us that the spectrum of the perturbations of $\mathcal{R}$ is Gaussian [3, 4]. For a Gaussian spectrum all information is contained in the 2-point function or equivalently the power spectrum via eq. (3.1). In this case, all odd correlations vanish and the higher even-point functions are given as functions of the 2-point function. Future CMB and BAO experiments might detect a deviation from a Gaussian spectrum, i.e., non-Gaussianities that potentially encode information about the details of the inflationary mechanism. In this case, the 3-point function which is often also referred to as the bispectrum has the form

$$< R(\mathbf{k_1})\mathcal{R}(\mathbf{k_2})\mathcal{R}(\mathbf{k_3}) >= (2\pi)^3\, \delta^3(\mathbf{k_1}+\mathbf{k_2}+\mathbf{k_3})\, F(\mathbf{k_1},\mathbf{k_2},\mathbf{k_3})\,, \tag{4.1}$$

where we parametrize $F(\mathbf{k_1},\mathbf{k_2},\mathbf{k_3})$ following [52] as

$$F(\mathbf{k_1},\mathbf{k_2},\mathbf{k_3}) = (2\pi)^4\, \frac{\Delta_s^4}{(k_1k_2k_3)^2}\, \frac{\mathcal{G}(k_1,k_2,k_3)}{k_1k_2k_3}\,, \tag{4.2}$$

i.e.,

$$< \mathcal{R}(\mathbf{k_1})\mathcal{R}(\mathbf{k_2})\mathcal{R}(\mathbf{k_3}) >= (2\pi)^7 \frac{\Delta_s^4}{k_1^2k_2^2k_3^2}\delta^3(\mathbf{k_1}+\mathbf{k_2}+\mathbf{k_3})\frac{\mathcal{G}(k_1,k_2,k_3)}{k_1k_2k_3}\,. \tag{4.3}$$

This parametrization is motivated by the fact that for scale-independent fluctuations $F(\mathbf{k_1},\mathbf{k_2},\mathbf{k_3})$ is symmetric in its arguments and a homogeneous function of degree -6. Furthermore, Δ_s^2 is the expansion parameter for the influence of higher order n-point functions on the observables, i.e., the 3-point function is proportional to Δ_s^4. Note that 3-point function calculations are sensitive to the time-evolution of the vacuum while this is a higher order effect in case of the 2-point function.

It is useful to divide the function $\mathcal{G}(k_1, k_2, k_3)/(k_1 k_2 k_3)$ into a part that measures the amplitude of the non-Gaussianities f_{NL} and a shape function $S(k_1, k_2, k_3)$ via [59]

$$\frac{\mathcal{G}(k_1, k_2, k_3)}{(k_1 k_2 k_3)} = f_{NL}\, S(k_1, k_2, k_3)\,, \tag{4.4}$$

with [1]

$$f_{NL} \equiv \frac{10}{9}\,\frac{\mathcal{G}(k, k, k)}{k^3}\,. \tag{4.5}$$

The potential wealth of information decoded in non-Gaussianities lies in the fact that it is not only characterized by a number but by a momentum dependent function $S(k_1, k_2, k_3)$. Since different inflationary Lagrangians imply different shape functions $S(k_1, k_2, k_3)$, a detection of non-Gaussianities could distinguish between different inflationary dynamics that are degenerate at the level of the 2-point function. In general, the shape refers to the dependence of $S(k_1, k_2, k_3)$ on the momentum ratios k_2/k_1 and k_3/k_1 when the overall momentum scale K is fixed, while the dependence of S on K when the momenta k_i are fixed gives the running of the bispectrum.

4.1 Summed resonant non-Gaussianities

We discuss the derivation of summed resonant non-Gaussianities in this section. After presenting a scalar potential with a sum of modulations we present the influence of these modulations on the power spectrum and the bispectrum.

4.1.1 Potential, solution and slow-roll parameters

From an effective field theory point of view, we can begin with a model of a single scalar field with canonical kinetic term and modulated potential

$$V(\phi) = V_0(\phi) + \sum_i A_i \cos\left(\frac{\phi + c_i}{f_i}\right), \tag{4.6}$$

where we have generalized the modulated potential in [52, 54] to the case where the modulation is a series of terms with varying phases. Superimposing modulated terms in the potential is directly connected to superimposing the associated non-Gaussianities as we will see in the following. The sum in eq. (4.6) is a small

[1] The prefactor in eq. (4.5) is chosen such that for the local shape $\mathcal{G}^{\rm local}(k_1, k_2, k_3)/(k_1 k_2 k_3) = f_{NL}^{\rm local}(k_1^3 + k_2^3 + k_3^3)/(k_1 k_2 k_3)$ which is often used to parametrize non-Gaussianities phenomenologically, $f_{NL} = f_{NL}^{\rm local}$.

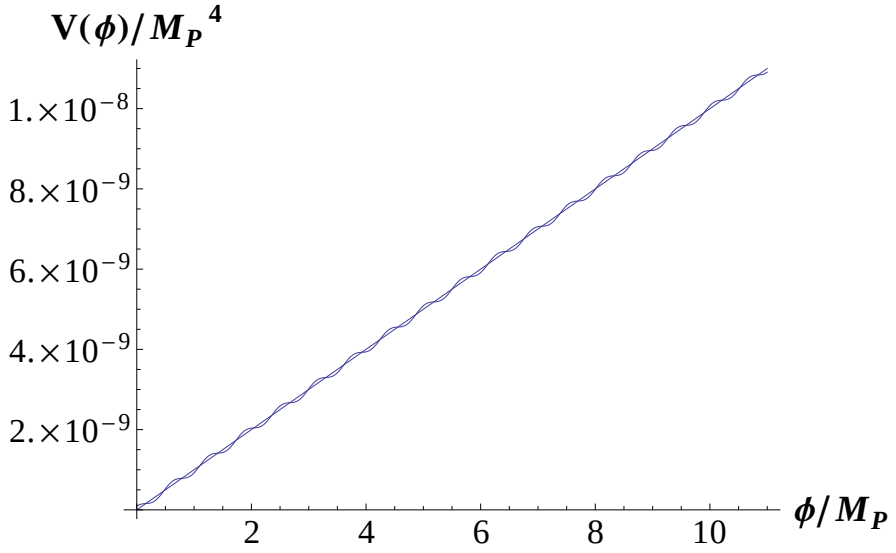

Figure 4.1: Modulated linear potential, for a convenient choice of c_i, f_i values.

perturbation to the equation of motion [13], i.e.,

$$\ddot{\phi} + 3H\dot{\phi} + V_0'(\phi) = \sum_i \frac{A_i}{f_i} \sin\left(\frac{\phi + c_i}{f_i}\right) , \tag{4.7}$$

instead of the first equation in eq. (2.36).

For suitable coefficients and values of f_i, the sum remains a small perturbation on the potential $V_0(\phi)$ (see Figure 4.1). It is shown in [13] that slow-roll inflation for this theory is supported for sufficiently large f_i, while a large time variation in the slow-roll parameters is possible, e.g.,

$$\frac{\dot{\delta}_1}{H} = \sum_i \frac{\sqrt{2\epsilon_\star}}{f_i} 3 b_i^\star \cos\left(\frac{\phi_0 + c_i}{f_i}\right) , \tag{4.8}$$

with $\delta \equiv \frac{\ddot{H}}{2\dot{H}H} = \frac{\eta}{2} - \epsilon$. It turns out [13, 54] that the perturbative expansion of the equations of motion eq. (4.7) is justified for $f_i \ll \sqrt{2\epsilon_\star}\,\forall\, i$ where the subscript $\star$ indicates evaluation at horizon exit, e.g., $\epsilon_\star \equiv \epsilon_{V_0}(\phi_\star)$. The parameter $b_i^\star$ in eq. (4.8) is defined as

$$b_i^\star \equiv \frac{A_i}{V_0'(\phi_\star) f_i} . \tag{4.9}$$

In Sections 4.1.2 and 4.1.3 we give the power spectrum and bispectrum respectively, finding that the bispectrum is given by a series of the resonant bispectra found for a singly modulated potential in [52, 54]. This bispectrum was first calculated in [52]; here we follow closely the notation and analysis in [54]. The details of our calculations are given in Appendix A of [13].

4.1.2 The power spectrum

To find the power spectrum we have to solve a differential equation, the Mukhanov-Sasaki equation for the mode function $\mathcal{R}_k$ of the curvature perturbation [54]

$$\frac{d^2\mathcal{R}_k}{dx^2} - \frac{2(1+\delta_1(x))}{x}\frac{d\mathcal{R}_k}{dx} + \mathcal{R}_k = 0, \tag{4.10}$$

where $x = -k\tau$ for τ the conformal time and δ_1 is the first order contribution in an expansion $\delta = \delta_0 + \delta_1 + \mathcal{O}(b_i^\star)$,

$$\delta_1 = -3\sum_i b_i^\star \sin\left(\frac{\phi_0 + c_i}{f_i}\right). \tag{4.11}$$

The differential eq. (4.10) can be solved by means of the stationary phase approximation [13, 54] with the solution outside the horizon $k/aH \ll 1$ i.e., $x = -k\tau = k/aH \ll 1$ (using the definition of conformal time and the fact that during inflation H is constant):

$$\begin{aligned}\mathcal{R}_k(x) = R_{k,0}^{(0)}\Bigg[1 + \sum_i 3b_i^\star\sqrt{\frac{f_i\pi}{2\sqrt{2\epsilon_\star}}}\cos\left(\frac{\phi_k + c_i}{f_i}\right) \\ - i\sum_i 3b_i^\star\sqrt{\frac{f_i\pi}{2\sqrt{2\epsilon_\star}}}\sin\left(\frac{\phi_k + c_i}{f_i}\right) + \mathcal{O}(x^3)\Bigg],\end{aligned} \tag{4.12}$$

where $\phi_k = \phi_\star - \sqrt{2\epsilon_\star}\ln\frac{k}{k_\star}$ is the value of the field when the mode with comoving momentum k exits the horizon. This implies

$$|\mathcal{R}_k^{(0)}|^2 = |\mathcal{R}_{k,0}^{(0)}|^2\left[1 + \delta n_s\right], \tag{4.13}$$

with

$$\delta n_s = \sum_i 3b_i^\star\left(\frac{2\pi f_i}{\sqrt{2\epsilon_\star}}\right)^{1/2}\cos\left(\frac{\phi_k + c_i}{f_i}\right), \tag{4.14}$$

which is just the generalization of eq. (2.30) in [54] one might have expected.

4.1.3 The bispectrum

The leading order to the bispectrum originates from the interaction Hamiltonian

$$H_I(t) \supset -\int d^3x a^3(t)\epsilon(t)\dot{\delta}(t)\mathcal{R}^2(\mathbf{x},t)\dot{\mathcal{R}}(\mathbf{x},t), \tag{4.15}$$

where to linear order in $b_i^\star$ we can use the approximations $\epsilon \approx \epsilon_\star, \delta \approx \delta_1$ and use the unperturbed mode functions $R_k(x)$.[2] Eq. (4.15) is one of many contributions

[2] To see why we can use the unperturbed mode functions, see Appendix A.2 of [13].

to the interaction Hamiltonian that can be derived from the effective Lagrangian of the perturbations. It is the leading contribution in our case since $\dot{\delta}(t)$ is large.

The single modulation analysis of [54] carries over to multi modulated case, with the 3-point function given by eq. (4.3) for

$$\frac{\mathcal{G}(k_1,k_2,k_3)}{k_1k_2k_3}=\frac{1}{8}\int_0^\infty dX\frac{\dot{\delta}_1}{H}e^{-iX}\left[-i-\frac{1}{X}\sum_{i\neq j}\frac{k_i}{k_j}+\frac{i}{X^2}\frac{K(k_1^2+k_2^2+k_3^2)}{k_1k_2k_3}\right]+c.c, \tag{4.16}$$

where $K\equiv k_1+k_2+k_3$, $X\equiv -K\tau$, and $\dot{\delta}_1$ is given by eq. (4.8). The integral has its dominant contribution in the vicinity of $X_{\text{res},i}=\frac{\sqrt{2\epsilon_\star}}{f_i}$ [13, 54], deep inside the horizon. Up to an overall phase,[3] the bispectrum is found to be a sum of the resonant bispectra found in [54]:

$$\begin{aligned}\frac{\mathcal{G}_{res}(k_1,k_2,k_3)}{k_1k_2k_3}=&\sum_i\frac{3\sqrt{2\pi}b_i^\star}{8}\left(\frac{\sqrt{2\epsilon_\star}}{f_i}\right)^{3/2}\left[\sin\left(\frac{\phi_K+c_i}{f_i}\right)\right.\\&-\frac{f_i}{\sqrt{2\epsilon_\star}}\sum_{\ell\neq m}\frac{k_\ell}{k_m}\cos\left(\frac{\phi_K+c_i}{f_i}\right)\\&\left.-\left(\frac{f_i}{\sqrt{2\epsilon_\star}}\right)^2\frac{K(k_1^2+k_2^2+k_3^2)}{k_1k_2k_3}\sin\left(\frac{\phi_K+c_i}{f_i}\right)\right]\\=&\sum_i\frac{3\sqrt{2\pi}b_i^\star}{8}\left(\frac{\sqrt{2\epsilon_\star}}{f_i}\right)^{3/2}\left[\sin\left(\frac{\sqrt{2\epsilon_\star}}{f_i}\ln\frac{K}{k_\star}+\frac{c_i}{f_i}\right)+\right.\\&\left.\frac{f_i}{\sqrt{2\epsilon_\star}}\sum_{\ell\neq m}\frac{k_\ell}{k_m}\cos\left(\frac{\sqrt{2\epsilon_\star}}{f_i}\ln\frac{K}{k_\star}+\frac{c_i}{f_i}\right)+...\right].\end{aligned} \tag{4.17}$$

As a consistency check of our calculation, we have confirmed that this sum of resonant bispectra satisfies the squeezed limit consistency relation [51, 60]. The details are presented in Appendix A.3 of [13].

4.2 Equilateral features from summed resonant non-Gaussianity

We now want to discuss what kind of non-Gaussianities could have a sizable overlap with summed resonant non-Gaussianity. One could also turn this question around

[3] Note that each term in the sum over i in eq. (4.17) actually has a different phase contribution which depends on the f_i. However, we can absorb these terms into the c_i which we are free to choose, such that eq. (4.17) is correct.

and ask what values the parameters $b_i^\star$, f_i and c_i have to take in order to generate a degeneracy. From an effective field theory point of view it is perfectly fine to choose ad hoc values for these parameters as long as they are not in conflict with observations such as the power spectrum and fulfill certain consistency conditions. For instance, the frequencies should certainly not be super Planckian, i.e., $f_i < 1$, and monotonicity of the inflaton potential requires $b_i^\star < 1$.

In [53, 61], bounds on oscillating features in the power spectrum were given for a quadratic and a linear inflaton potential respectively. The bound that was found in both works is

$$b_i^\star f_i < \frac{10^{-5}}{\sqrt{2\epsilon_\star}}\,, \tag{4.18}$$

for a single modulation in the potential, which may be avoided if the symmetry under time translations is collectively broken [62]. In the following, we assume that this bound is valid for multiple modulating terms in the potential. For more detail on when this bound, eq. (4.18), is applicable, see the discussion in Section 4.2.4.

Let us briefly discuss the general form of the bispectrum. Due to the appearance of the delta function in eq. (4.3), a momentum configuration is completely characterized by the absolute values of the three momenta k_1, k_2 and k_3. Furthermore, for a scale-invariant spectrum this reduces to two variables. Then, one usually considers the bispectrum as a function of the two rescaled momenta $x_2 = k_2/k_1$ and $x_3 = k_3/k_1$. A region that includes only inequivalent momentum configurations is given by $1 - x_2 \leq x_3 \leq x_2$.

Let us switch to the variables $x_\pm = x_2 \pm x_3$, with $1 < x_+ < 2$ and $0 < x_- < 1$. Note that the resonant non-Gaussianity eq. (4.17) is to first order in $f_i/\sqrt{2\epsilon_\star}$ only a function of x_+ and k_1 but not of x_- since

$$\sin\left(\frac{\sqrt{2\epsilon_\star}}{f_i}\,\ln\frac{K}{k_\star}\right) = \sin\left(\frac{\sqrt{2\epsilon_\star}}{f_i}\,(y + \ln k_1/k_\star)\right)\,, \tag{4.19}$$

having defined $y \equiv \ln(1 + x_+)$. Summed resonant non-Gaussianities are therefore not scale invariant, as is clear from in the explicit dependence on k_1 in eq. (4.19). We will discuss the issue of scale dependence in Section 4.2.2.

Furthermore, eq. (4.19) implies that as far as other types of non-Gaussianities are concerned, we can only expect degeneracies with the summed resonant type if they are predominantly a function of x_+. We will show in Section 4.2.1, that this is primarily the case for equilateral non-Gaussianity, typically arising in non-canonical models of inflation.

To measure the degree of degeneracy between different kinds of non-Gaussianities we follow [59]. The cosine of two shapes is defined via the normalized scalar prod-

uct

$$C(S,S') = \frac{F(S,S')}{\sqrt{F(S,S)F(S',S')}}, \tag{4.20}$$

where

$$F(S,S') = \int_{\mathcal{V}} \frac{d\mathcal{V}}{K} S(k_1,k_2,k_3)S'(k_1,k_2,k_3)\,. \tag{4.21}$$

The integration is defined via

$$\frac{d\mathcal{V}}{K} = \frac{dk_1\,dk_2\,dk_3}{k_1+k_2+k_3} = \frac{1}{2}k dk\,d\alpha\,d\beta\,, \tag{4.22}$$

where we have switched to the variables k, α and β defined according to [59]

$$\begin{aligned} k &= \frac{1}{2}(k_1+k_2+k_3)\,, \quad k_1 = k(1-\beta)\,, \\ k_2 &= \frac{k}{2}(1+\alpha+\beta)\,, \quad k_3 = \frac{k}{2}(1-\alpha+\beta)\,, \end{aligned} \tag{4.23}$$

with the integration boundaries

$$\alpha \in [-1+\beta, 1-\beta]\,, \qquad \beta \in [0,1] \qquad \text{and} \qquad k \in [k_{min}, k_{max}]\,. \tag{4.24}$$

4.2.1 Equilateral and local shapes for $x_- \to 0$

Let us check which shape functions can be well approximated by the limit $x_- \to 0$ by calculating the respective cosines defined in eq. (4.20). Out of the many known types of non-Gaussianities,[4] we discuss the following two representative types: The equilateral type

$$\frac{\mathcal{G}_{equil}(k_1,k_2,k_3)}{k_1k_2k_3} = f_{NL}^{equil}\, S_{equil}(k_1,k_2,k_3)\,, \tag{4.25}$$

with

$$S_{equil}(k_1,k_2,k_3) = \frac{(k_1+k_2-k_3)(k_1+k_3-k_2)(k_3+k_2-k_1)}{k_1k_2k_3}\,, \tag{4.26}$$

is characteristic of non-canonical inflation. The local type is given by

$$\frac{\mathcal{G}_{local}(k_1,k_2,k_3)}{k_1k_2k_3} = f_{NL}^{local}\, S_{local}(k_1,k_2,k_3)\,, \tag{4.27}$$

with

$$S_{local}(k_1,k_2,k_3) = \frac{k_1^3+k_2^3+k_3^3}{k_1k_2k_3}\,, \tag{4.28}$$

and is dominant for instance in multi-field inflation.

[4] For an overview see e.g., [63].

In the limit $x_- \to 0$, the shape functions are given by

$$S_{equil}^{x_-\to 0}(x_+) = \frac{4(x_+ - 1)}{x_+^2}\,, \tag{4.29}$$

$$S_{local}^{x_-\to 0}(x_+) = \frac{4 + x_+^3}{x_+^2}\,. \tag{4.30}$$

Now, the cosine in eq. (4.20) can be evaluated to find the overlap of S_{equil} and $S_{equil}^{x_-\to 0}(x_+)$:

$$C(S_{equil}, S_{equil}^{x_-\to 0}) = 0.93\,. \tag{4.31}$$

Hence, the equilateral shape is well approximated by its $x_- \to 0$ limit. For the local shape the overlap is much smaller. S_{local} diverges for squeezed momentum configurations which makes it necessary to regulate the integrals that enter the cosine eq. (4.20). We only give an upper bound $C(S_{local}, S_{local}^{x_-\to 0}) < 0.7$, which was obtained by cutting the integration boundaries eq. (4.24) as follows:

$$\beta \in [\Delta, 1 - \Delta] \qquad \text{with} \qquad \Delta = 5 \cdot 10^{-5}\,. \tag{4.32}$$

Notice that the shape function $S_{non-can}$ from non-canonical inflation shows a slightly more complicated momentum dependence than the equilateral shape function eq. (4.26), see [47]. We find $C(S_{non-can}, S_{non-can}^{x_-\to 0}) > 0.93$, so the approximation by the $x_- \to 0$ limit is even better in the case of $S_{non-can}$.

4.2.2 Scale invariance vs. scale dependence

Let us now discuss how well the scale-invariant equilateral shape can be approximated by a scale-dependent shape, such as summed resonant non-Gaussianity. It is obvious that the overlap cannot be made arbitrarily large; however, we will show in the following that the overlap can still be considerable.

Let $S_{equil}^{per}(y)$ be the periodic generalization of

$$S_{equil}^{x_-\to 0}(y) = 4\frac{e^y - 2}{(e^y - 1)^2}\,, \qquad y \in [\ln 2, \ln 3]\,, \tag{4.33}$$

to $y \in \mathbb{R}$, i.e., $S_{equil}^{per}(y + \Delta y) = S_{equil}^{per}(y)$ with $\Delta y = \ln 3 - \ln 2$. This definition is motivated by the fact that we are going to Fourier expand on the interval $y \in [\ln 2, \ln 3]$ and this expansion will itself be periodic with period Δy.

Furthermore, let us consider the scale-dependent shape $S_{equil}^{per}(y + \ln k_1/k_\star) = S_{equil}^{per}(\ln K/k_\star)$ which is a shape that can be approximated by the shape of some combination of resonant non-Gaussianities, since they have the same functional

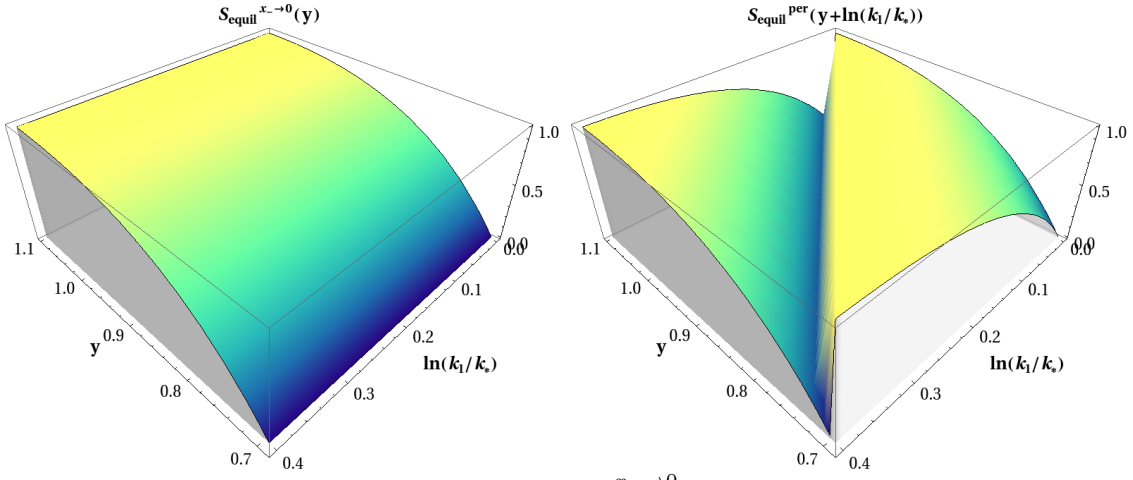

Figure 4.2: The scale-invariant shape $S_{equil}^{x_-\to 0}(y)$ (left) and scale-dependent shape $S_{equil}^{per}(y + \ln k_1/k_\star)$ (right) for $y \in [\ln 2, \ln 3]$ and $\ln k_1/k_\star \in [0, \Delta y]$

dependence, see eq. (4.19). The different shapes in $(y, \ln k_1/k_\star)$ space are shown in Figure 4.2.

The calculation of the cosine eq. (4.20) between the shapes $S_{equil}^{per}(\ln 2k/k_\star)$ and $S_{equil}(\alpha, \beta)$ simplifies due to the reduced dependencies on the integration variables k, α and β to

$$C\left(S_{equil}, S_{equil}^{per}\right) = \frac{\int d\alpha\, d\beta\, S^{equil}(\alpha,\beta)}{\left(2\int d\alpha\, d\beta\, S^{equil\,2}(\alpha,\beta)\right)^{1/2}} \times \frac{2\int_{k_{min}}^{k_{max}} dk\, k\, S_{equil}^{per}(\ln 2k/k_\star)}{\left([k_{max}^2 - k_{min}^2]\int_{k_{min}}^{k_{max}} dk\, k\, S_{equil}^{per\,2}(\ln 2k/k_\star)\right)^{1/2}}\,. \tag{4.34}$$

We find that eq. (4.34) is to a very good approximation independent of the values of k_{min} and k_{max}, if $k_{min} \ll k_\star$ and $k_{max} \gg k_\star$. This is due to the periodicity of $S_{equil}^{per}(\ln 2k/k_\star)$, yielding the second fraction on the RHS of eq. (4.34) essentially independent of these values. For $k_{max} = 10^4 k_\star$ and $k_{min} = 10^{-4} k_\star$, we find

$$C\left(S_{equil}, S_{equil}^{per}\right) = 0.83\,. \tag{4.35}$$

Let us also mention that the overlap would be greater than 83%, if we had considered not the equilateral shape function eq. (4.26), but the exact shape function [47] that arises in non-canonical single field models of inflation. This is due to the fact that the overlap between $S^{x_-\to 0}$ and S is larger than for the equilateral shape function eq. (4.26), as discussed at the end of Section 4.2.1. Finally, as we will see in the following Section 4.2.3, oscillatory features remain in the squeezed limit even if the periodic equilateral shape is synthesized in a Fourier analysis. An

observation of such oscillatory features in the CMB bispectrum, see [64], would break the degeneracy with the equilateral shape.

4.2.3 Fourier analysis

Having found that the equilateral shape function has a non-negligible degeneracy with the one dimensional function $S^{per}_{equil}(y + \ln k_1/k_\star)$, the question of degeneracy with summed resonant non-Gaussianities can be expressed in terms of a Fourier analysis. Let us set $k_1 = k_\star$ for conciseness in the remainder of this section; however the following analysis is valid for all values of k_1.

Let us define

$$B_i = \frac{3\sqrt{2\pi}b_i^\star}{8}\left(\frac{\sqrt{2\epsilon_\star}}{f_i}\right)^{3/2} \quad \text{and} \quad F_i = \frac{\sqrt{2\epsilon_\star}}{f_i}\,. \tag{4.36}$$

Then, summed resonant non-Gaussianity, eq. (4.17), can, to first order in $f_i/\sqrt{2\epsilon_\star}$, be written in the form[5]

$$\frac{\mathcal{G}_{res}}{k_1k_2k_3}(y) = \sum_{i=1}^{2N} B_i \sin(F_i y + C_i) = \sum_{i=1}^{N} B_i \cos(F_i y) + B_{N+i}\sin(F_i y)\,, \tag{4.37}$$

where in the last equality of eq. (4.37), we have chosen the phases C_i such that there appears a sine and a cosine for each frequency F_i. Clearly, eq. (4.37) has the form of a Fourier expansion with vanishing constant term. Ref. [13] performs the Fourier expansion, i.e., calculates the coefficients B_i in terms of f_{NL}^{equil} and F_i demanding $\mathcal{G}^{per}_{equil}(y) \simeq \mathcal{G}_{res}(y)$ for $N = 5$ and $N = 10$. For $N = 5$ we find using eq. (4.36)

$$f_i = \frac{\sqrt{2\epsilon_\star}}{F_i} = 0.06\frac{\sqrt{2\epsilon_\star}}{i} \qquad \text{and} \qquad b_i^\star = \frac{8}{3\sqrt{2\pi}}\frac{B_i}{F_i^{3/2}} \leq \frac{f_{NL}^{equil}}{f_{NL}^{max}}\,, \tag{4.38}$$

with $f_{NL}^{max} \equiv 140$ where the number originates from the maximal B_i and minimal F_i that were found numerically in the Fourier decomposition.

There are two things we can conclude from eq. (4.38). First of all, frequencies are necessarily sub-Planckian as is required for consistency. Second, we see that for $f_{NL}^{equil} > f_{NL}^{max}$ the monotonicity condition $b_i^\star < 1$ is violated. Hence $f_{NL}^{max} \equiv 140$ is the maximal equilateral non-Gaussianity that could be matched by summed resonant non-Gaussianity if there were no constraints from the power spectrum.

[5] Due to the suppression by $f_i/\sqrt{2\epsilon_\star} \ll 1$, the second order contribution to $\mathcal{G}_{res}/(k_1k_2k_3)$ induces a non-negligible correction only in the squeezed momentum configurations which we discuss at the end of this section.

To conclude this section let us discuss the role of the second order corrections that become sizable in the very squeezed limit to the resonant bispectrum given in eq. (4.17). Since these corrections come with an inverse power of the Fourier frequencies $F_i = \sqrt{2\epsilon_\star}/f_i$ and generically $u_1 \gg u_i$ for $i \lesssim N$, the corrections are dominated by the low frequency terms $i \gtrsim 1$. Hence, assuming that S^{per}_{equil} can be approximated to arbitrary precision in a Fourier analysis we define the shape function

$$S^{per-corr}_{equil} \equiv S^{per}_{equil} + \frac{1}{F_1} \sum_{l \neq m} \frac{k_l}{k_m} \cos\left(F_1 \ln \frac{K}{k_\star}\right) , \tag{4.39}$$

with $F_1 \simeq 15.5$ to estimate the effect of these corrections. We find

$$C\left(S_{equil}, S^{per-corr}_{equil}\right) = 0.77 , \tag{4.40}$$

compared to 83% correlation between S_{equil} and S^{per}_{equil}. As expected, the second order terms further break the degeneracy with the equilateral shape in the very squeezed limit. However, the effect is moderate.

4.2.4 Constraints from the power spectrum

Let us discuss the constraint on the product $b^\star_i f_i$ from the power spectrum, i.e., eq. (4.18). Non-observation of oscillating contributions to the 2-point function can place tight constraints on the maximum amount of resonantly generated non-Gaussianity with equilateral characteristics. However, the power spectrum constraint can be evaded when the time translation symmetry (which gives rise to scale invariance) is collectively broken as in [62]. Here, we discuss the bound on f_{NL} arising from the constraints on oscillations in the power spectrum, and also the mechanism of collective symmetry breaking whereby this constraint may be avoided.

First, using eq. (4.38), we find

$$b^\star_i f_i < \frac{8}{3\sqrt{2\pi}} \frac{\sqrt{2\epsilon_\star}\, f^{equil}_{NL}\, u_i}{F_i^{5/2}} < 5 \cdot 10^{-4} f^{equil}_{NL} \sqrt{2\epsilon_\star} , \tag{4.41}$$

where the product on the far right is the maximum value of $b^\star_i f_i$. Since the maximum value of $b^\star_i f_i$ has to be smaller than the upper bound given in eq. (4.18) this implies

$$\epsilon_\star\, f^{equil}_{NL} < 10^{-2} . \tag{4.42}$$

Given the values for $b^\star_i$ and f_i obtained for the Fourier expansion, we can check the behavior of eq. (4.14). We find that to leading order it behaves like a single

oscillation with f_i given by the lowest frequency f_1. This means that the 2-point function bounds found for the singly modulated potential will still apply in our case, assuming no other U(1)s are present, as in [62].

Note, that eq. (4.18) was derived for large-field models (linear axion monodromy inflation [53] and a quadratic potential [61]), and thus should not have validity for, $\epsilon_\star \lesssim 10^{-3}$. Therefore, from this result we can argue at most for a resonantly generated $f_{NL}^{equil} \lesssim \mathcal{O}(1)$.

This constraint from the 2-point function bound can be understood from the fact that the resonant N-point functions in inflationary models with periodically broken shift symmetry display a hierarchical suppression with increasing N [65]. However, if the mechanism of shift symmetry breaking is collective (such that scale invariance is protected by several independent symmetries), this hierarchy is no longer present. Any scale-dependent correlation function must depend on all the couplings required to break the symmetry, so that it is possible to have a nearly scale-invariant power spectrum and large non-Gaussianity (scale dependence in the bispectrum), as was shown for resonantly generated non-Gaussianity in [62]. In this case, for instance when an extra global U(1) symmetry is present, the constraints discussed above can be avoided. A sizable equilateral type f_{NL} (up to 140) could be produced via the summation discussed here, without implying large oscillations in the power spectrum.

The limit eq. (4.42) was derived for a large-field model by imposing the limit which the 2-point function data places on this model in eq. (4.18). As such, we cannot apply our bound to small-field models. In the absence of a collective breaking of the shift symmetry, e.g., by additional global U(1) symmetries [62], the structure of the resonant N-point functions places a tight constraint $f_{NL} \sim \mathcal{O}(5)$ [65], regardless of the field range during inflation. For a parametrically small-field model ($\Delta\phi_{60\,e-folds} \ll 1$), we would have to get multiple instanton contributions with axion decay constants with even parametrically smaller values in order to produce many wiggles in the potential within the 60 e-fold field range. As the axion decay constants are typically given by an $\mathcal{O}(1)$ inverse power of the size of the extra dimensions, they are difficult to suppress. Therefore, we expect parametrically small-field models to appear generically with few or no significant oscillatory contributions within their 60 e-folds field range. If this is true, then small-field models might be generically expected to produce no oscillations in the 2-point function and no resonant non-Gaussianity at all.

As we saw in Section 4.1 and this section, a potential that is modulated by a sum of small oscillating terms as given in eq. (4.6) leads to a bispectrum that is

a sum of resonant bispectrum terms, eq. (4.6). This sum can be interpreted as a Fourier series of resonant bispectra that, for appropriate choices of the parameters A_i, f_i and c_i, can lead to a significant degeneracy with the equilateral bispectrum shape. An important question is a string theoretic motivation for this scenario which can be found in Section 4 of [13] where a possible origin of the sum of oscillating terms in the potential in the context of axion monodromy inflation [53, 66] is discussed.

To conclude Part I of this thesis, we showed that for inflationary theories of a single scalar field there can be significant observational degeneracy. More precisely, the equilateral type of non-Gaussianities that are characteristic for non-canonical inflation are found to have sizable overlap with summed resonant non-Gaussianity from a canonical theory. Due to constraints from the non-observation of oscillatory features in the power spectrum, this degeneracy generically only holds up to $f_{NL} \sim \mathcal{O}(1)$ such that the observation of a larger f_{NL} of the equilateral shape would be a decisive sign for non-canonical inflation. At the level of 2-point function observables there is generically much more space for degeneracies between models as only two numbers have been measured so far: Δ_s^2 and n_s. Within the error bars of the measurements it is typically hard to distinguish between different theories of inflation. We identified the conditions on the agreement of Δ_s^2, n_s and so far unobserved Δ_t^2 when constructing a canonical from a non-canonical theory by mapping the phase space trajectories of the two theories. We find that for DBI inflation these two theories agree at the level of these observables for a whole range of efolds N_e but do not find any other examples for this matching. To conclude, it might not be as easy as previously thought to distinguish between canonical and non-canonical single field inflation from cosmological observations.

Part II

De Sitter vacua in string theory

Chapter 5

De Sitter model building

We discuss how the phenomenon of dark energy arises in the context of the string theory landscape. Similar to Part I of this thesis, we start with a review chapter. After briefly summarizing the experimental evidence for dark energy in Section 5.1, we give a short introduction to string theory, in particular type IIB, in Section 5.2. Next, we discuss the connection between the vacuum energy of string theory and dark energy in terms of an effective cosmological constant in Section 5.3. Finally, in Section 5.4 we focus on the structure of effective 4D $\mathcal{N} = 1$ effective scalar potentials of the moduli fields that arise from the compactification of string theory and give a brief introduction into moduli stabilization in type IIB. We end this chapter with an outline for Chapters 6-8.

5.1 The experimental case for dark energy

The discovery of the late-time acceleration of the universe has imposed an enormous challenge on theoretical particle physics. The first direct evidence came from type IA supernovae [1, 2]. Being so called standard candles, their intrinsic peak brightness is known, such that one can determine their luminosity distance d_L by the observed effective brightness and the redshift

$$1 + z \equiv \frac{\lambda_{obs}}{\lambda_{emit}} = \frac{a(t_{obs})}{a(t_{emit})}\,, \tag{5.1}$$

via the observed wavelength of the peak. Now in a FLRW universe, the luminosity distance can be expressed as a function of redshift as well as the cosmological parameters H_0, Ω_Λ, Ω_m and Ω_k. Experimental data from type IA supernovae up to a redshift of $z \sim 1$ favors a flat universe with a positive cosmological constant [1, 2].

Furthermore, there is observational evidence for dark energy from the temperature power spectrum of the CMB. From the WMAP satellite, the location of the first peak in the temperature spectrum implies $\Omega_{tot} = 1$, i.e., a flat universe. The contribution of photons and neutrinos to Ω_{tot} is negligible and the height of the first peak in the temperature spectrum implies $\Omega_m \simeq 0.3$ for the non-relativistic matter in the universe, i.e., baryons and cold dark matter. Since Ω_Λ is the only missing component, it follows indirectly that $\Omega_\Lambda \simeq 0.7$. However, taking data from the Atacama Cosmology Telescope (ACT), the South Pole Telescope (SPT) and BAO into account [3–7], the CMB by itself also directly implies a flat universe with a positive cosmological constant.

So far the experimental data is consistent with equation of state $w = -1$ [3, 4, 34, 67] for the portion of the universe that makes up dark energy. As we saw in eq. (2.8), this is characteristic of a cosmological constant. A deviation $w > -1$ would rule out a cosmological constant as the origin of dark energy.[1]

5.2 String theory

Before we discuss how dark energy can arise in string theory, let us elaborate on some basics of the theory.[2] String theory is a promising candidate for a theory of quantum gravity, reconciling quantum mechanics and general relativity. Furthermore, string theory can describe the gauge interactions and particle content of the standard model of particle physics, hence potentially describing all known fundamental forces and forms of matter. Whereas quantum field theory is a quantum theory of relativistic point-like particles, string theory is a quantum theory of relativistic strings, i.e., objects that are extended in one spatial dimension. The usual concept of quantum mechanics is kept in string theory. As a result of the space-like extension of the string, world lines of particles become world sheets of strings. Point-like interaction vertices of quantum field theory are replaced by world sheets with a certain topology, effectively smearing out all interaction vertices. This implies the finiteness of scattering amplitudes in string theory order by order in perturbation theory. Since the low energy limit of some string theories includes general relativity, string theory is therefore related to as the UV completion of general relativity.

One can formulate the dynamics of a one-dimensional string in D-dimensional space-time in terms of a two-dimensional conformal field theory (CFT) with a

[1] A future experiment that is designed to determine w more precisely is e.g., [68].

[2] For an introduction to string theory see e.g., [69–72].

D dimensional target space, i.e., a so-called sigma model of bosonic fields. This theory has one dimensionful free parameter α' which is the string tension and a dimensionless parameter g_s, the string coupling constant. The latter is determined by the VEV of the dilaton $\phi^{(10)}$ which is a scalar field arising in the string spectrum as we will discuss below. In order to obtain fermionic degrees of freedom in the spectrum of the string, one has to add fermionic fields to the worldsheet CFT. For consistency reasons, CFTs that obey a so-called worldsheet supersymmetry, hence leading to superstring theories, are of particular interest. To cancel the conformal anomaly, which is required by mathematical consistency, one has to either consider a 10D target space or introduce more complicated CFTs whose low energy effective actions are generically difficult to construct. The spectrum of superstring theories can be obtained by quantizing the left- and right-moving modes of the string independently. It consists of an infinite tower of string excitations which form irreducible representations of the target space Lorentz group. The higher string excitations inherit higher masses with mass spacing given by α'.

Phenomenologically, we are interested in superstring theories that have zero-mass states since only those theories can potentially include a massless graviton. Furthermore, the theory should not contain any tachyonic states for the sake of stability and admit a flat background. Under these conditions, there are five superstring theories that live in a 10D target space. If both left- and right-moving modes are described by a supersymmetric theory, the theory is referred to as type II which has 32 supercharges in 10D. There are two different type II theories: type IIA which is non-chiral and type IIB which is chiral with respect to the 10D Lorentz group. Type I string theory can be obtained by orientifolding, i.e., identifying left- and right-moving modes of type IIB string theory which has 16 supercharges in 10D. To cancel the anomalies in type I, one has to add open string states to the theory. The other possibility to obtain 16 supercharges in 10D is by introducing a supersymmetric theory for the right-moving excitations and a bosonic theory for the left-moving excitations. These are the heterotic string theories. There are two heterotic string theories which differ by their gauge group in 10D. These five string theories are connected to each other and also to 11D supergravity by a net of dualities, some of which are non-perturbative in nature. Due to these connections, it is conjectured that the five string theories describe certain limits of a more fundamental theory, called M-theory, whose low energy limit is given by 11D supergravity [73].

In the low energy limit of string theory, only the massless states of the spectrum play a role due to the large masses of the higher excitations. The massless spectra of the five string theories coincide with the massless spectra of the five mathematically

consistent supergravities in 10D: The type IIA and IIB which are $\mathcal{N} = 2$, the $SO(32)$ type I, and the $E_8 \times E_8$ and $SO(32)$ heterotic supergravities which are $\mathcal{N} = 1$. As these supergravities describe locally supersymmetric field theories in 10D, they always include a metric field g_{MN} and hence contain general relativity. Note that the non-renormalizability of these supergravities is not a problem since they are considered as effective theories being UV completed by string theory. Apart from the field content, supergravity includes extended solitonic objects in p spatial dimensions, so-called Dp-branes. The defining property for Dp-branes is that they define a Dirichlet boundary condition for open strings.

For the remainder of this work, we will study type IIB string theory in its supergravity limit together with D3- and D7-branes. The spectra of the left- and right-moving massless modes appear in vector or spinor representations of $SO(8)$ which is the little group of the 10D Lorentz group. They are referred to as the Neveu-Schwarz (NS) and Ramond (R) sector, respectively. Since left- and right-moving modes can be treated independently, there are four combinations of representations that determine the overall massless spectrum. In the case of type IIB string theory, the NSNS sector consists of the dilaton $\phi^{(10)}$ which is related to the string coupling via $g_s = e^{\phi^{(10)}}$, the Kalb-Ramond anti-symmetric 2-form field B_2 and the metric g_{MN}. The RR sector is built by the antisymmetric n-form fields C_n, for $n = 0, 2, 4$ while the NSR and RNS sectors are space-time fermions. The anti-symmetric form fields induce the field strengths

$$F_n \equiv dC_{n-1} \quad (n = 1, 3, 5)\,, \qquad H_3 \equiv dB_2\,, \tag{5.2}$$

with F_5 being self-dual, i.e., $F_5 = *_{10}F_5$, where $*_{10}$ denotes the 10D Hodge-star operator. Even though there is no manifestly covariant action for selfdual p-forms [74], we can formulate an effective $\mathcal{N} = 2$, 10D supergravity action and impose the self-duality condition later at the level of the equations of motion. To do so we redefine the fields as

$$\begin{aligned} \tau &\equiv C_0 + ie^{-\phi^{(10)}}\,, \qquad G_3 \equiv F_3 - \tau H_3\,, \\ \tilde{F}_5 &\equiv F_5 - \frac{1}{2}C_2 \wedge H_3 + \frac{1}{2}B_2 \wedge F_3\,. \end{aligned} \tag{5.3}$$

The IIB action in the 10D Einstein frame, which is related to the 10D string frame via a Weyl transformation $g^E_{MN} = e^{-\phi^{(10)}/2}g_{MN}$, can be written as [70, 75]

$$\begin{aligned} S = \frac{2\pi}{l_s^8}\Bigg[\int d^{10}x\sqrt{-g^E}\,\mathcal{R}^{(10)} - \frac{1}{2}\int \frac{1}{(\mathrm{Im}\tau)^2}d\tau \wedge *_{10}d\bar{\tau} \\ + \frac{1}{\mathrm{Im}\tau}G_3 \wedge *_{10}\bar{G}_3 + \frac{1}{2}\tilde{F}_5 \wedge *_{10}\tilde{F}_5 + C_4 \wedge H_3 \wedge F_3\Bigg]\,, \end{aligned} \tag{5.4}$$

where $l_s = 2\pi\sqrt{\alpha'}$ is the string length and $\mathcal{R}^{(10)}$ is the 10D Ricci scalar with respect to g^E_{MN}. The action in eq. (5.4) is invariant under $SL(2,\mathbb{Z})$ transformations

$$\begin{gathered}\tau \to \frac{a\tau + b}{c\tau + d} \qquad \text{with} \qquad a, b, c, d \in \mathbb{Z} \quad \text{and} \quad ad - bc = 1\,, \\ \begin{pmatrix} H_3 \\ F_3 \end{pmatrix} \to \begin{pmatrix} d & c \\ b & a \end{pmatrix} \cdot \begin{pmatrix} H_3 \\ F_3 \end{pmatrix}\,,\end{gathered} \tag{5.5}$$

which implies

$$G_3 \to \frac{G_3}{c\tau + d}\,. \tag{5.6}$$

As we discussed above, type IIB string theory has to be formulated in 10D for mathematical consistency, so 6Ds have to be compactified in order to make contact with our 4D world. The choice of compactification corresponds to a choice of a 6D compact manifold whose metric typically has a large number of non-trivial deformations (moduli) which correspond to volume and shape characteristics of the manifold. These moduli are described as massless scalar fields in a 4D effective low energy theory, i.e., their potential is flat for simple compactifications. This effective theory is obtained via a Kaluza-Klein (KK) reduction [76, 77]: The 6 extra dimensions manifest themselves via an infinite tower of massive states that can be integrated out of the effective 4D action if the energy scale is below the KK scale, which is the mass scale of the first excitations. Often, 4D $\mathcal{N} = 1$ space-time supersymmetry is imposed for phenomenological reasons [3] and for its power to keep control over quantum corrections to the effective theory above the supersymmetry breaking scale. This singles out a class of 6D manifolds which include Calabi-Yau (CY) manifolds [79] [4] that we will focus on in the remainder of this work. Defining properties of CY manifolds are being compact, complex, Kähler and of $SU(3)$ holonomy. The moduli of CY manifolds can be divided into Kähler/volume moduli and complex structure/shape moduli. Their number is counted by the Hodge numbers $h^{1,1}$ and $h^{2,1}$ respectively.

5.3 De Sitter vacua in string theory

What are possible explanations for dark energy? The only definite experimental data that is available right now is that we observe a non-vanishing contribution

[3] Low energy SUSY can be used to stabilize the Higgs mass at the electroweak scale and often comes with an interesting phenomenology, for instance connecting particle physics and cosmological constraints, see e.g., [78].

[4] For a comprehensive review see e.g., [80].

to the energy density of the universe $\Omega_\Lambda = 0.68$ with an equation of state that is consistent with $w = -1$. These are the characteristics of our universe being in a state of a de Sitter vacuum, i.e., a homogeneous and isotropic universe that is dominated by a positive cosmological constant. A negative cosmological constant would characterize an anti-de Sitter (AdS) vacuum.

As we discussed in Section 2.2, scalar fields are useful ingredients to model exponential expansion of the universe. Hence, let us once again consider a canonically normalized scalar field ϕ minimally coupled to gravity

$$S = \int d^4x\sqrt{g}\left[\frac{M_{\rm P}^2}{2}\mathcal{R} + \frac{1}{2}(\partial_\mu\phi)^2 - V(\phi)\right] . \tag{5.7}$$

In a local minimum $\phi = \phi_0$ of the scalar potential $V(\phi)$ this has an equation of state eq. (2.37)

$$w = \frac{\frac{1}{2}(\partial_\mu\phi)^2 - V(\phi)}{\frac{1}{2}(\partial_\mu\phi)^2 + V(\phi)} = -1\,, \tag{5.8}$$

using $\partial_\mu\phi = 0$. The energy-momentum tensor that is induced by the *effective* scalar potential $V_{eff}(\phi)$ is $T^V_{\mu\nu} = -V_{eff}(\phi_0)\eta_{\mu\nu}$, where V_{eff} is the scalar potential that includes the tree-level contribution V as well as perturbative V_p and non-perturbative V_{np} quantum corrections and finite temperature contributions V_T. This energy-momentum tensor can be absorbed into an effective cosmological constant

$$\Lambda_{eff} = \Lambda + V_{eff}(\phi_0) = \Lambda + V(\phi_0) + V_p(\phi_0) + V_{np}(\phi_0) + V_T(\phi_0)\,, \tag{5.9}$$

in Einsteins eq's (2.3) in a free-fall frame $g_{\mu\nu} = \eta_{\mu\nu}$.

It is important to note that the Lagrangian in eq. (5.7) is not renormalizable. Hence, it only makes sense to consider this Lagrangian as an effective theory of a UV complete quantum theory of gravity below some cutoff scale. String theory is arguably the best understood candidate for such a theory of quantum gravity that currently exists.

Now, what is the natural value of the energy density $\rho_\Lambda = \Lambda_{eff}$ in a theory of quantum gravity? The scale of quantum gravity is the Planck scale $M_{\rm P}$ and hence in the absence of any dynamical mechanism that keeps Λ_{eff} at small values or any fine-tuning, the terms in eq. (5.9) are expected to add up such that $\rho_\Lambda \sim M_P^4 \simeq 10^{76}\text{GeV}^4$. However, the observed value of $\Omega_\Lambda \sim 1$ corresponds to $\rho_\Lambda \sim 10^{-46}\text{GeV}^4$. This imposes maybe the most severe problem in todays theoretical physics, the cosmological constant problem: *Why is the observed cosmological constant* 10^{-122} *times smaller than its expected natural value in theories of quantum gravity?*

Even before the discovery of $\Omega_\Lambda > 0$ in the late 1990's, the reason why we do not observe a large cosmological constant in our universe needed to be explained. A possible anthropic explanation was that galaxies and therefore observers could never have formed in such a universe with $|\rho_\Lambda| \sim M_P^4$ due to its extremely accelerated expansion [20]. The observational fact of $\Omega_\Lambda > 0$ added significantly to the severity of the cosmological constant problem since it is usually easier to explain that a number is exactly zero by some mechanism [5] as opposed to being extremely small in its natural units.

As we discussed in the previous section, there is a large number of scalar moduli fields for string theory compactified on CY manifolds. Moduli fields are not charged under the standard model gauge group but couple only gravitationally. Hence, their action can be brought into the form eq. (5.7) and in case their effective potential V_{eff} stabilizes them in a (meta-)stable minimum, they directly influence the value of the cosmological constant via eq. (5.9). Let us make some phenomenological comments on moduli stabilization: If the moduli would have small masses $< 10^{-2}$ GeV, they would induce fifth-forces, modifying the strength of gravity, e.g., at solar system distance scales. Furthermore, they can cause cosmological problems. As Planck-coupled fields, their characteristic decay rate is $\Gamma \sim \frac{1}{16\pi}\frac{m_\phi^3}{M_P^2}$. If moduli are abundant during the hot big bang phase they tend to overclose the universe, i.e., the energy density Ω_ϕ stored in the moduli fields acts as a form of dark matter that dominates the energy density of the universe [6] and typically spoils the predictions of BBN. These cosmological problems are typically solved if $m_\phi \gtrsim 30$ TeV which makes Γ large enough that the moduli decay gravitationally well before BBN.

Hence, in order to accommodate the non-observation of light scalar fields that couple gravitationally in nature, the moduli have to be stabilized at a rather high mass scale. This corresponds to adding further ingredients to the effective theory, i.e., considering more complicated compactifications, that lift the flat directions, developing a potential for these moduli. These ingredients depend on the details of the considered compactification and will be discussed in the following. A pressing question at this point is the following: what allows us to add or not add these ingredients into the theory and which 6D manifold do we choose? The conceptual understanding of string theory is so far largely based on perturbative formulations.

[5] For instance, the photon is believed to be exactly massless due to gauge invariance.

[6] Light axion-like fields ϕ can act as cold dark matter if they are produced non-thermally via a vacuum realignment mechanism [81–83]. This mechanism fixes the value of ϕ for $H \gtrsim m_\phi$ which causes a coherent oscillation around the VEV at late times $m_\phi \gtrsim 3H$, which effectively resembles a state of cold dark matter.

However, there are strong indications that there is already a large abundance of perturbatively consistent backgrounds that could potentially describe a universe with a small positive cosmological constant. How many of these backgrounds could accommodate a standard model like gauge group, hence rendering a description of our world, remains an open question since at a more detailed level explicit constructions of such phenomenological backgrounds turn out to be difficult. The remainder of this work will mainly be concerned with the following quest: *The construction of explicit vacua in type IIB string theory that allow a fine-tuning of the cosmological constant to the extremely small observed value.*[7]

We choose to work in the context of type IIB because moduli stabilization is arguably best understood in this theory, using quantized VEVs for the gauge field strengths F_3 and H_3, i.e., *fluxes*. In this context, the number of de Sitter vacua is exponentially large due to the large number of fluxes. A topologically distinct flux has to be used to stabilize each complex structure modulus and the number of complex structure moduli of CYs is typically $\mathcal{O}(100)$ which leads to the number of isolated de Sitter vacua scaling like $e^{\mathcal{O}(1)h^{2,1}}$. This extremely large number of de Sitter vacua is usually referred to as the landscape of string vacua [17–19]. Due to general statistical arguments for a flat number density of the effective cosmological constant [23, 24], the landscape can provide an anthropic explanation for the smallness of the cosmological constant since the number of vacua is large enough to produce vacuum energies with average spacing $\lesssim 10^{-122}$. In other words, string theory *can* accommodate a universe with such a small vacuum energy which can already be considered a success given the severity of the cosmological constant problem and the fact that quantum field theory by itself does not teach us anything about the cosmological constant. In this work, we will go beyond statistical arguments for the distribution of the cosmological constant and explicitly construct large sets of vacua.

The anthropic selection of our vacuum is generically thought [19] to proceed in a population process of the landscape by Coleman-deLuccia tunneling and eternal inflation. Coleman-deLuccia tunneling [84] describes the quantum tunneling from a false vacuum, which is a classically stable excited state that is quantum-mechanically unstable, to the true vacuum state of the theory, including gravitational effects. The false vacuum decay proceeds via the nucleation of bubbles in the false vacuum, where each bubble is an open universe. The theory of eternal inflation [85] is based on the fact that there can be large quantum fluctuations

[7] The very important task of constructing a standard model sector with the corresponding gauge groups and representations will only be touched upon by in principle allowing such a sector locally in the compactification.

produced during inflation. These can increase the energy density in some parts of the universe to such an extent that these regions expand at a much greater rate than their parent domains. Conversely, large quantum fluctuations inside these domains lead to regions with even larger energy density and hence expansion rate and so on. In this sense, the universe is eternally inflating. Combining eternal inflation and Coleman-deLuccia tunneling with the string theory landscape, every vacuum of the theory is expected to be accessible in some region of the universe. If the anthropic selection of our vacuum in such a population process of the landscape is the end of the story or if there might be a selection mechanism that does not have to rely on anthropic reasoning remains an open question.

Before we discuss de Sitter model building in greater detail in Section 5.4, let us briefly summarize the state of the art for de Sitter model building in Type IIB string theory/F-theory on CY with orientifolds. As far as moduli stabilization is concerned, the complex structure moduli are stabilized by fluxes [14] while the Kähler moduli are stabilized by non-perturbative effects [15, 16] or a combination of perturbative and non-perturbative effects [86, 87]. As a first result, one often ends up with an AdS vacuum such that an uplifting sector has to be added to the effective theory. Uplifting mechanisms are, for instance, anti D3-branes [16], D-terms [88–90], F-terms from matter fields [91], metastable vacua in gauge theories [92], dilaton dependent non-perturbative effects [93] and F-terms of the Kähler moduli [21, 22, 86, 94]. We will focus on F-terms of the Kähler moduli in the remainder of this work since it is especially suitable for an explicit construction of a de Sitter vacuum.

Orientifolds have to be introduced since type II compactified on CY yields an $\mathcal{N} = 2$ effective theory in 4D. Including orientifold planes in the compactification effectively truncates the $\mathcal{N} = 2$ moduli space to $\mathcal{N} = 1$. Orientifold planes arise from the orientifold projection, which combines a discrete symmetry that identifies left- and right-moving modes on the worldsheet with a discrete symmetry of the target space. The orientifold plane is given as the fixed point of the discrete target space symmetry which can be defined in terms of an isometric and holomorphic involution σ of the CY. One can define Op planes with $p = 3, 5, 7, 9$ spatial dimensions. In this work, we only consider O7 planes, with σ leaving invariant a two complex dimensional submanifold of the CY. Apart from reducing the supersymmetry from $\mathcal{N} = 2$ to $\mathcal{N} = 1$, Op planes have negative Dp-brane charge. Hence, including O7 planes in the compactification allows us to include D7-branes with an overall zero D7-charge. The overall Dp-charge, the so-called Dp-tadpole, has to be canceled inside the compactification manifold because otherwise stationary solutions to the equations of motion are not possible. According to Gauss' law,

a net charge would source field lines that would cause decompactification since a stationary solution is only possible in a 10D non-compact space. Furthermore, harmonic (p,q)-forms are either even or odd eigenstates of the holomorphic involution which in particular splits the number of Kähler and complex structure moduli in $h^{1,1}_{\pm}$ and $h^{2,1}_{\pm}$. After orientifolding the number of Kähler moduli and complex structure moduli that remain in the spectrum are given by $h^{1,1}_{+}$ and $h^{2,1}_{-}$ respectively. Furthermore, there are $h^{1,1}_{-}$ chiral multiplets with purely axionic scalar fields and $h^{2,1}_{+}$ vector multiplets. In the following, we refer to $h^{1,1}_{+}$ by $h^{1,1}$ and to $h^{2,1}_{-}$ by $h^{2,1}$, for simplicity, unless stated otherwise.

F-theory [95] arises from the observation that the axio-dilaton of type IIB can be interpreted as the complex structure modulus of an elliptic curve fibred over the base of the CY 3-fold.[8] Hence, F-theory can geometrically be considered as a 12D theory that is compactified on a CY 4-fold that is elliptically fibred. In the limit of weak string coupling, F-theory is equivalent to type IIB (Sen limit [98]). The attraction of F-theory is due to the geometrization of non-perturbative gauge theory effects as well as its property of being intrinsically non-perturbative away from the Sen limit.

5.4 Moduli stabilization in type IIB string theory

Let us consider the effective 4D $\mathcal{N}=1$ supergravity scalar potential V of the following set of chiral multiplets: the $h^{1,1}$ Kähler moduli $T_i = t_i + i\,c_i$, the $h^{2,1}$ complex structure moduli $U_a = \nu_a + i\,u_a$ of a CY 3-fold X_3 and the axio-dilaton $\tau = \sigma + i\,s$. The real scalar fields c_i, ν_a and σ are referred to as axions since they have axion-like couplings to gauge fields. For instance, the coupling of the c_i's to $U(1)$ gauge field strengths can be found in the effective action of D7-branes wrapping 4-cycles D_i whose volume is given by t_i [99]. The real part $s = \mathrm{Im}(\tau)$ is related to the string coupling g_s as $s = g_s^{-1}$.

The scalar potential V is determined by the Kähler potential K and the holomorphic superpotential W as

$$V = e^K \left(K^{\alpha\bar{\beta}} D_\alpha W \overline{D_\beta W} - 3|W|^2 \right) , \tag{5.10}$$

where $D_\alpha W = W_\alpha + K_\alpha W$, $K^{\alpha\bar{\beta}}$ is the inverse of $K_{\alpha\bar{\beta}}$ and the indices α and β run over all geometric moduli. The Kähler potential and superpotential are given

[8] For reviews see [75, 96, 97].

as [100]

$$\begin{aligned} K &= K_{\rm k}(T_i, \bar{T}_i, \tau, \bar{\tau}) + K_{\rm cs}(U_a, \bar{U}_a) - \log(-i(\tau - \bar{\tau}))\,, \\ W &= W_0(U_a, \tau) + W_{\rm np}(T_i, U_a, \tau)\,, \end{aligned} \tag{5.11}$$

where $K_{\rm k}$ is the Kähler potential of the Kähler moduli, $K_{\rm cs}$ of the complex structure moduli, W_0 the tree-level superpotential and $W_{\rm np}$ includes non-perturbative corrections to the superpotential. While K includes perturbative as well as non-perturbative corrections, W only receives non-perturbative corrections due to its holomorphicity. The perturbative corrections to K come in various powers of α' and g_s. Since these corrections are only known to leading order at present, one has to ensure that higher order corrections do not spoil any phenomenological implications that have been derived from the scalar potential that only includes the leading order corrections. This issue of trustability of the effective potential can generically be avoided by considering theories in which the moduli are stabilized such that $g_s \ll 1$ and the overall volume of the CY $\mathcal{V} \gg 1$.

Note that W does not depend on the Kähler moduli at tree-level. Furthermore, eq. (5.10) obeys a no-scale structure [101, 102] in the Kähler moduli sector:

$$K^{i\bar{j}} D_i W \overline{D_j W} = 3|W|^2\,, \qquad \text{for } i, j = 1, .., h^{1,1}\,, \tag{5.12}$$

such that

$$V = e^K K^{c\bar{d}} D_c W \overline{D_d W} \geq 0\,, \tag{5.13}$$

where the indices c and d run over the moduli U_a and τ. Hence, at the tree-level only the U_a and τ develop a scalar potential if $W_0 \neq 0$. We will discuss their stabilization in Section 5.4.1. The Kähler moduli potential remains flat at tree-level such that perturbative and/or non-perturbative corrections have to be taken into account for their stabilization. This will be discussed in Section 5.4.2.

5.4.1 Complex structure moduli stabilization

In this section, we discuss the stabilization of the complex structure moduli and axio-dilaton by fluxes.[9] The number of complex structure moduli is related to the number of 3-cycles $b_3 = 2h^{2,1} + 2$ in the CY 3-fold X_3. We choose a symplectic basis $\{A_a, B^b\}$ for the b_3 3-cycles

$$\int_{A_a} \alpha^b = \int_{X_3} \alpha^b \wedge \beta_a = \delta_a^b\,, \qquad \int_{B^b} \beta_a = \int_{X_3} \beta_a \wedge \alpha^b = -\delta_a^b\,, \tag{5.14}$$

[9] For recent reviews see [103–105].

where $\{\alpha_b, \beta^a\}$ are the Poincaré dual cohomology elements to the 3-cycles and $a, b = 0, .., h^{2,1}$.

Having chosen a symplectic basis for the 3-cycles, this defines a choice of coordinates ω_a on complex structure moduli space via the period integrals over the holomorphic 3-form Ω via

$$\omega_a = \int_{A_a} \Omega \,, \qquad\qquad \mathcal{G}_b = \int_{B^b} \Omega \,. \tag{5.15}$$

Note, that there are $h^{2,1}+1$ coordinates $\omega_0, .., \omega_{h^{2,1}}$ even though there are only $h^{2,1}$ complex structure moduli. This is because ω_0 refers to the normalization of the holomorphic 3-form Ω. The complex structure moduli can be defined via $U_a = \omega_a/\omega_0$ for $i = a, .., h^{2,1}$. The period vector $\Pi(\omega_a) = (\mathcal{G}_b, \omega_a)$ is inherited from a holomorphic function $\mathcal{G}(\omega_a)$ of degree two in the ω_a known as the prepotential via $\mathcal{G}_b = \partial_b \mathcal{G}$ of the underlying $\mathcal{N} = 2$ CY compactification.

The Kähler potential of the complex structure moduli U_a can then be written as

$$\begin{aligned} K_{\rm cs}(U_a, \bar{U}_a) &= -\log\left(-i\int_{X_3} \Omega(U_a)\wedge\bar{\Omega}(\bar{U}_a)\right) \\ &= -\log\left(i(\bar{\omega}_a\mathcal{G}_a - \omega_a\bar{\mathcal{G}}_a)\right) \\ &= -\log\left(-i\Pi^\dagger\cdot\Sigma\cdot\Pi\right) \,, \end{aligned} \tag{5.16}$$

where in the third line of eq. (5.16) we have introduced the symplectic matrix

$$\Sigma = \begin{pmatrix} 0 & \mathbb{1} \\ -\mathbb{1} & 0 \end{pmatrix} \,, \tag{5.17}$$

and used the intersection formula

$$\int_{X_3} X\wedge Y = \sum_{a=0}^{h^{2,1}} \left(\int_{A_a} X \int_{B^a} Y - \int_{A_a} Y \int_{B^a} X\right) \,, \tag{5.18}$$

for general 3-forms X and Y.

The Gukov-Vafa-Witten flux superpotential is determined by the flux of F_3 and H_3 via [106]

$$W_0(U_a, \tau) = \frac{1}{2\pi}\int_{X_3} (F_3 - \tau H_3)\wedge\Omega(U_a) \,. \tag{5.19}$$

Due to the quantization of the 3-form flux

$$\begin{aligned} &\frac{1}{(2\pi)^2\alpha'}\int_{A_a} F_3 = f_{1a} \in \mathbb{Z} \,, \qquad &&\frac{1}{(2\pi)^2\alpha'}\int_{B^a} F_3 = f_{2a} \in \mathbb{Z} \,, \\ &\frac{1}{(2\pi)^2\alpha'}\int_{A_a} H_3 = h_{1a} \in \mathbb{Z} \,, \qquad &&\frac{1}{(2\pi)^2\alpha'}\int_{B^a} H_3 = h_{2a} \in \mathbb{Z} \,, \end{aligned} \tag{5.20}$$

eq. (5.19) can be written as

$$W_0(U_a,\tau) = 2\pi\left[(f_{1_a} - \tau\, h_{1a})\mathcal{G}_a - (f_{2_a} - \tau\, h_{2a})U_a\right] , \tag{5.21}$$

where we have set $\alpha' = 1$ and used again eq. (5.18) and the definition of the periods eq. (5.15).

The D3-tadpole induced by turning on RR and NS flux is given by

$$L \equiv \frac{1}{(2\pi)^4(\alpha')^2}\int_{X_3} H_3 \wedge F_3 = h\cdot\Sigma\cdot f = h_1 f_2 - h_2 f_1 \,. \tag{5.22}$$

It has been realized in [107], that localized sources of D3-charge such as orientifolds have to be included in the compactification in order to cancel the contribution in eq. (5.22) that is induced by non-vanishing H_3 and F_3 fluxes.

The no-scale structure eq. (5.12) is broken by α' corrections [108] and string loop corrections [109] in K, as well as non-perturbative corrections to the superpotential and K. However, these corrections are parametrically small in every moduli stabilization scenario where the overall volume $\mathcal{V}$ of X_3 is large as we already mentioned above. Hence, the scalar potential for the dilaton and complex structure moduli eq. (5.13) is positive semi-definite in this limit and a supersymmetric extremum given by a solution to the system of equations

$$D_\tau W = 0 \qquad \text{and} \qquad D_{U_a} W = 0\,, \qquad \text{for } a = 1,..,h^{2,1}\,, \tag{5.23}$$

will always be a minimum, i.e., all eigenvalues of the second derivative matrix V_{ab} are positive [87].

Note that due to the appearance of the symplectic matrix, the tadpole eq. (5.22) is at first not positive definite. However, as has been discussed in [14, 24], imposing the supersymmetry conditions $D_a W = 0$ results in $G_3 = F_3 - \tau\, H_3$ being imaginary self-dual (ISD), i.e., $*_6 G_3 = i\, G_3$. Since the ISD component of G_3 always results in positive semi-definite contributions to the tadpole while the anti-ISD ($*_6 G_3 = -i\, G_3$) component of G_3 always yields negative semi-definite contributions, a supersymmetric point always has $L \geq 0$. This can be seen nicely if the ISD condition is displayed as [110]

$$*_6\, s\, H_3 = -(F_3 - \sigma H_3)\,, \tag{5.24}$$

i.e., only $h^{2,1}+1$ of the original $2h^{2,1}+2$ fluxes are independent once the ISD condition is invoked and

$$L \sim \int_{X_3} H_3\wedge F_3 \sim \int_{X_3} H_3 \wedge *_6 H_3 \sim \int_{X_3}\sqrt{\tilde{g}}|H_3|^2 > 0\,, \tag{5.25}$$

where we have used eq. (5.24). As is easily verified, the $SL(2,\mathbb{Z})$ transformations in eq. (5.5) leave the D3-tadpole eq. (5.22) invariant. When determining the solution space of flux vacua of X_3 we have to make sure to consider only inequivalent vacua under the transformations eq. (5.5).

5.4.2 Kähler moduli stabilization

Including the leading α' correction [108] as well as non-perturbative corrections to the superpotential [111] the effective 4D theory of the Kähler moduli is defined by

$$\begin{aligned} K_{\rm k} &= -2\log\left(\mathcal{V}(t_i) + \frac{1}{2}\hat{\xi}(\tau,\bar{\tau})\right) , \\ W_{\rm np} &= \sum_{i=1}^{h^{1,1}} A_i(U_a,\tau)\, e^{-a_i T_i} , \end{aligned} \tag{5.26}$$

where

$$\hat{\xi}(\tau,\bar{\tau}) = -\frac{\zeta(3)\,\chi}{4\sqrt{2}(2\pi)^3}(-i(\tau-\bar{\tau}))^{3/2} , \tag{5.27}$$

is the leading α' correction to the Kähler potential with χ representing the Euler number of X_3.[10] There are additional corrections to $K_{\rm k}$ that we will mostly neglect in the following: string loop corrections entering $K_{\rm k}$ [109] are suppressed by g_s, as well as higher orders of $\mathcal{V}$ in V due to the extended no-scale structure of V [112]. Also, higher order α' corrections [113] are neglected due to their volume suppression.[11] Finally, non-perturbative corrections to $K_{\rm k}$ are generically expected to be subleading compared to perturbative corrections due to their exponential suppression.

The exponential terms in the non-perturbative superpotential in eq. (5.26) can originate from two sources: Euclidean D3-brane [12] instantons with $a_i = 2\pi$ wrapping around 4-cycles of X_3, or gaugino condensation in pure non-Abelian 4D $\mathcal{N}=1$ super-Yang-Mills theories on stacks of D7-branes wrapping around 4-cycles of X_3. In the latter, $a_i = 2\pi/N_i$ where N_i is the Coxeter number of the corresponding gauge group that is realized by the stack of D7-branes. The dependence of the one-loop determinants $A_i(U_a,\tau)$ on the complex structure moduli and the axio-dilaton is, in general, poorly understood. However, these moduli are generically stabilized at tree level and hence at a higher scale compared to the Kähler moduli which are

[10] In the following, we set $\alpha' = 1$ in natural units.

[11] This is of course only valid if there are no large coefficients in front of these higher order terms in the $1/\mathcal{V}$ expansion of the scalar potential.

[12] An euclidean D3-brane is related to a standard D3-brane with 4D world volume by a Wick rotation of the time coordinate, so it is an object with four spatial dimensions.

stabilized by subleading effects with respect to an expansion of the potential V in $\mathcal{V}$. Therefore, the A_is can generically be considered constant for the purpose of Kähler moduli stabilization. In the following, we will often consider D7-branes, wrapping divisors, which are 4-cycles that are submanifolds of X_3 with complex codimension one, i.e., complex dimension two. The value of A_i is related to a geometric property of the corresponding divisor D_i: $A_i \neq 0$ only if D_i is rigid, i.e., does not allow continuous deformation into other divisors. Hence, rigid divisors are particularly interesting for the purpose of Kähler moduli stabilization.

The scenarios of moduli stabilization that we discuss in the following, i.e., the Kachru-Kallosh-Linde-Trivedi (KKLT) scenario [16], the large volume scenario (LVS) [86, 87] and the Kähler uplifting scenario [21, 86, 94], all rely on the effects summarized in eq. (5.26) but operate in different regions of the parameter space of the effective 4D theory. This parameter space is spanned by $\{W_0, \hat{\xi}, A_i, a_i\}$. The leading terms in an expansion in $\mathcal{V}^{-1}$ of the scalar potential that follows from eq. (5.26) can be written schematically as

$$V \sim \frac{W_{\rm np}^2}{\mathcal{V}} - \frac{W_{\rm np} W_0}{\mathcal{V}^2} - \frac{\hat{\xi}\, W_0^2}{\mathcal{V}^3}\,. \tag{5.28}$$

KKLT vacua

In the KKLT scenario, the fluxes in eq. (5.20) are fine-tuned such that $|W_0| \ll 1$, typically $|W_0| < 10^{-5}$. The smallness of W_0 implies that the terms $\propto \hat{\xi}$ in eq. (5.28) are strongly suppressed such that the first 2 terms on the LHS have to be balanced against each other in order to construct a minimum. These minima are supersymmetric, i.e., solutions to the equations $D_{T_i} W = 0$. For one Kähler modulus T, $K_{\rm k} = -3\log(T+\bar{T})$ and one non-perturbative effect $W_{\rm np} = A\, e^{aT}$, the minimum $T = t_0$ ($c_0 = 0$) lies at

$$W_0 = -A\, e^{-a t_0} \left(1 + \frac{2}{3} a t_0\right)\,. \tag{5.29}$$

Hence, W_0 has to be small and negative in order for $\mathcal{V} \sim t_0^{3/2} \sim -\log|W_0|$ to be large enough to justify the supergravity approximation $\mathcal{V} \gg 1$. For $h^{1,1} > 1$, moduli stabilization in the KKLT scenario generically requires a non-perturbative effect for each Kähler modulus. However, in a variation of the KKLT scenario [114], a single non-perturbative effect on an ample divisor [13] can lead to a minimum for all t_i and one linear combination of the c_i. In this case, the remaining axionic directions remain flat.

[13] An ample divisor D_{amp} in a basis $\{D_i\}$ of divisors for $i = 1, .., h^{1,1}$ is given as $D_{amp} = \sum_i^{h^{1,1}} n_i D_i$ with exclusively positive coefficients $n_i > 0$.

Since all moduli are stabilized supersymmetrically, i.e., $D_\alpha W = 0$, the vacuum energy at the minimum is at first negative

$$V_{\text{AdS}} = -3\, e^K\, W^2\,, \tag{5.30}$$

such that a positive contribution to the potential, an uplifting term, is needed to construct a de Sitter vacuum. Of the uplifting mechanisms discussed in Section 5.3, anti D3-branes, F-terms from matter fields and F-terms from metastable vacua in gauge theories can be used. D-terms are not available in this scenario since the vanishing of the F-terms of the geometric moduli $D_\alpha W = 0$ implies vanishing of the D-terms as well. Even though the Kähler moduli sector by itself develops a stable minimum in the sense of a positive definite Hessian in the KKLT scenario, consideration of the complete mass matrix that includes the axio-dilaton and complex structure moduli might reveal directions that become tachyonic upon uplifting [115].[14]

LVS vacua

In the LVS scenario, all three terms in eq. (5.28) are balanced against each other to yield a stable minimum for the Kähler moduli. The simplest example of the LVS can be realized for a manifold with two Kähler moduli T_b and T_s with a 'swiss-cheese' volume form $\mathcal{V} \sim t_b^{3/2} - t_s^{3/2}$ and one non-perturbative effect on T_S, $W_{\text{np}} = Ae^{-aT_s}$. The potential takes the form

$$V \sim \frac{a^2 A^2 \sqrt{t_s}\, e^{-2at_s}}{\mathcal{V}} - \frac{at_s\, A\, e^{-at_s} W_0}{\mathcal{V}^2} + \frac{\hat{\xi}\, W_0^2}{\mathcal{V}^3}\,. \tag{5.31}$$

All three terms are of similar magnitude if $t_s \sim \log \mathcal{V}$ for arbitrary values of W_0. This is a natural way to achieve exponentially large $\mathcal{V}$ with $W_{\text{np}} \ll W_0$ and hence very good control over higher order corrections to the effective potential. Evaluating the potential V at the minimum yields an AdS vacuum that has to be uplifted to de Sitter. However, in this case the F-terms of the Kähler moduli are not zero such that D-terms can be used for the uplift. Furthermore, dilaton dependent non-perturbative effects as well as the uplifting options that apply in the KKLT scenario are available.

[14] A supersymmetric AdS minimum is always stable as was first pointed out by Breitenlohner and Freedman [116].

Kähler uplifting vacua & outline

In the Kähler uplifting scenario, the last two terms in eq. (5.28) are relevant

$$V \sim -\frac{W_{\rm np} W_0}{\mathcal{V}^2} - \frac{\hat{\xi}\, W_0^2}{\mathcal{V}^3}\,. \tag{5.32}$$

The $W_{\rm np}^2/\mathcal{V}$ term can be neglected since $\mathcal{V} \sim \mathcal{O}(10^2 - 10^3)$ is not exponentially large and $a \ll 1$ such that $W_{\rm np} \ll 1$. Contrary to the KKLT and LVS scenario de Sitter vacua can be realized by the potential in eq. (5.32) alone, there is no need for an additional uplifting sector. Due to the fact that moduli stabilization of the geometric moduli without further input makes the construction of Kähler uplifted de Sitter vacua possible, this scenario is especially suitable for the following attempts that we will pursue in the remainder of this work:

- *A model-independent analysis for a sufficient condition for de Sitter vacua in the context of Kähler uplifting*: In Chapter 6, we elaborate on a sufficient condition for the compactification parameters to realize a de Sitter vacuum. After presenting the analysis for the Kähler moduli sector in Section 6.1, we include the complex structure moduli and the dilaton and show in a perturbative analysis in Section 6.2 under which condition all moduli are stabilized simultaneously. This chapter is a summary of [21].

- *The construction of explicit examples of Kähler uplifted de Sitter vacua*: In Chapter 7, which summarizes [22], we present a globally consistent brane and gauge flux configuration that realizes a de Sitter vacuum along the lines of the sufficient condition given in Chapter 6. After discussing general constraints on large gauge group ranks N (that imply small a) in Section 7.1, we focus on a specific manifold to construct a globally consistent de Sitter model: $\mathbb{CP}^4_{11169}[18]$. The analysis is presented from the IIB perspective in Section 7.2 and from the equivalent F-theory perspective in Appendix C.2.

- *Explicit flux compactifications that lead to an estimate of the tunability of the cosmological constant*: Finally, in Chapter 8 we construct the full solution spaces of supersymmetric flux vacua of the reduced moduli space of $\mathbb{CP}^4_{11169}[18]$. The reduction of this moduli space is discussed in Section 8.1. The construction of the full solution space via the polynomial homotopy continuation method is considered in Section 8.2, while an alternative method, the minimal flux method, is summarized in Section 8.3. This chapter gives an overview of the results obtained in [25] and [26].

Chapter 6

De Sitter vacua by Kähler uplifting

6.1 A meta-stable de Sitter vacuum for the Kähler modulus

We will at first restrict ourselves to one-parameter models with $h^{1,1} = 1$ and $h^{2,1} > 1$ so that the Euler number $\chi = 2(h^{1,1} - h^{2,1}) < 0$ (which will be shown to be part of the the sufficient condition for the existence of de Sitter vacua). Later, we will extend the analysis to all so-called 'swiss-cheese' CY 3-folds with arbitrary $h^{1,1} > 1$ and $h^{2,1} > h^{1,1}$, giving a strong indication that the mechanism discussed in this section works for all 3-folds with $\chi < 0$.

For one-parameter models, we have $\mathcal{V} = \gamma(T + \bar{T})^{3/2}$ with $\gamma = \sqrt{3}/(2\sqrt{\kappa})$ and κ denotes the self-intersection number of the single Kähler modulus $T = t + ic$. Following [86, 94, 108] we can write the resulting scalar potential eq. (5.10) in the form

$$V(T) = e^K \left(K^{T\bar{T}} \left[W_T \overline{W_T} + (W_T \cdot \overline{WK_T} + c.c) \right] + 3\hat{\xi} \frac{\hat{\xi}^2 + 7\hat{\xi}\mathcal{V} + \mathcal{V}^2}{(\mathcal{V} - \hat{\xi})(\hat{\xi} + 2\mathcal{V})^2} |W|^2 \right) . \tag{6.1}$$

The non-trivial task is to find stationary points of $V(T)$ with respect to t. It is straightforward to show that the axionic direction has an actual minimum at $c = 0$. The Kähler potential does not depend on c and the exponential in eq. (5.26) introduces trigonometric functions $\sin(ac)$ and $\cos(ac)$ into $V(T)$. Then it can be shown that $V_c = 0$ for $c = n\pi/a$ for $n \in \mathbb{Z}$. We restrict ourselves to the case $c = 0$

so that after insertion of W_T we obtain

$$\begin{aligned} V(t) =& e^K \left(K^{T\bar{T}} \left[a^2 A^2 e^{-2at} + (-aAe^{-at}\overline{WK_T} + c.c) \right] \right. \\ &\left. + 3\hat{\xi} \frac{\hat{\xi}^2 + 7\hat{\xi}\mathcal{V} + \mathcal{V}^2}{(\mathcal{V} - \hat{\xi})(\hat{\xi} + 2\mathcal{V})^2} |W|^2 \right) . \end{aligned} \tag{6.2}$$

6.1.1 Approximating $V(T)$ in the large volume limit

In [94], it was shown that one can get de Sitter minima for T at parametrically large volume $\mathcal{V} \simeq \mathcal{O}(10^2 \dots 10^3)$ and weak string coupling $g_s \simeq 0.1$. The stable minimum is realized at $\hat{\xi}/(2\mathcal{V}) \simeq 0.01$ such that neglecting higher orders in the α' expansion is well justified and string loop effects are double-suppressed due to the smallness of g_s and the extended no-scale structure [112]. This minimum can be constructed under the following conditions

- Put a stack of $N \simeq \mathcal{O}(30 \dots 100)$ D7-branes on the single 4-cycle that undergoes gaugino condensation.[1]
- Choose the flux induced superpotential $W_0 \simeq \mathcal{O}(-30)$ and the parameter $\hat{\xi} \simeq \mathcal{O}(10)$. Note that a W_0 of this rather large magnitude does not induce problematic back reactions, as in type IIB the fluxes are imaginary self-dual (ISD) and of (1,2) or (0,3) type which restricts the back reaction to the warp factor.

In this setup, one typically obtains a minimum at $T \simeq \mathcal{O}(40)$ so that the non-perturbative contribution to the superpotential Ae^{-aT} is small enough to also trust the Ansatz for the non-perturbative superpotential.

In this context, we can give a parametric understanding of the scenario by approximating the scalar potential eq. (6.2) under the constraint of the typical values of the parameters $a, A, W_0, \hat{\xi}, \gamma$. We use the condition $\hat{\xi}/(2\mathcal{V}) \simeq 0.01$ and the validity of the non-perturbative superpotential:

$$\mathcal{V} \gg \hat{\xi}, \qquad |W_0| \gg Ae^{-at} . \tag{6.3}$$

Under these approximations, the leading terms in the scalar potential eq. (6.2) are [21]

$$V(x) \simeq \frac{-W_0 a^3 A}{2\gamma^2} \left(\frac{2C}{9x^{9/2}} - \frac{e^{-x}}{x^2} \right), \quad C = \frac{-27 W_0 \hat{\xi} a^{3/2}}{64\sqrt{2}\gamma A} . \tag{6.4}$$

[1] In the context of compact F-theory models very large gauge groups have been constructed [117], e.g., $SO(7232)$.

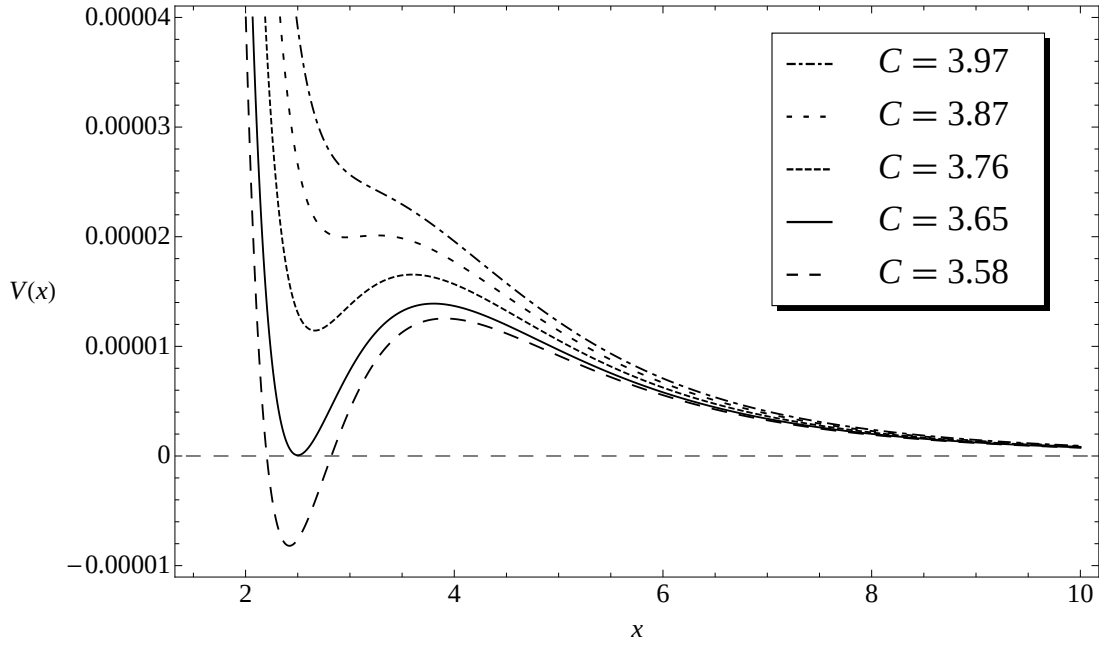

Figure 6.1: The approximate 2-term scalar potential $V(x)$ from eq. (6.4) for different values of C.

with $x = a \cdot t$ and $C > 0$ for $W_0 < 0$. The stationary point in the axionic direction $c = 0$ is always a minimum since the mass $V_{cc} > 0$ for $W_0 < 0$ [21].

6.1.2 A sufficient condition for meta-stable de Sitter vacua

To calculate extrema of eq. (6.4) we need to calculate the first and second derivative with respect to x ($V' = \frac{\partial V}{\partial x}$)

$$V'(x) = \frac{-W_0 a^3 A}{2\gamma^2} \frac{1}{x^{11/2}} \left(C - x^{5/2}(x+2)e^{-x}\right) \ , \tag{6.5}$$

$$V''(x) = \frac{-W_0 a^3 A}{2\gamma^2} \frac{1}{x^{13/2}} \left(\frac{11}{2} C - x^{5/2}(x^2+4x+6)e^{-x}\right) \ . \tag{6.6}$$

Solving for an extremum $V'(x) = 0$ yields

$$x^{5/2}(x+2)e^{-x} = C \tag{6.7}$$

which cannot be solved explicitly in an analytic way. Plotting the approximate expression eq. (6.4) of $V(x)$ for different values of the constant C in Figure 6.1 we observe the following behavior: We see that with growing C we first obtain an AdS minimum. This minimum breaks supersymmetry since

$$F_T \simeq \frac{-3W_0}{2t\mathcal{V}} \neq 0 \ . \tag{6.8}$$

Then at some point the minimum transits to de Sitter, and for even larger C the potential eventually develops a runaway in the x direction. We can analytically calculate the window for C where we obtain a meta-stable de Sitter vacuum by identifying:

- Lower bound on C: $V(x_{min}) = V'(x_{min}) = 0 \quad \Rightarrow \{x_{min}, C\} \simeq \{2.5, 3.65\}$
- Upper bound on C: $V'(x_{min}) = V''(x_{min}) = 0 \quad \Rightarrow \{x_{min}, C\} \simeq \{3.11, 3.89\}$

These numerical values for $\{x_{min}, C\}$ are the only solutions with $x_{min} > 0$. The region close to $\{x_{min}, C\}$ is the one relevant for obtaining a small positive cosmological constant suitable for describing the late-time accelerated expansion of the universe. For $a = 2\pi/100$, the lower bound on x corresponds to a volume $\mathcal{V} \simeq 100$ so we are indeed at parametrically large volume. The allowed window for C to obtain meta-stable de Sitter vacuum is approximately

$$3.65 \lesssim \frac{-27 W_0 \hat{\xi} a^{3/2}}{64\sqrt{2}\gamma A} \lesssim 3.89\,. \tag{6.9}$$

The following details regarding this sufficient condition for metastable de Sitter vacua can be found in [21]:

- When focusing on the leading order α' correction to the scalar potential we have to make sure that flux induced α' corrections are suppressed. It is shown in Section 2.4 of [21], that these corrections can be tuned irrelevant by choosing small $W_0 \lesssim \mathcal{O}(1)$ and $g_s \lesssim 0.01$ such that eq. (6.9) is fulfilled.
- In Section 2.5 of [21] we give an equivalent formulation of this sufficient condition in the context of F-theory. The topological data of the 3-fold, i.e., the parameters ξ, γ, χ and $h^{2,1}$ translate to 4-fold parameters while the gauge group rank entering a is determined by the ADE singularity enforced at the degeneration point of the elliptically fibred torus. The condition on $W_0(G_3)$ becomes a condition on the 4-form flux G_4. In this sense, the sufficient condition eq. (6.9) becomes purely geometrical (except for G_4) in the F-theory picture.
- There is a necessary condition for de Sitter vacua in general 4D $\mathcal{N} = 1$ supergravity that imposes a condition on the curvature of the scalar field space induced by the Kähler potential [118]. For consistency, this necessary condition needs to be fulfilled if the sufficient condition in eq. (6.9) is satisfied. This is checked in Section 2.6 of [21].

- A numerical example that shows the validity of the above approximations to obtain the sufficient condition by comparing the full scalar potential, eq. (6.2), versus the approximated version, eq. (6.4), can be found in Section 2.7 of [21].
- A discussion of the decay rate of these metastable vacua via quantum tunneling [84, 119–121] is found in Section 2.8 of [21]. The tunneling is predominantly in the direction of the volume modulus while the other Kähler moduli do not show a finite barrier. At first approximation it turns out that the lifetime of these metastable vacua is extremely large with respect to the age of the universe.

In Section 6.2, we will show that fulfilling condition eq. (6.9) is still sufficient to obtain a meta-stable minimum of the scalar potential when all the remaining moduli fields of the CY, i.e., the dilaton and the complex structure moduli, are included in the stabilization analysis. Hence, this is truly a sufficient condition for meta-stable de Sitter vacua and no tachyonic instabilities occur by including further moduli, contrary to the standard KKLT scenario [115, 122].

6.1.3 $h^{1,1} > 1$

We will now proceed to show explicitly that the above argument can be extended to the full class of all CY 3-folds with $h^{1,1} > 1$ arbitrary and $\chi < 0$ which are of 'swiss cheese' type.[2] A 'swiss cheese' type CY is characterized by a classical volume given by

$$\mathcal{V} = \gamma \left(T + \bar{T}\right)^{3/2} - \sum_{i=2}^{h^{1,1}} \gamma_i \left(T_i + \bar{T}_i\right)^{3/2} . \tag{6.10}$$

We will look for de Sitter vacua which satisfy $\mathrm{Re}\, T_i \ll \mathrm{Re}\, T$ for $i = 2 \ldots h^{1,1}$ such that $\mathcal{V} \sim \gamma \left(T+\bar{T}\right)^{3/2}$, i.e., the $h^{1,1}-1$ blow-up Kähler moduli form the 'holes' of the 'swiss cheese'. This entails choosing the a_i for $i = 2 \ldots h^{1,1}$ of the nonperturbative superpotential effects on the associated 4-cycles such that $a_i \gg a \equiv a_1$ while enforcing $a_i t_i > 1$ to maintain the validity of the one-instanton approximation.

We will again determine the leading terms in $\hat{\xi}/\mathcal{V}$ as before. The scalar poten-

[2] For the two Kähler moduli of $\mathbb{CP}^4_{[1,1,1,6,9]}$ the Kähler uplifted de Sitter minimum was found numerically first in [123].

tial reads

$$V = e^K \Bigg(K^{T_I \bar{T}_J} \left[a_I a_J A_I A_J e^{-a(T_I+\bar{T}_J)} + (-a_I A_I e^{-aT_I} \overline{W K_{T_J}} + c.c) \right] + 3\hat{\xi} \frac{\hat{\xi}^2 + 7\hat{\xi}\mathcal{V} + \mathcal{V}^2}{(\mathcal{V}-\hat{\xi})(\hat{\xi}+2\mathcal{V})^2} |W|^2 \Bigg) \quad . \tag{6.11}$$

Guided by eq. (6.4), the leading terms in the scalar potential can be determined to be [21]

$$V = \frac{4W_0}{\mathcal{V}^2} \left(atAe^{-at}\cos(ac) + \sum_{i=2}^{h^{1,1}} a_i t_i A_i e^{-a_i t_i} \cos(a_i c_i) \right) + \frac{3\hat{\xi} W_0^2}{4\mathcal{V}^3} + \sum_{i=2}^{h^{1,1}} \frac{4}{3} \frac{a_i A_i^2}{\mathcal{V}^2} \frac{\sqrt{t_i}}{\gamma_i} e^{-2a_i t_i} \left[\frac{\mathcal{V}}{\sqrt{2}} + 3\gamma_i \sqrt{t_i}(a_i t_i + 1) \right] \quad . \tag{6.12}$$

Although the terms $\sim e^{-2a_i t_i}$ appear subleading, at the prospective minimum one can show that $e^{-at} \sim e^{-a_i t_i} \sim \hat{\xi}/\mathcal{V}$. This implies that the terms $\sim e^{-2a_i t_i}$ are in fact $\sim \hat{\xi}^2/\mathcal{V}^3$ (including the factor of $\mathcal{V}$ in the rectangular bracket) and are thus of relevant order for minimization.

This potential has a full minimum at $at \simeq a_i t_i \simeq 3$ for $i = 2 \ldots h^{1,1}$, and $c = c_i = 0$, implying

$$\mathcal{V} \simeq \gamma (2t)^{3/2} \simeq \gamma N^{3/2} \,, \tag{6.13}$$

if the quantity C defined in eq. (6.4) satisfies a structurally similar bound on C as in the one-parameter case discussed above. However, the numerical interval of C-values allowed by the metastability conditions increases slowly with $h^{1,1}$. The size of $C \sim |W_0|$ for given $\hat{\xi}$, intersection numbers, and gauge group ranks.

6.2 Inclusion of the dilaton and complex structure moduli

Turning on ISD 3-form fluxes generically leads to a supersymmetric stabilization of all complex structure moduli and the axio-dilaton at an isolated supersymmetric extremum in moduli space. Due to the no-scale structure eq. (5.12), the scalar potential of the complex structure moduli and the axio-dilaton eq. (5.13) is positive semi-definite. Hence, every flux-induced isolated supersymmetric extremum for the axio-dilaton and the complex structure moduli has a positive-definite mass matrix, and is a true local minimum. In both the LVS and the Kähler uplifting scenario, all no-scale breaking terms are suppressed by an extra inverse power $1/\mathcal{V}$ of the

volume compared to the flux-induced part above [21, 87]. As the flux-induced piece is positive semi-definite and $\mathcal{O}(1/\mathcal{V}^2)$, any negative term must come from no-scale breaking contributions which are $\mathcal{O}(1/\mathcal{V}^3)$. Hence, any small shift of τ or one of the U_a will see a positive $\mathcal{O}(1/\mathcal{V}^2)$ increase in the scalar potential overwhelming any possible decreasing $\mathcal{O}(1/\mathcal{V}^3)$ contribution from Kähler moduli stabilization as long as the overall volume is large.

Thus, *any* choice of flux producing an isolated SUSY extremum $D_\tau W = D_{U_a} W = 0$ will be a minimum of the full potential once the LVS or Kähler uplifting generate a local minimum for the Kähler moduli at large volumes. Hence, there is no need for a detailed model-by-model calculation of flux-induced mass matrix for the complex structure moduli and the axio-dilaton (a task practically unfeasible for typical values $h^{2,1} = \mathcal{O}(100)$).

After these general remarks, let us now explicitly include the dilaton τ and an arbitrary number $h^{2,1}$ of complex structure moduli U_a into our stabilization analysis. A commonly used example of a CY 3-fold with one Kähler modulus are smooth hypersurfaces in $\mathbb{CP}^4$, for instance the quintic $\mathbb{CP}^4_{11111}$. In this case, we generically have $\mathcal{O}(100)$ complex structure moduli so the Euler number of our CY 3-fold will be of the order

$$\chi = 2(h^{1,1} - h^{2,1}) \sim \mathcal{O}(-200) \ . \tag{6.14}$$

For a perturbative treatment, we demand the expansion parameter $\hat{\xi}/\mathcal{V} \lesssim 0.1$ to be small. For typical volumes in Kähler uplifting $\mathcal{V} \sim \mathcal{O}(10^2 - 10^3)$ we thus expect the leading α' correction to the Kähler potential to be $\hat{\xi} = \mathcal{O}(10)$. This needs the dilaton $\mathrm{Im}(\tau) = g_s^{-1}$ to be at weak coupling: $g_s \simeq \mathcal{O}(0.1)$ using eq. (5.27). Finding meta-stable minima of an effective scalar potential of $\mathcal{O}(100)$ complex scalar fields is, in general, a challenging and cumbersome task. A further difficulty enters by the fact that the explicit form of the Kähler potential eq. (5.26) and the superpotential eq. (5.19) of the complex structure sector

$$\begin{aligned} K_{\mathrm{k}} &= -2\log\left(\gamma(T+\bar{T})^{3/2} + \frac{\hat{\xi}(\tau,\bar{\tau})}{2}\right) \ , \\ W &= C_1(U_a) + i\, C_2(U_a)\cdot\tau + A e^{-aT} \ , \end{aligned} \tag{6.15}$$

with C_1 and C_2 depending on the 3-form fluxes and the U_a given in eq. (5.21), are only known explicitly for some special CY 3-folds [124]. We assume A to be constant, neglecting its dependence on the complex structure sector. Note that A is always paired with an exponential term e^{-aT} in the superpotential and, hence, also in the scalar potential which suppresses its influence on moduli stabilization

for large t. However, since in general the function $A(\tau, U_a)$ is not known, we cannot go beyond this qualitative argument in a model-independent way. This leaves us with a possible caveat: a very steep functional dependence of $A(\tau, U_a)$ might derail our perturbative treatment of complex structure moduli stabilization in certain examples.

We can split the full scalar potential into four parts

$$V = V^{(T)} + V^{(T,\tau)} + V^{(\tau)} + V^{(U)}, \quad \text{with} \quad V^{(T,\tau)} = e^K \left(K^{T\bar{\tau}} D_T W \overline{D_\tau W} + c.c\right),$$
$$V^{(\tau)} = e^K \left(K^{\tau\bar{\tau}} |D_\tau W|^2\right), \qquad V^{(U)} = e^K K^{U_a \bar{U}_b} D_{U_a} W \overline{D_{U_b} W}. \tag{6.16}$$

where $V^{(T)}$ contains the F-terms of T and the $-3|W|^2$ term given in eq. (6.1) and $V^{(\tau)}$ and $V^{(U)}$ are the F-terms of τ and the U_a, respectively and $V^{(T,\tau)}$ mixes the F-terms of T and τ. The latter are non-zero since $K_{\rm k}$ induces non-zero $K_{T\bar{\tau}}$.

We expect a meta-stable minimum of the effective scalar potential which includes the dilaton and complex structure moduli to have the following properties: 1) The complex structure moduli should be stabilized approximately in a supersymmetric minimum like the dilaton since they enter the scalar potential similarly. 2) They are even further decoupled from the SUSY breaking Kähler modulus since there is no mixing term in the Kähler potential for the complex structure moduli. We show in Appendix A.1 that the deviation is, in general, a 1-st order effect and hence the fields are stabilized supersymmetrically to 0-th order.

6.2.1 Mass scales & SUSY breaking

Let us neglect the complex structure moduli U_a in this subsection for simplicity, qualitatively the mass scales and SUSY breaking of these moduli are represented by that of the dilaton which we include in the analysis. To 1-st order in $\hat{\xi}/\mathcal{V}$ or $A\, e^{-at}/|W_0|$ the first three terms in eq. (6.16) can be found in Section 3.1 of [21].[3] The 0-th order potential for the field s is $\sim (C_1 + C_2 s)^2$ if we neglect terms that are suppressed either by ξ or e^{-at} relative to the quadratic potential. Hence, the supersymmetric locus is

$$s_0 = -\frac{C_1}{C_2} > 0 \quad \Rightarrow \quad C_1 C_2 < 0. \tag{6.17}$$

The shift of s to this supersymmetric minimum due to the 1-st order terms $V^{(T)}$ and $V^{(T,\tau)}$ will be discussed in Section 6.2.2 to first order. The extremum of t to

[3] For a numerical example that compares the approximated and full expression for the potential V, see Section 3.4 of [21].

1-st order is governed by $V^{(T)}$ only since $V^{(T,\tau)} \propto D_\tau W$ and $D_\tau W$ equals zero to 0-th order so that $V^{(T,\tau)}$ is actually a 2-nd order term. Finally, the axion field derivatives V_c and V_σ can be minimized for $c = n\pi/a$ for $n \in \mathbb{Z}$ and $\sigma = 0$. As in Section 6.1, we restrict to $c = 0$.

Using the approximate scalar potential $V(t, s, \tau, \sigma)$ of eq. (6.16) we can calculate the mass matrix of the moduli as the second derivative with respect to the real fields. The masses of the canonically normalized scalar fields are $m_t^2, m_c^2 \sim \hat{\xi}/\mathcal{V}^3$ and $m_s^2, m_\sigma^2 \sim 1/\mathcal{V}^2$.[4] In this approximation, the fields s and σ have the same mass which expresses that they are in the same chiral multiplet and supersymmetry is unbroken in the τ direction to 0-th order.

The hierarchy between the masses of the t- and s-modulus is given parametrically as $m_t^2/m_s^2 \sim \hat{\xi}/\mathcal{V}$. As we will see now, this implies that supersymmetry is predominantly broken in the T direction, i.e., $F_T \gg F_\tau$ where

$$F_i = e^{K/2} D_i W \ . \tag{6.18}$$

The direction F_T has a non-vanishing 0-th order contribution [21]

$$F_T \simeq -\frac{3C_1}{\sqrt{-2C_1/C_2}\, t\mathcal{V}} \ . \tag{6.19}$$

As expected, the first non-vanishing contribution to F_τ is 1-st order [21]:

$$F_\tau \simeq -\frac{9C_1\hat{\xi}}{10\sqrt{2}\,\mathcal{V}^2\,(-C_1/C_2)^{3/2}} \simeq -F_T \cdot \frac{3\,t\,C_2}{10C_1} \cdot \frac{\hat{\xi}}{\mathcal{V}} \tag{6.20}$$

so supersymmetry is predominantly broken in the T direction which is what one would expect since t is stabilized in a minimum with spontaneously broken supersymmetry.

The gravitino mass can be approximated to 0-th order to

$$m_{3/2}^2 = e^K |W|^2 \simeq -\frac{2\,C_1 C_2}{\mathcal{V}^2} = -\frac{C_1 C_2}{4\gamma^2 t^3} \sim 10^{-4} \ldots 10^{-3} \,, \tag{6.21}$$

in units of $M_{\rm P}^2$ which is of order $\sim M_{\rm GUT}^2$ for typical volumes.

We note that $m_{3/2} < m_s \,, m_\sigma$ which renders the supersymmetric starting point for them a self-consistent approximation. Moreover, the KK scale here is given for a single volume modulus (i.e., no anisotropies are possible) and the volume given in units of α' as $\mathcal{V} = L^6$ as

$$m_{KK} = \frac{1}{L\sqrt{\alpha'}} \sim \frac{1}{\mathcal{V}^{2/3}} \,, \tag{6.22}$$

[4] A detailed calculation of the masses including canonical normalization and diagonalization of the inverse Kähler metric can be found in Section 3.2 of [21].

in units of M_P^2 while the gravitino mass as well as the moduli masses scale at least $\sim 1/\mathcal{V}$. Here we have used the relation between 10D string frame and 4D Einstein frame

$$\frac{1}{\alpha'} = \frac{(2\pi)^7}{2} M_P^2 \frac{g_s^2}{\mathcal{V}} \quad . \tag{6.23}$$

Therefore, the use of a 4D effective supergravity description is justified, although the separation

$$\frac{m_{3/2}}{m_{KK}} \sim \frac{1}{\mathcal{V}^{1/3}} , \tag{6.24}$$

will typically be only of $\mathcal{O}(0.1)$ here. Nevertheless, there is a parametric hierarchy between the moduli mass scale, the SUSY and the KK-scale in the limit of large volume $\mathcal{V} \to \infty$. This suppresses potential mixing between the moduli masses and KK masses alleviating their danger of causing additional tachyonic directions.

6.2.2 F-term induced moduli shifts

The 1-st order terms of the scalar potential include terms that are proportional to either e^{-at} or $\hat{\xi}$ so we write it as a perturbance $\delta V^{(1)} = V^{(T)} + V^{(T,\tau)}$ of the 0-th order scalar potential $V^{(0)} = V^{(\tau)} + V^{(U)}$. Expanding this to first non-vanishing order in $\vec{\theta} = (s, u_a)$ around the supersymmetric minimum $\vec{\theta}_0 = (s_0, u_{0a})$ gives [5]

$$V = V^{(0)} + \frac{1}{2} \underbrace{(\vec{\theta} - \vec{\theta}_0)}_{\delta\vec{\theta}} V^{(0)}_{\vec{\theta}_0 \vec{\theta}_0} (\vec{\theta} - \vec{\theta}_0) + \delta V^{(1)} + \delta V^{(1)}_{\vec{\theta}_0} (\vec{\theta} - \vec{\theta}_0) + \dots \ , \tag{6.25}$$

where subscript $\vec{\theta}_0$ denotes differentiating with respect to $\vec{\theta}$, evaluated at $\vec{\theta}_0$. Notice that we again only expand around the real parts of the moduli fields since the supersymmetric minimum for all axionic VEVs equal to zero is an exact minimum of the scalar potential. Demanding that $\delta\vec{\theta}$ still is a minimum of V, we get an expression for $\delta\vec{\theta}$ in terms of 0-th order terms:

$$V_{\delta\vec{\theta}} = 0 \quad \Leftrightarrow \quad \delta\vec{\theta} = -\left(V^{(0)}_{\vec{\theta}_0 \vec{\theta}_0}\right)^{-1} \cdot \delta V^{(1)}_{\vec{\theta}_0} \ . \tag{6.26}$$

First, let us note that the matrix $V^{(0)}_{\vec{\theta}_0 \vec{\theta}_0}$ has to be positive definite. It is not sufficient to demand the weaker condition of Breitenlohner-Freedman vacuum stability [116] since we are spontaneously breaking supersymmetry in the T direction to obtain a de Sitter vacuum. Hence, the feature of AdS space that keeps a tachyon

[5] For a general supergravity analysis of the influence of supersymmetrically stabilized heavy moduli on the stabilization of lighter moduli see [125, 126], where the $\mathcal{O}(\xi/\mathcal{V})$ shifts of the heavy moduli were also found.

from exponentially rolling down a negative definite $V^{(0)}_{\vec{\theta}_0\vec{\theta}_0}$ is absent in our case. As is shown in Appendix A.1,

$$\delta\vec{\theta}_i \sim \frac{\hat{\xi}}{\mathcal{V}}\,. \tag{6.27}$$

Furthermore, it is also demonstrated that $\delta\vec{\theta}_i$ does not depend on positive powers of $h^{2,1}$, such that a large number of complex structure moduli cannot increase the induced shifts. We supplemented this line of thinking by an explicit example based on T^6 in Section 5 of [21]: the dependence is harmless as there we find $\delta s \sim const.$, and $\delta\vec{u} \sim 1/h^{2,1}$.

As 1-st order terms in the scalar potential induce a 1-st order shift $\delta\vec{\theta}$ on $\vec{\theta}$, 2-nd order terms induce a 1-st order shift δt of the Kähler modulus. This calculation is summarized in Appendix A.2. δt could potentially induce a shift in m_t^2, especially for large $h^{2,1}$. This has to be checked case by case for a specific model as we cannot make a general statement regarding the $h^{2,1}$ dependence of this mass shift. However, for the torus example based on T^6 in Section 5 of [21], we find that the shift is always in a region where it does not induce any tachyonic directions for the t-modulus.

At this point, we have succeeded now in determining the combined scalar potential of the volume modulus T,the dilaton τ, and an arbitrary number $h^{2,1}$ of complex structure moduli U_a in a fully analytical form to first order in a perturbation expansion around the supersymmetric locus for the τ, U_a. The resulting full minimum is a tunable de Sitter minimum of the same form and type as found in the previous section for T, and it is perturbatively stable under the inclusion of the dynamics of the dilaton τ and all U_a (with certain caveats, as there may be non-generic dependence on $h^{2,1}$ in the coefficients of the perturbation expansion).

Chapter 7

Explicit stabilization of the Kähler moduli

As we have seen in the previous section eq. (6.13), the volume of a Kähler uplifted de Sitter vacuum on a swiss-cheese manifold scales as $\mathcal{V} \sim N^{3/2}$, where N is the Coxeter number of the gauge group realized by the stack of D7-branes on the large divisor.[1] Thus, we will address the question of large gauge group ranks in IIB compactifications in Section 7.1 since they induce a large volume. There is a number of consistency constraints that have to be fulfilled in order to construct a globally consistent D7-brane configuration that can realize a Kähler uplifted de Sitter vacuum. These constraints are addressed in general in Section 7.1 and summarized for the explicit example of the manifold $\mathbb{CP}^4_{11169}[18]$ in Section 7.2.[2] In Section 7.3, we present the effective stabilization of the Kähler moduli in a de Sitter vacuum.

7.1 Constraints on large gauge group rank in the landscape

In this section, we discuss generic constraints on obtaining large gauge group gaugino condensation which is a crucial input for the method of Kähler uplifting. In the context of non-compact CYs, it was already discussed in [106] that arbitrarily high gauge group ranks are possible. As we will see, the situation in the compact case is more restrictive. We will mostly discuss the perturbative type IIB picture. However, an equivalent treatment in F-theory is possible.

[1] For another possibility to realize the Kähler uplifting scenario with large $\mathcal{V}$ see [127].

[2] An equivalent discussion in the F-theory picture can be found in C.2.

Our laboratory will be the landscape of complex three-dimensional CY manifolds that are hypersurfaces in toric varieties. These were classified in [128] by constructing all 473,800,776 reflexive polyhedra that exist in four dimensions, yielding 30,108 distinct Hodge numbers of the corresponding CY manifolds X_3. For simplicity we will study a subset of these, i.e., the set of 184,026 maximal polytopes yielding 10,237 distinct Hodge numbers. These can be represented by a weight system of positive integers $n_1, ..., n_5$. One of the projective coordinates $\{u_1, ..., u_4, \xi\}$ of a four-dimensional toric space can be associated to each integer n_i:

$$\begin{array}{ccccc} u_1 & u_2 & u_3 & u_4 & \xi \\ \hline n_1 & n_2 & n_3 & n_4 & n_5 \end{array} \qquad \text{with} \qquad 0 < n_1 \leq n_2 \leq n_3 \leq n_4 \leq n_5 \ . \tag{7.1}$$

The integers n_i determine the scaling equivalence relation the coordinates satisfy:

$$(u_1, ..., u_4, \xi) \sim (\lambda^{n_1} u_1, ..., \lambda^{n_4} u_4, \lambda^{n_5} \xi) \, , \qquad \text{with} \quad \lambda \in \mathbb{C}^* \, . \tag{7.2}$$

The divisors $D_i : \{u_i = 0\}$ and $D_\xi : \{\xi = 0\}$ are called toric divisors. A hypersurface in such toric space is a CY (i.e., its first Chern class vanishes) if the degree of the defining equation is equal to $\sum_i^5 n_i$.

Eq. (7.2) defines the complex four-dimensional projective space $\mathbb{CP}^4_{n_1 n_2 n_3 n_4 n_5}$. If one of the weights n_i is greater than one, the ambient space is not smooth. This is the case for any toric CY that is not the quintic, which is given by $n_i = 1$, $\sum_i^5 n_i = 5$. The corresponding singularities have to be resolved if they intersect the CY hypersurface. The resolution process yields additional weights, i.e., eq. (7.1) becomes a $k \times (k + 5)$ matrix, called the weight matrix, that defines the resolved toric ambient space X_4^{amb}. Generically, the greater the n_i in eq. (7.1), the more lines of weights have to be added to obtain a smooth CY. Often there is more than one choice to resolve the singularities, corresponding to different triangulations of the corresponding polytope. The number of lines of the weight matrix k gives the dimension of $H^{1,1}(X_4^{\text{amb}}, \mathbb{Z})$. Since some divisors of X_4^{amb} might either intersect X_3 in two or more disconnected and independent divisors of X_3, or even not intersect X_3 at all, $\dim H^{1,1}(X_4^{\text{amb}}, \mathbb{Z})$ is not necessarily the same as $h^{1,1} = \dim\, H^{1,1}(X_3, \mathbb{Z})$. However, increasing k will generically also increases $h^{1,1}$.

To realize an $\mathcal{N} = 1$ supersymmetric compactification of type IIB in four dimensions and to consistently include D-branes and fluxes we introduce O7 orientifold planes in the construction. For simplicity, we only consider orientifold projections acting via the holomorphic involution

$$\sigma : \quad \xi \mapsto -\xi \, , \tag{7.3}$$

i.e., the sign of the coordinate with the highest weight is reversed. We demand

$$n_\xi \equiv n_5 = \sum_{i=1}^{4} n_i \,, \tag{7.4}$$

such that the CY hypersurface equation symmetric under (7.3) is given by

$$\xi^2 = P_{(2\sum_i^4 n_i, \dots)} \,. \tag{7.5}$$

The dots denote possible additional weights that have to be added to obtain a 3-fold free of singularities. Note that eq. (7.5) only holds if $n_\xi = \sum n_i$ also for the resolution weights which we assume is in many cases possible and which we have verified in various examples.

Hence, all information of the CY 3-fold is stored in the weights $n_1, \dots, n_4$ and the chosen triangulation. Moreover, the resolution of the three dimensional manifold $\mathbb{CP}^3_{n_1 n_2 n_3 n_4}$ is the base B_3 of the elliptically fibered 4-fold that realizes the uplift of the type IIB model to F-theory. For this reason, models fulfilling eq. (7.4), are named models of the 'F-theory type'. These are 97,036 weight systems leading to 7,602 distinct pairs of Hodge numbers. The first Chern class of B_3 defines a non-trivial line bundle, the anti-canonical bundle $\bar{K}$, with $\bar{K} = c_1(B_3)$ (we use the same symbol to denote the line bundle and its corresponding divisor class). Due to eq. (7.4) the homology class of the O7-plane at $\xi = 0$ is given as $[O7] = \bar{K}$.

Now, we discuss the inclusion of D7-branes from the IIB perspective. The presence of the O7-plane induces a negative D7-charge of $-8[O7]$. This has to be compensated by the positive charge of the D7-brane stacks $[D7]$. This tadpole condition can be formulated in terms of a polynomial equation on certain polynomials in the complex coordinates u_i of the resolved base manifold B_3 (for details see Appendix B.1). The D7-brane that is defined by these polynomials is called in the literature 'Whitney brane', as it has the singular shape of the so called Whitney umbrella [129]. It can split into stacks of $2N_i$ branes on a toric divisor $D_i : \{u_i = 0\}$ via a factorization of the polynomials in $u_i^{2N_i}$. This realizes an $Sp(N_i)$ gauge group. For the branes to be supersymmetric, the polynomials have to be holomorphic functions so N_i cannot be arbitrarily large. In Appendix B.1, we derive that a sufficient condition for holomorphicity is

$$N_i \leq 3\frac{n_\xi}{n_i} \,. \tag{7.6}$$

Due to the ordering of the n_i, eq. (7.1), we expect to be able to put the largest number of branes on the divisor D_1 and the constraining quantity is the largest integer N_{lg} that is smaller than $3n_\xi/n_1$. N_{lg} will serve as our large gauge group indicator in the following.[3] N_{lg} only serves as an easily computable estimate for

[3] For a detailed discussion of the meaningfulness of N_{lg}, see Section 2.2 of [22].

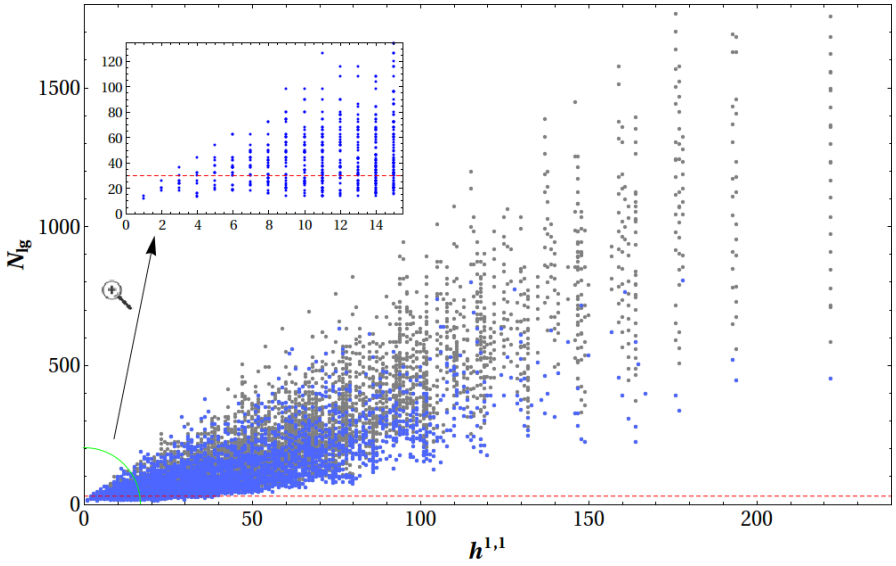

Figure 7.1: The large gauge group indicator N_{lg} as a function of $h^{1,1}$. The gray dots denote the general set of models, while the blue dots denote the conservative set (for explanations see text). The red dashed line denotes the critical gauge group rank for Kähler uplifting $N_{lg}^{\text{crit.}} = 30$.

the largest gauge group rank one can obtain in a 3-fold of the F-theory type. To see if one can stabilize the Kähler moduli in a large volume, one has to check the additional constraints case by case. We will do this in Section 7.2, constructing a consistent model of a Kähler uplifted de Sitter vacuum.

7.1.1 Maximal gauge group ranks

In this section, we give the results of our scan for the maximal gauge group indicator N_{lg} in the 97,036 models of the F-theory type contained in the classification of [128]. We use *PALP* to calculate the Hodge numbers resulting in 7,602 distinct pairs of Hodge numbers. We refer to this set of weight systems as the general set. We also gather all weight systems that lead to the same pair of Hodge numbers and choose as the representative the weight system with the smallest N_{lg} corresponding to the most conservative estimate for the maximal gauge group. This set of weight systems is referred to as the conservative set. We restrict our attention to manifolds with negative Euler number $\chi = 2(h^{1,1} - h^{2,1})$, further reducing the set of weight systems to 8,813 corresponding to 3,040 distinct pairs of $(h^{1,1}, h^{2,1})$. We do this since $\chi < 0$ is a necessary condition to apply the method of Kähler uplifting.

Our results are summarized in Figure 7.1. The maximal N_{lg} we obtain is 2,330 in the general set and 806 in the conservative set. The minimal N_{lg} is 12 in both

sets corresponding to the base $\mathbb{CP}^3_{1111}$. The mean $\bar{N}_{lg}$ we find is 204.5 in the general set and 132.8 in the conservative set. Generically, the critical value for Kähler uplifting to be in large volume regime ($\mathcal{V} \gtrsim 100$) is $N_{lg}^{\text{crit.}} = 30$. Since the actual volume also depends on the intersection numbers and the stabilized volumes of the divisors other than D_1, $N_{lg}^{\text{crit.}} = 30$ can only serve as an estimate for large volume. The subset of weight systems with $N_{lg} < N_{lg}^{\text{crit.}}$ is 444 in the general set and 267 in the conservative set, corresponding to only 5% respectively 9% of the models where the method of Kähler uplifting is not applicable.

Another important feature we notice is the dependence of N_{lg} on $h^{1,1}$. We see from Figure 7.1 that N_{lg} tends to increase with $h^{1,1}$. In other words, if one wants to have very large gauge groups one has to buy this by a rather high number of Kähler moduli which of course has the disadvantage of increasing the complexity of the model, especially if it is not swiss cheese.[4] The tendency of $N_{lg} \propto h^{1,1}$ can be explained from the weight system: As $n_\xi = \sum_i^4 n_i$ becomes large, a large number of lines has to be added to the weight matrix to make the 3-fold singularity free which generically increases the number of Kähler moduli.

We conclude this section with the remark that the possibility to engineer large enough gauge groups to obtain a large volume in the framework of Kähler uplifting is a generic feature of the landscape region we have analyzed.

7.2 The type IIB perspective of $\mathbb{CP}^4_{11169}[18]$

In this section, we present an explicit example of a brane and gauge flux setup on a 3-fold of the landscape region studied in Section 7.1. To keep the analysis tractable, we study a 3-fold with small $h^{1,1}$. Looking at Figure 7.1, we see that there is a model with $h^{1,1} = 2$ that has $N_{lg} = 27$, which is close to the critical value $N_{lg}^{\text{crit.}} = 30$. This is the CY 3-fold X_3 that is a degree 18 hypersurface in $\mathbb{CP}^4_{11169}$ (it is usually denoted as $\mathbb{CP}^4_{11169}[18]$). The corresponding weight system of the ambient toric space after resolving the singularities is

$$X_4^{\text{amb}}: \quad \begin{array}{cccccc|c} u_1 & u_2 & u_3 & u_4 & u_5 & \xi \\ \hline 1 & 1 & 1 & 6 & 0 & 9 \\ 0 & 0 & 0 & 1 & 1 & 2 \end{array} \quad . \tag{7.7}$$

The two lines determine the two scaling equivalence relations that the coordinates satisfy (see eq. (7.2)). We will see in Section 7.3 that on this manifold we can stabilize the two Kähler moduli to values corresponding to a volume $\mathcal{V} \simeq 52$.

[4] For an algorithm to check for the swiss cheese property of a 3-fold see [130].

Let us mention some geometric properties of X_3 that will be needed during the following analysis. The CY is a hypersurface in the ambient space (7.7), defined by the equation

$$\xi^2 = P_{18,4}(u_i) \equiv u_5\, Q_{18,3}\,, \tag{7.8}$$

where the factorization of the polynomial $P_{18,4}$ is enforced by its weights. The Hodge numbers of X_3 are $h^{1,1} = 2$ and $h^{2,1} = 272$. The (holomorphic) orientifold involution is given by $\xi \mapsto -\xi$. This involution has $h^{1,1}_- = 0$ and then the number of invariant Kähler moduli is $h^{1,1}_+ = h^{1,1} = 2$. Due to the factorization of eq. (7.8), there are two O7-planes $O7_{u_5}$ and $O7_Q$ at the fixed locus $\xi = 0$ that do not intersect. One can show that the divisor $O7_{u_5}$ is a rigid divisor in the 3-fold X_3. Its homology class in the ambient space is $D_\xi \cdot D_5 = [X_3] \cdot \frac{D_5}{2}$. We see that the class of this integral 4-cycle in the 3-fold is $D_5^{\text{fix}} = \frac{D_5}{2}$. So we can use it as an element of an integral basis.

Using the triple intersection numbers of $\mathbb{CP}^4_{11169}[18]$ in terms of D_1 and D_5^{fix}, we find an approximately swiss cheese volume of the 3-fold [22]

$$\mathcal{V} = \frac{1}{6}\int_X J\wedge J\wedge J = \sqrt{\frac{2}{3}}\left(\mathcal{V}_1 + \frac{1}{3}\mathcal{V}_5\right)^{3/2} - \frac{\sqrt{2}}{9}\mathcal{V}_5^{3/2}\,, \tag{7.9}$$

with $\mathcal{V}_i = \text{Re}(T_i)$ being the volumes of the respective divisors. D_5^{fix} is rigid and hence fulfills the sufficient condition to contribute to the gaugino condensation superpotential. D_1 is not rigid, but one can choose a proper gauge flux on the wrapped D7-branes, that fixes the $h^{2,0} = 2$ deformations as is discussed in Appendix B.2.2.

In constructing an explicit brane and gauge flux setup on X_3 we address the following issues that are crucial in constructing a global model [90, 131–134]:

- The choice of the orientifold involution determines the class of the O7-plane. D7-tadpole cancellation then implies $[D7] = -8[O7]$, fixing the degrees of the polynomial defining the D7-brane configuration. Requiring the presence of a D7-brane stack on D_1 with maximal gauge group rank N_{lg} might force the defining polynomial to factorize further, leading to the presence of another large rank stack (For details see Appendix B.2.1). Due to the swiss cheese structure of the volume form, this might destroy the large volume approximation and one has to check that this does not happens. As we discuss in Appendix B.2.1, we can realize an $Sp(24)$ gauge group on D_1 which enforces an $SO(24)$ gauge group on D_5^{fix}.

- To lift unwanted zero modes that might destroy gaugino condensation on some D7-brane stacks, one needs to 'rigidify' the wrapped non-rigid toric

divisors (in the present case D_1). To do this, the gauge flux $\mathcal{F}_{D_1}$ has to be properly adjusted. Furthermore, it breaks the $Sp(24)$ gauge group to $SU(24)$ and induces a D3-charge of $Q_{D3}^{\mathcal{F}_{D_1}} = 144$. (For details see Appendix B.2.2.)

- To avoid the introduction of additional zero modes, due to non-zero gauge flux (possibly forced by Freed-Witten anomaly cancellation [135, 136]) and D-terms for the Kähler moduli, one has to choose such a flux in a proper way. As we show in Appendix B.2.3, $\mathcal{F}_{D_1}$ can be chosen without any problematic consequences in our case even though for intersecting stacks this is generically not possible.

- One has to saturate the D3-tadpole cancellation condition. The compactification ingredients that induce a D3-charge are the (fluxed) D7-branes, the O7-planes, the D3-branes and the RR and NS field strengths F_3 and H_3. The total D3-brane charge that has to be canceled by the RR and NS fluxes, eq. (5.22), is

$$L = Q_{D3}^{\text{O7s}} + Q_{D3}^{\text{stacks}} + Q_{D3}^{W} = \begin{cases} -104 & \text{for } Q_{D3}^{W} = -81 \\ -96 & \text{for } Q_{D3}^{W} = -73\,, \end{cases} \tag{7.10}$$

  where Q_{D3}^{W} is the D3-brane charge of the Whitney brane. (For details see Appendix B.2.4.)

At this point, we have a fully consistent picture of the D-brane and gauge flux setup in our 3-fold X_3 that ensures that gaugino condensation from the divisors D_1 and D_5^{fix} contributes to the superpotential of the four dimensional $\mathcal{N} = 1$ effective supergravity.

7.3 Kähler uplifted de Sitter vacua of $\mathbb{CP}^4_{11169}[18]$

The two Kähler moduli T_1 and T_2 of $\mathbb{CP}^4_{11169}[18]$ can be stabilized in a de Sitter minimum by Kähler uplifting as we discuss in the following. The Kähler potential of T_1 and T_2 is given as

$$K = -2\log\left[\frac{1}{\sqrt{12}}\left((T_1+\bar{T}_1)+\frac{1}{3}(T_2+\bar{T}_2)\right)^{3/2} - \frac{1}{18}(T_2+\bar{T}_2)^{3/2} + \frac{1}{2}\hat{\xi}(\tau,\bar{\tau})\right], \tag{7.11}$$

with the leading order α' correction $\hat{\xi}$ given in eq. (5.27) with Euler number $\chi = 2(2-272) = -540$ and we have used eq. (7.9) for the volume of the CY. To apply the method of Kähler uplifting we need to balance the leading order α' correction

to the Kähler potential with non-perturbative contributions to the superpotential. These originate from gaugino condensation of an $SU(24)$ and $SO(24)$ pure super Yang Mills from respectively 24 D7-branes wrapping the divisors D_1 and $D_5^{\rm fix}$ corresponding to T_1 and T_2 respectively. The induced superpotential is

$$W = W_0 + A_1\, e^{-\frac{2\pi}{24}T_1} + A_2\, e^{-\frac{2\pi}{22}T_2}\,. \tag{7.12}$$

Our analysis in Section 7.2 has shown that $A_1, A_2 \neq 0$. The induced D3-tadpole by this gauge flux and the geometric contributions from the D7-branes is $L = 96$ or 104, see eq. (7.10). The one-loop determinants A_1 and A_2 depend on the complex structure moduli, the dilaton and also potentially D7-brane moduli. As we have discussed above, the explicit dependence on these moduli is unknown, however for the purpose of Kähler moduli stabilization the values of A_1 and A_2 can be assumed be constant since complex structure moduli are stabilized at a higher scale. Since there is a large number of flux parameters due to $h^{2,1} = 272$, it seems a reasonable assumption that one should be able to use the freedom in this sector to mildly tune A_1 and A_2 to a value desired for the stabilization of the Kähler moduli.

Choosing $A_1 = A_2 = 1$, it was found numerically in [22], that the pairs of W_0 and s that are suitable to realize a de Sitter vacuum with small positive tree level vacuum energy [5] lie on the curve

$$W_0^{\rm dS}(s) = 70.2\, s^{-2.35} \qquad \text{with} \qquad s \geq 4\,. \tag{7.13}$$

Actually, it is a band rather than a curve, the lower bound of the band corresponding to Minkowski vacua and the upper bound corresponding to the minimum becoming an inflection point. For a single Kähler modulus this corresponds to the upper and lower bound in eq. (6.9), respectively. Since the width of the band is rather small and we are interested in vacua with a small cosmological constant, we choose to display the lower bound in eq. (7.13).

The volume of the divisors at theses de Sitter vacua can be numerically determined as $\langle T_1 \rangle \simeq 10.76$ and $\langle T_2 \rangle \simeq 12.15$ which implies $\mathcal{V} \simeq 52$ in units of α'. The not too large overall volume emerges from the fact that we have only realized an $N_1 = 24$ gauge group on D_1 which is actually lower than the critical gauge group rank ~ 30. Note that we were forced to choose the rank smaller than the maximal rank $N_{lg} = 27$ in order to consistently incorporate the subtleties in the D7-brane configuration and construct a fully consistent model, see Appendix B.2.1. Since models with a larger number of Kähler moduli allow in principle larger maxi-

[5] In this case, small refers to how small we can tune $\langle V \rangle$ by choosing numerical values for W_0 and s to a certain decimal place and is not related to the tuning of the cosmological constant.

mal gauge group rank, one may also realize larger overall volumes in these more complicated cases.

Chapter 8

Constructing explicit flux vacua

In this chapter, we study the flux vacua of a particular CY: The degree 18 hypersurface in a 4 complex dimensional projective space $X_3 \equiv \mathbb{CP}^4_{11169}[18]$ in the large complex structure limit [25].[1] This manifold is the standard working example of both the LVS and the Kähler uplifting scenario and its geometric properties have been worked out in great detail in [137]. We switch on flux along six 3-cycles that correspond to two complex structure moduli that are invariant under a certain discrete symmetry that can be used to construct the mirror manifold [138]. For this purpose we review a known argument that a supersymmetric vacuum in these two complex structure moduli corresponds to a supersymmetric vacuum of *all* 272 complex structure moduli [139, 140].

For an explicit construction of the flux vacua, we use the fact that the prepotential $\mathcal{G}$ of the two complex structure moduli space has been worked out in [137] in the large complex structure limit. We apply two computational methods to find flux vacua on this manifold:

- *The polynomial homotopy continuation method* [141] allows us to find *all* stationary points of the polynomial equations that characterize the supersymmetric vacuum solutions. The fluxes $f_i \in \mathbb{Z}$ appear as parameters in these equations and are restricted by the D3-tadpole L which depends on the chosen brane and gauge flux configuration imposed on the manifold. Since the restriction is of the form $\sum f_i^2 \leq L$, this method allows us to explicitly construct, for the first time, *all flux vacua* in the large complex structure limit that are consistent with a given D3-tadpole L. This is done by applying the polynomial homotopy continuation method at each point in flux parameter space. This method has the attractive feature of being highly

[1] For an analogous study of the manifold $\mathbb{CP}^4_{11111}[5]$ see [26].

parallelizable.

- *The minimal flux method* [140] finds flux parameters that are consistent with a given D3-tadpole L for a given set of vacuum expectation values (VEVs) of the complex structure moduli. Hence it is in a sense complementary to the polynomial homotopy continuation method where the role of parameters and solutions is exchanged with respect to this method. However, it is not possible to find all flux vacua for a given tadpole L with this method.

Our results are complementary to statistical analysis by [23, 24].[2] The uniform distribution of physical quantities such as the gravitino mass and the vacuum energy density in the landscape have recently been questioned both in general [145–147] and in the context of Kähler uplifting [148–150]. Hence, our results present an important check of the general results found in [23, 24] on a very realistic example, X_3. This is especially true since we are able to construct the complete solution space of flux vacua for a given tadpole L.

In Section 8.1, we review the reduction of the full moduli space of the 272 complex structure moduli to two complex structure moduli. The scans for flux vacua with the polynomial homotopy continuation method and the minimal flux method are presented in Section 8.2 and Section 8.3, respectively.

8.1 Effective reduction of the moduli space

As we discuss in Appendix D in greater detail, the 272 dimensional complex structure moduli space of $\mathbb{CP}^4_{11169}[18]$ can be reduced to a two dimensional moduli space by making use of a global symmetry. Also, we show that it is possible to achieve $D_a W = 0$ for *all* 272 complex structure moduli, and hence find a minimum of the positive definite tree-level no-scale scalar potential eq. (5.13). This is possible if flux is only switched on for the cycles that transform trivially under the above mentioned global symmetry, i.e.,

$$f = (f_{1_1}, f_{1_2}, f_{1_3}, f_{2_1}, f_{2_2}, f_{2_3}, 0, ..., 0) \quad \text{and} \quad h = (h_{1_1}, h_{1_2}, h_{1_3}, h_{2_1}, h_{2_2}, h_{2_3}, 0, ..., 0)\,. \tag{8.1}$$

Effectively, one is left with the task of solving the equations

$$D_I W = 0 \qquad \text{for} \quad I = \tau, U_1, U_2\,. \tag{8.2}$$

[2] For explicitly constructed vacua on two different two parameter models in the vicinity of the Landau-Ginzburg respectively conifold point see [142]. For a study of flux vacua of X_3 in the context of accidental inflation [143] see [144].

In [137], the prepotential $\mathcal{G}$ for the two complex structure moduli $U_1 = \omega_1/\omega_0$ and $U_2 = \omega_2/\omega_0$ was derived via mirror symmetry in the large complex structure limit to be

$$\mathcal{G}(\omega_0,\omega_1,\omega_2) = \xi\omega_0^2 + \frac{17\omega_0\omega_1}{4} + \frac{3\omega_0\omega_2}{2} + \frac{9\omega_1^2}{4} + \frac{3\omega_1\omega_2}{2} - \frac{9\omega_1^3 + 9\omega_1^2\omega_2 + 3\omega_1\omega_2^2}{6\omega_0}\,, \tag{8.3}$$

with $\xi = \frac{\zeta(3)\chi}{2(2\pi\,i)^3} \simeq -1.30843\,i$ determined by the Euler number χ of the CY.

Eq. (8.3) receives instanton corrections which are given as

$$\mathcal{G}_{\text{inst.}}(q_1,q_2) = \frac{1}{(2\pi\,i)^3}\left(540q_1 + \frac{1215q_1^2}{2} + 560q_1^3 + 3q_2 - 1080q_1q_2 + 143370q_1^2q_2 - \frac{45q_2^2}{2} + 2700q_1q_2^2 + \frac{244q_2^3}{9} + \dots\right)\,, \tag{8.4}$$

with $q_a = \exp(2\pi\,i\,U_a)$ and we have set $\omega_0 = 1$. The dots in eq. (8.4) denote higher powers in the q_a which are suppressed in the large complex structure limit $u_a = \text{Im}(U_a) \gtrsim 1$. We define the large complex structure limit via

$$\frac{|\mathcal{G}_{\text{inst.}}|}{|\mathcal{G}|} \leq \epsilon_{LCS}\,, \qquad \frac{540e^{-2\pi u_1}}{(2\pi)^3|\mathcal{G}|} \leq \epsilon_{LCS} \qquad \text{and} \qquad \frac{3e^{-2\pi u_2}}{(2\pi)^3|\mathcal{G}|} \leq \epsilon_{LCS}\,, \tag{8.5}$$

for small ϵ_{LCS}. The two last condition in eq. (8.5) are imposed to ensure that there are no cancellations between the terms in $\mathcal{G}_{\text{inst.}}$, i.e., the leading correction in $e^{-2\pi u_a}$ is actually small.

8.2 The polynomial homotopy continuation method

We want to solve the non-linear eqs. (8.2) derived from the prepotential eq. (8.3) for the 6 real variables $x_i = u_1, u_2, s, \nu_1, \nu_2$ and σ. The parameters of these equations are the 12 fluxes f_1, f_2, h_1 and h_2 in eq. (8.1). Though systems of non-linear equations are extremely difficult to solve in general, if the non-linearity in the system is polynomial-like, then the recently developed algebraic geometry methods can rescue the situation. In particular, we use the so-called numerical polynomial homotopy continuation (NPHC) method [141] which finds all the solutions of the given system of polynomial equations. This method has been used in various problems in particle theory and statistical mechanics in [151–161].

8.2.1 The algorithm

Let us briefly explain the NPHC method.[3] For a system of polynomial equations $P(x) = (p_1(x), \ldots, p_m(x))^T = 0$ with $x = (x_1, \ldots, x_m)^T$ there is a maximal number of isolated solutions in $\mathbb{C}^m$ for generic values of the coefficients which is $\prod_{i=1}^m d_i$, where d_i is the degree of the ith polynomial. This is the *classical Bézout bound* (CBB) [141, 162].

To find solutions to $P(x) = 0$ one can take advantage of the CBB. Now, a so called homotopy can be constructed

$$H(x,t) = \gamma(1-t)Q(x) + t\,P(x)\,, \tag{8.6}$$

where γ is a generic complex number, $t \in [0,1)$ and $Q(x) = (q_1(x), \ldots, q_m(x))^T$ is another system of polynomial equations. Note that $H(x,0) = \gamma Q(x)$ and $H(x,1) = P(x)$, such that we can track each solution of $Q(x) = 0$ from $t = 0$ to $t = 1$, finding *all* solutions to $P(x) = 0$ if the following 2 conditions are fulfilled: 1) the solution set of $H(x,t) = 0$ for $0 \leq t \leq 1$ consists of a finite number of smooth paths, called homotopy paths, each parameterized by $t \in [0,1)$, and 2) every isolated solution of $H(x,1) = P(x) = 0$ can be reached by some path originating at a solution of $H(x,0) = Q(x) = 0$. It is then convenient to choose a system $Q(x)$ where the solution space is easily obtained, e.g.,

$$Q(x) = \left(x_1^{d_1} - 1, \ldots, x_m^{d_m} - 1\right)\,, \tag{8.7}$$

where d_i is the degree of the i^{th} polynomial of the original system $P(x) = 0$. The CBB of $Q(x)$ and $P(x)$ are equal. Hence, the task of finding solutions of $P(x) = 0$ is transfered to efficiently track all paths from the easily obtained $Q(x) = 0$ solution. A strong advantage of the NPHC lies in the fact that the path tracking is highly parallelizable.

For solving eq. (8.2) we use a method known as Cheater's homotopy [26, 163, 164] which is based on the NPHC but does not use the CBB, since this bound often overestimates the actual number of solutions to $P(x) = 0$. We want to solve a parametric system, $\vec{f}(\vec{q};\vec{x}) = \vec{0}$ where $\vec{x}$ are variables and $\vec{q}$ are parameters (in our case the fluxes). Cheater's homotopy first solves the system at a generic parameter point and uses those solutions as the starting point for the systems at all other parameter-points. It makes use of the fact that the maximum number of complex solutions at any parameter point is the number of solutions at a generic parametric point, as has been shown in [163, 164].

[3] For a more detailed explanation of the NPHC method see Section 3.1 of [25] and Section 3 of [26].

8.2.2 The scan

We define a set of flux parameters on which we apply the algorithm described in the previous Section 8.2.1. Since we are only interested in supersymmetric flux vacua, we can make use of the ISD condition eq. (5.24) and define a flux configuration via

$$H_3 = \begin{pmatrix} h_1 \\ h_2 \end{pmatrix} \qquad \text{and} \qquad F_3 = \begin{pmatrix} -h_2 \\ h_1 \end{pmatrix}, \tag{8.8}$$

with $h_1, h_2 \in \mathbb{Z}^3$. Note that since we have two complex structure moduli, we have initially $2 \cdot 2 + 2 = 6$ flux parameters for both H_3 and F_3 but the ISD condition eq. (5.24) reduces this to the six parameters given in eq. (8.8). Furthermore, the D3-tadpole eq. (5.22) becomes manifestly positive semi-definite, i.e.,

$$L = h_1^2 + h_2^2 \,. \tag{8.9}$$

To scan efficiently, we apply the paramotopy algorithm to only $SL(2,\mathbb{Z})$ inequivalent flux configurations. In Section 3.2 of [25] it is derived that these are given as

$$\begin{pmatrix} h_1 \\ h_2 \end{pmatrix} \cong \begin{pmatrix} -h_1 \\ -h_2 \end{pmatrix} \cong \begin{pmatrix} -h_2 \\ h_1 \end{pmatrix} \cong \begin{pmatrix} h_2 \\ -h_1 \end{pmatrix} . \tag{8.10}$$

where the 3-rd and 4-th flux vector in eq. (8.10) are related to the 1-st by a transformation $\tau' = -1/\tau$, while the 2-nd is related to the the 1-st via $\tau' = \tau$. The number of $SL(2,\mathbb{Z})$ inequivalent flux configurations in a spherical region defined by a spherical constraint eq. (8.9) can be estimated as $\pi^3/(4\,\Gamma[4])(\sqrt{L})^6$, using the formula for the volume of the n-sphere $V_n(r) = \pi^{n/2}/\Gamma(n/2+1)\,r^n$. The factor $1/4$ accounts for the 4 equivalent configurations in eq. (8.10). If more flux configurations are switched on, $n > 6$, the number of lattice points grows very rapidly $\sim L^{n/2}$.

For our scan, we choose $L = 35$ such that we scan over 52,329 parameter points (the above estimate yields 55,391). On the *FermiLab cluster* using 100 nodes each with 32 cores (each core with 2.0 GHz cloak speed), the calculation time in total is around $75,000$ hours, with $60 - 100$ minutes per parameter point.

8.2.3 Distribution of parameters

In this section, we want to discuss the distribution of the following parameters as results of the scan defined in the previous Section 8.2.2:

- u_1 and u_2, to see how many points reach the large complex structure limit as defined in eq. (8.5).

- τ, to identify regions of weak and strong coupling.
- The number of solutions for a given D3-tadpole L.
- W_0, the flux superpotential.
- The masses of the moduli m^2 and the gravitino mass $m_{3/2}^2$.
- The available fine-tuning $\Delta\Lambda$ of the cosmological constant Λ.
- The amount of flux vacua for which a de Sitter vacuum can be constructed via Kähler uplifting in 8.2.4.

For the 52,329 parameter points, we find a total of 531,370 solutions to the eqs. (8.2). This corresponds to an average of 10.2 solutions per parameter point. For 1,360 parameter points, we do not find any solutions. Many of the solutions are unphysical and hence have to be sorted out: 288,160 fulfill the criterion of a physical string coupling $g_s > 0$, and 26,297 and 16,235 are in accordance with the large complex structure criterion eq. (8.5) for $\epsilon_{LCS} = 10^{-1}$ and $\epsilon_{LCS} = 10^{-2}$, respectively. Due to the strong suppression of the large complex structure limit in the general solution space of eq. (8.2), the minimal flux method has the advantage of directly searching for solutions in this region.

For the distribution of the dilaton, we can use $SL(2,\mathbb{Z})$, to transform each solution to the fundamental domain

$$-\frac{1}{2} \leq \mathrm{Re}(\tau) \leq \frac{1}{2} \qquad \text{and} \qquad |\tau| > 1\,, \tag{8.11}$$

via the successive transformations

$$\tau' = \tau + b\,, \quad G_3' = G_3\,, \tag{8.12}$$

i.e., $a = 1$, $b \in \mathbb{Z}$, $c = 0$, $d = 1$ and

$$\tau' = -1/\tau\,, \quad G_3' = G_3/\tau\,, \tag{8.13}$$

i.e., $a = 0$, $b = -1$, $c = 1$, $d = 0$.
We show the distribution of the obtained values for $\tau = \sigma + i\,s$ in Figure 8.1. We see that the the strongly coupled region $s = 1/g_s \sim 1$ is preferred and large values of $s > 10$ are obtained for a fraction of 5%.

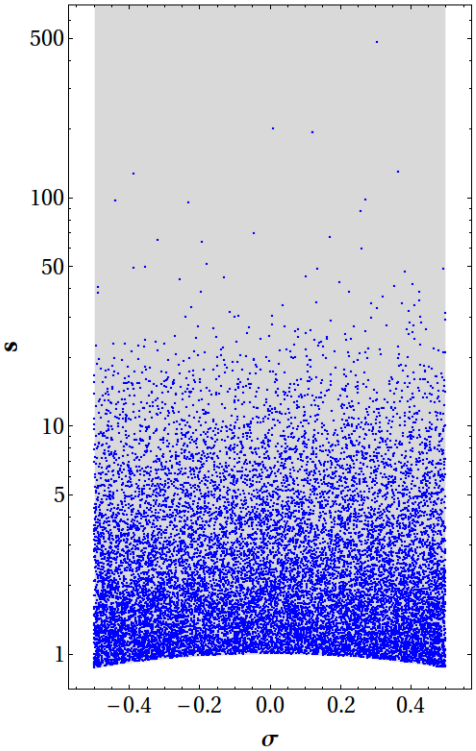

Figure 8.1: Distribution of τ for the paramotopy scan with $\epsilon_{LCS} = 10^{-2}$.

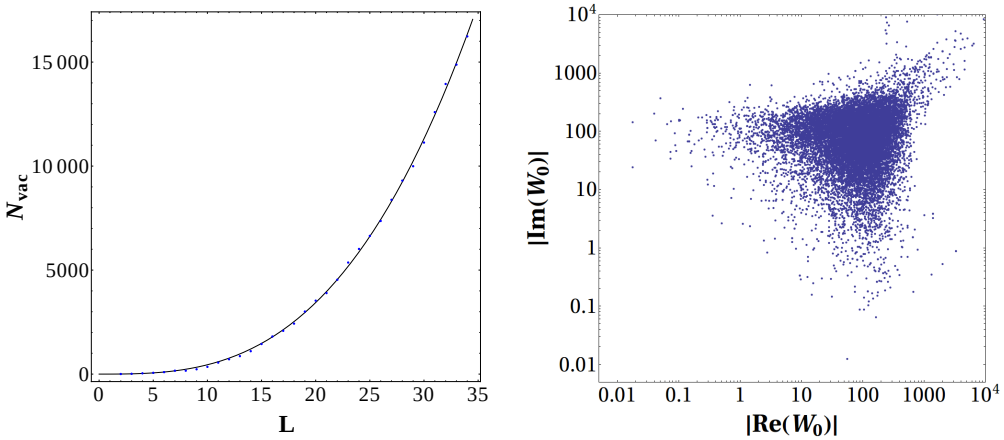

Figure 8.2: The number of vacua N_{vac} with $h^2 < L$ (left) and the logarithmic distribution of the flux superpotential W_0 (right) in the large complex structure limit with $\epsilon_{LCS} = 10^{-2}$.

The number of vacua of X_3 in the large complex structure limit for a given D3-tadpole L was estimated in [140] as [4]

$$N_{vac} = \frac{(2\pi L)^3}{3!} \int \det(-\mathcal{R} - \mathbf{1} \cdot \omega) \,, \tag{8.14}$$

with Kähler form ω and the curvature 2-form $\mathcal{R}$ of the moduli space. The integral in eq. (8.14) was estimated in [140] to be be 1/1296, using the Γ symmetry of the moduli space such that

$$N_{vac} \simeq 0.03\, L^3 \,. \tag{8.15}$$

Since paramotopy allows us to find all solutions for a given flux configuration we can check not only the L dependence of eq. (8.14), but also the normalization. This depends on the value chosen for ϵ_{LCS}, i.e., a greater ϵ_{LCS} will yield a larger normalization factor. Fitting the number of solutions with $h^2 \leq L$ in the large complex structure limit to the tadpole L we find

$$N_{vac} \simeq (0.50 \pm 0.04)\, L^{2.94 \pm 0.03} \qquad \text{for} \qquad \epsilon_{LCS} = 10^{-2} \,, \tag{8.16}$$

$$N_{vac} \simeq (0.85 \pm 0.06)\, L^{2.93 \pm 0.03} \qquad \text{for} \qquad \epsilon_{LCS} = 10^{-1} \,. \tag{8.17}$$

The dependence of N_{vac} on L and the fit in eq. (8.16) are shown in Figure 8.2. Considering the very general arguments that are used to derive the estimate eq. (8.14), the agreement within an order of magnitude with the factual number of vacua strongly confirms the statistical analysis of [23, 24]. In the following, we set $\epsilon_{LCS} = 10^{-2}$.

[4] Note that $N_{vac} \sim L^6$ in [140] which is due to the fact that 12 independent fluxes have been switched on while we effectively switch on 6 independent fluxes, see eq. (8.8).

The distribution of the flux superpotential is shown in Figure 8.2. We find that for most vacua $\mathcal{O}(10^1 - 10^3)$ values are preferred. To calculate the masses of the moduli we have to know the value of the volume $\mathcal{V}$ of X_3. Note that we have not specified the stabilization mechanism for the Kähler moduli in this chapter and hence have no information about the value of $\mathcal{V}$. Therefore, we can only calculate the physical masses m as a function of $\mathcal{V}^{-1}$, i.e.,

$$m = \frac{m_{\rm cs}}{\mathcal{V}}\,, \tag{8.18}$$

where $m_{\rm cs}$ is the mass calculated from the effective theory of the complex structure moduli only, i.e., $K = K_{\rm cs}$ and $W = W_0$.

Let us discuss the distribution of the physical moduli masses m^2 in terms of $m^2_{\rm cs}$, i.e., the eigenvalues of the Hessian $\partial_a\partial_b V$ of the no-scale potential eq. (5.13) for $a, b = u_1, u_2, s, \nu_1, \nu_2, \sigma$ as well as the gravitino mass $m^2_{3/2}$ in terms of the quantity

$$m^2_{\rm cs,\,3/2} \equiv m^2_{3/2}\,\mathcal{V}^2 = e^{K_{\rm cs}}|W_0|^2\,. \tag{8.19}$$

This quantity, $m^2_{\rm cs,\,3/2}$, governs the scale of the typical AdS cosmological constant induced by the flux superpotential ignoring the contributions from the Kähler moduli sector. The distribution of $m^2_{3/2}$ peaks at $\langle m^2_{3/2}\rangle = 3.5\times 10^{-2}\cdot(\frac{100}{\mathcal{V}})^2$ with a standard deviation $3\times 10^{-2}\cdot(\frac{100}{\mathcal{V}})^2$. The complex structure moduli and the dilaton are stabilized at $m^2 \sim \mathcal{O}(10^{-3} - 10^2)(\frac{100}{\mathcal{V}})^2$. These ranges for the moduli and gravitino masses are compatible with the values obtained for a single explicit flux choice in the same construction [21, 22].

The AdS/dS cosmological constant before tuning is up to $\mathcal{O}(1)$ factors estimated to be

$$\Lambda \sim \frac{m^2_{3/2}}{\mathcal{V}} = \frac{m^2_{\rm cs,\,3/2}}{\mathcal{V}^3}\,, \tag{8.20}$$

in both the LVS and Kähler uplifting scenarios. In particular, the tunability of $m_{\rm cs,\,3/2}$ by 3-form flux directly translates into the tunability of the cosmological constant via

$$\frac{\Delta\Lambda}{\Lambda} \sim 2\,\frac{\Delta m_{\rm cs,\,3/2}}{m_{\rm cs,\,3/2}}\,. \tag{8.21}$$

Note that the RHS of eq. (8.21) is independent of the volume $\mathcal{V}$, i.e., fine-tuning of $m_{\rm cs,\,3/2}$ only has a tiny effect on the VEVs of the Kähler moduli.

Since the polynomial homotopy continuation method allows us to calculate all solutions for a given tadpole L, we can estimate $\Delta\Lambda/\Lambda$ by determining the average spacing $\Delta m_{\rm cs,\,3/2}$ for all values of $m_{\rm cs,\,3/2}$ that are to be found in a σ-interval around $\langle m_{\rm cs,\,3/2}\rangle$. Since the number of vacua is given as a power-law in L, with

the exponent linear in the number of flux carrying complex structure moduli $h^{2,1}_{\text{eff}}$, we expect $\Delta m_{\text{cs},\,3/2}/m_{\text{cs},\,3/2}$ to be of the form

$$\frac{\Delta m_{\text{cs},\,3/2}}{m_{\text{cs},\,3/2}} \sim \frac{C}{L^{a\,(h^{2,1}_{\text{eff}}+1)}}\,, \tag{8.22}$$

with $C, a > 0$. We can determine these parameters by fitting the LHS of eq. (8.22) as a function of L for $h^{2,1}_{\text{eff}} = 2$. Choosing a 3-σ interval around $\langle m_{\text{cs},\,3/2}\rangle$ we find the available tuning for the cosmological constant to be

$$\frac{\Delta\Lambda}{\Lambda} \simeq (6.0 \pm 0.3)\, L^{-(0.95\pm 0.005)\,(h^{2,1}_{\text{eff}}+1)}\,, \tag{8.23}$$

where we have included the statistical errors of the fit parameters C and a.

Let us assume that eq. (8.23) is valid and $\langle m_{\text{cs},\,3/2}\rangle \sim \mathcal{O}(10)$ also for larger values of $L \sim \mathcal{O}(10^3)$ and larger values of $h^{2,1}_{\text{eff}} \sim \mathcal{O}(10^1 - 10^2)$. [5] Then, we can extrapolate the values of the cosmological constant eq. (8.20) and its tunability to more realistic scenarios, see Table 8.1.

$h^{2,1}_{\text{eff}}$	L	$\Delta\Lambda/\Lambda$
2	34	$7\cdot 10^{-3} \pm 5\cdot 10^{-4}$
2	500	$5\cdot 10^{-5} \pm 4\cdot 10^{-6}$
40	34	$3\cdot 10^{-58} \pm 2\cdot 10^{-58}$
40	500	$10^{-102} \pm 10^{-102}$

Table 8.1: The tunability $\Delta\Lambda/\Lambda$ of the cosmological constant for different values of $h^{2,1}_{\text{eff}}$ and L with statistical errors propagated from eq. (8.23). The untuned values of the cosmological constant are estimated via eq. (8.20) to be $\mathcal{O}(10^{-4} - 10^{-22})$ in units of M_{P}^4 for $\mathcal{V}$ of $\mathcal{O}(10^2 - 10^8)$. The first row of this table is directly calculated from our dataset while the last three rows are obtained as an extrapolation via eq. (8.23).

To tune the cosmological constant to the accuracy given in Table 8.1, one has to make the assumption that every supersymmetric flux vacuum has no tachyonic directions after uplifting and stabilizing the Kähler moduli. In particular, for large values of $h^{1,1}$ there could be strong suppressions of tachyonic free configurations [145–147]. In the following section, we will determine how many de Sitter vacua can be constructed from our dataset on X_3 via the method of Kähler uplifting.

[5] This assumption is reasonable when the prepotential $\mathcal{G}$ is of the same structure as eq. (8.3), i.e., we are considering the large complex structure limit away from e.g., conifold singularities via a mirror construction. It may be interesting to consider such examples with $h^{2,1}_{\text{eff}} = h^{1,1} > 2$, e.g., by choosing random pre-factors in a general polynomial prepotential of degree 2 in the ω_i.

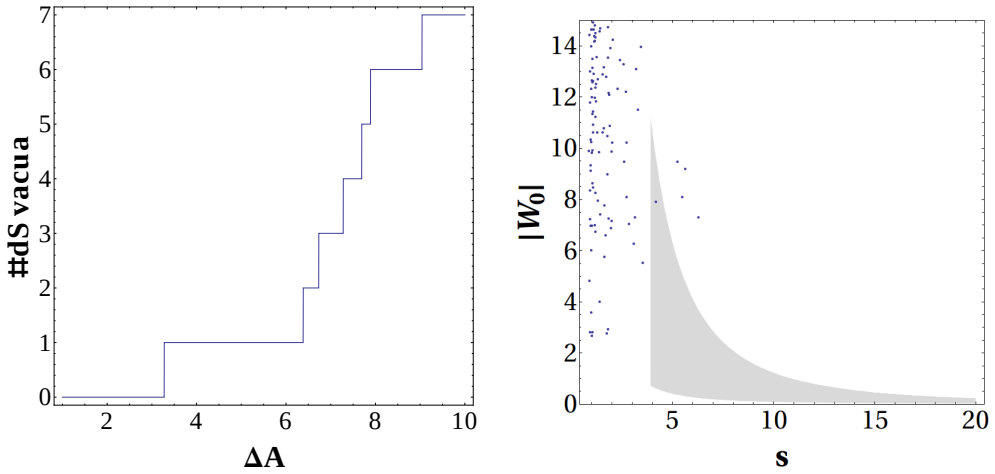

Figure 8.3: The number of Kähler uplifted de Sitter vacua as a function of ΔA (left) and data points $(s, |W_0|)$ (right). Kähler uplifting can be applied in the shaded region ($\Delta A = 4$).

8.2.4 de Sitter vacua via Kähler uplifting

Let us discuss for what proportion of flux vacua the class of Kähler uplifted de Sitter vacua constructed in Section 7.3 is applicable. For the specific point in moduli space $A_1 = A_2 = 1$, we found that the parameters W_0 and s have to lie on the curve eq. (7.13). To extend this class of vacua to more general values of A_1 and A_2, we introduce the parameter ΔA and the scaling relations

$$W_0 \to W_0 \cdot \Delta A\,, \qquad A_1 \to A_1 \cdot \Delta A\,, \qquad A_2 \to A_2 \cdot \Delta A\,, \tag{8.24}$$

under which the position of a minimum of the potential eq. (5.10) is invariant since $V \to V \cdot \Delta A^2$. For a given uncertainty in the one-loop determinants $\Delta A^{-1} \leq A_i \leq \Delta A$ around $A_1 = A_2 = 1$ we can then define the criterion

$$\frac{W_0^{\rm dS}(s)}{\Delta A} \leq |W_0| \leq W_0^{\rm dS}(s) \cdot \Delta A \qquad \text{and} \qquad s \geq 4\,, \tag{8.25}$$

for a given data point $(s, |W_0|)$ to allow a de Sitter vacuum via Kähler uplifting.

We show the number of Kähler uplifted de Sitter vacua depending on ΔA in Figure 8.3. Due to the low number of weakly coupled vacua with $s \gg 1$ and $\mathcal{O}(1)$ values of the superpotential, the number of vacua that can be uplifted to de Sitter via Kähler uplifting is strongly suppressed. For $\Delta A = 10$, only 7, i.e., a fraction of $\sim 10^{-4}$ of the total number of flux vacua allow such an uplifting.

The available tuning of the cosmological constant via fluxes can be estimated again via eq. (8.21). The Kähler moduli stabilization yields a volume of $\mathcal{V} \simeq 53$ such that the untuned cosmological constant is $\Lambda \sim 6 \cdot 10^{-6}$ and

$$\frac{\Delta\Lambda}{\Lambda} \simeq 0.38 \pm 0.27\,, \tag{8.26}$$

for $\Delta A = 10$. We remind the reader that this is calculated for $L = 34$ which is the maximal value we reach in our paramotopy scan and hence less than $L = 104$, eq. (7.10), which is maximally allowed by the gauge flux and D7-brane construction realized for a Kähler uplifted de Sitter vacuum in Section 7.3.

To summarize this section, the polynomial homotopy continuation method allows us to find all flux vacua for a given D3-tadpole L. The number of these vacua is well estimated by the statistical analysis of [23, 24]. We find that strongly coupled vacua $s \gtrsim 1$ are preferred as well as $\mathcal{O}(10^1 - 10^3)$ values of W_0. Our results can be used to estimate the tunability of the cosmological constant by fluxes and the number of flux vacua that can be Kähler uplifted to a de Sitter vacuum.

8.3 The minimal flux method

In this section we briefly describe the minimal flux method that was first used by Denef, Douglas and Florea [140]. In contrast to the polynomial homotopy continuation method described in Section 8.2, we fix starting values for the VEVs $\langle U_1 \rangle_{fix}$, $\langle U_2 \rangle_{fix}$ and $\langle \tau \rangle_{fix}$ and solve for the flux values f and h.

Due to the linear dependence of W_0 on f and h, see eq. (5.21), the quantities $D_I W_0 = W_{0I} + K_I W_0$ for $I = \tau, U_1, U_2$ are linear in these flux vectors. Hence, if we want to solve the system of equations

$$(W_0, D_\tau W_0, D_{U_1} W_0, D_{U_2} W_0) = 0\,, \tag{8.27}$$

this can be written as

$$M \cdot (f, h) = 0\,, \tag{8.28}$$

with $M \in \mathbb{R}^{8\times 12}$ for general VEVs $\langle U_1 \rangle, \langle U_2 \rangle, \langle \tau \rangle \in \mathbb{C}$. The dimensions of M result from the fact that we have 8 real equations in eq. (8.27), and there are 12 flux integers in total in f and h. Note that we have also included the condition $W_0 = 0$ in eq. (8.27). However, we are not interested in flux vacua where W_0 is strictly zero since none of the well studied moduli stabilization mechanisms KKLT [16], LVS [87] and Kähler uplifting [21, 22, 86, 94] apply in this situation. As such, eq. (8.27) will only serve as a starting point and we will eventually end up with vacua where $W_0 \neq 0$ and $\mathcal{O}(1)$.

For $M \in \mathbb{R}^{8\times 12}$ there is no hope to find a solution of eq. (8.28) since the flux parameters need to be integers. However, if we neglect instanton corrections induced by eq. (8.4) and choose rational starting values $\langle U_1 \rangle, \langle U_2 \rangle, \langle \tau \rangle \in \mathbb{Q} + i\,\mathbb{Q}$ in the superpotential, the only transcendental number in eq. (8.28) is $\xi = \frac{\zeta(3)\chi}{2(2\pi\, i)^3} =$

$-1.30843..\,i$. If we approximate ξ by a rational number ξ_{rat}, for instance $\xi_{rat} = -13/10\,i$, we have accomplished $M \in \mathbb{Q}^{8\times 12}$.

Now we can hope to find a solution of eq. (8.28) although the entries of f and h will generically be quite large for generic M, since one expects them to be at least of the order of the lowest common denominator of the entries of M. This puts tension on the D3-tadpole constraint eq. (5.22) since generally the geometry of the compactification manifold and D7-brane configuration generates $L \sim 10^2 - 10^4$. We use the same algorithms [165] as the authors of [140], to generate as small as possible values for the entries of f and h in order to generate a not too large D3-tadpole $L < L_{max}$ where we choose $L_{max} = 500$ to be the maximal value for the D3-tadpole that we consider.

Since the system of equations eq. (8.28) is under-determined, the solution space is given by all linear combinations of linearly independent vectors $(f,h)_i$ for $i = 1,..,4$, where each $(f,h)_i$ is a solution to eq. (8.28), i.e.,

$$(f,h)_{sol} = \sum_{i=1}^{4} a_i\,(f,h)_i \qquad \text{with } a_i \in \mathbb{Z}\,. \tag{8.29}$$

For obvious practical reasons, we cannot consider all possible values of the a_i. We find that basis vectors of solutions with $L((f,h)_i) < 10$ are extremely rare in our scan. Hence, since $L(a_i(f,h)_i) = a_i^2 L((f,h)_i)$, we can safely restrict ourselves to all values of the a_i with $-3 \leq a_i \leq 3$ in order to fulfill $L((f,h)_{sol}) < L_{max}$.

In the next step, we are looking for solutions to eq. (8.2), including instanton corrections eq. (8.4) to the prepotential and also setting ξ to its transcendental value. We insert the flux solution $(f,h)_{sol}$ into the equations

$$(D_\tau W_0, D_{U_1} W_0, D_{U_2} W_0) = 0 \qquad \text{(with instanton corrections)}\,, \tag{8.30}$$

leaving the VEVs $\langle U_1\rangle$, $\langle U_2\rangle$ and $\langle\tau\rangle$ unfixed. These are six real equations for six real variables and we can numerically search for a solution in the vicinity of $\langle U_1\rangle_{fix}$, $\langle U_2\rangle_{fix}$ and $\langle\tau\rangle_{fix}$. A check needs to be carried out on a case by case basis to determine if the complex structure limit is still valid for these perturbed solutions. The shift of the VEVs from their fixed values may also induce a shift in the superpotential, i.e., W_0 is not zero anymore. However, note that the value that W_0 will take in the end is not in any way under our control and it has to be checked if one obtains useful values for the purpose of moduli stabilization.

The above outlined algorithm can be iterated by sampling over a set of VEVs $\langle U_1\rangle_{fix}$, $\langle U_2\rangle_{fix}$ and $\langle\tau\rangle_{fix}$ and approximate ξ values ξ_{rat}.

For the minimal flux method, we find ~ 1000 flux vacua with $L < 500$ out of $\sim 10^7$ parameter points of our scan. A detailed presentation of the results can

be found in Section 4.3 of [25]. This method allows us to control the region in W_0 and moduli space where we are intending to find flux vacua. Hence, we more easily access the regions of weak string coupling and of the large complex structure limit compared to the polynomial homotopy continuation method. For this much smaller set of flux vacua constructed with the minimal flux method, the fraction of Kähler uplifted de Sitter minima is approximately 10%. This is a considerably higher proportion of vacua compared to the polynomial homotopy continuation method (which was only $\sim 0.01\,\%$). This is due to the fact that the minimal flux method naturally finds values for g_s and W_0 in a region where Kähler uplifting is applicable.

Chapter 9

Conclusions and Outlook

Let us start by concluding Part II of this thesis (as Part I was already concluded at the end of Chapter 4). Following the motivation of providing a proof of existence for de Sitter vacua in string theory, we derived a sufficient condition for de Sitter vacua in the Kähler uplifting scenario in the low energy supergravity limit of type IIB string theory in Chapter 6. This condition can be expressed in terms of the compactification parameters, more precisely the geometry of the Calabi-Yau manifold and the fluxes. This sufficient condition provides guidance in the construction of explicit examples for de Sitter vacua. In Chapter 7, we constructed such an example on the manifold $\mathbb{CP}^4_{11169}[18]$, taking into account all known consistency constraints such as tadpole conditions and anomaly cancellations. The question of whether this set of de Sitter vacua can include a subset with extremely small vacuum energy as in our universe was addressed in Chapter 8. The explicit treatment of $\mathcal{O}(100)$ fluxes which are needed to tune the cosmological constant to $\mathcal{O}(10^{-120})M_{\rm P}^4$ is technically extremely difficult. Hence, we restrict our explicit analysis to 6 fluxes on $\mathbb{CP}^4_{11169}[18]$ and extrapolate our results to higher dimensional flux spaces. In agreement with semi-analytical results [23, 24], our extrapolation strongly indicates that such a fine-tuning of the cosmological constant is indeed possible.

So did we succeed in constructing an explicit example of a de Sitter vacuum in string theory? Certainly we can answer this question affirmative if higher order corrections in α' and g_s that are as yet unknown do not spoil the analysis presented in this work. Due to the large volume and weak coupling limit we take, this is generically the case if the coefficients of these higher order corrections are not too large. Hence, it is an important task for the future to calculate these higher order corrections and check their effect on moduli stabilization and inflationary

model building.[1] If one does not have to rely on its IIB limit, a particular suitable approach is F-theory since it is non-perturbative in g_s such that all corrections originating from g_s are automatically included. Another very important task is to verify that the standard model of particle physics can be included in a globally consistent compactification of string theory. In particular, these global constructions should allow for an extremely small cosmological constant and an early phase of inflation in order to be more realistic.[2]

The attempt to construct fully realistic models of our universe in the sense of both particle physics and cosmology is crucial to find out if string theory does in fact describe our world. Due to the highly non-trivial constraints such as the cosmological constant fine-tuning that reality imposes on string phenomenology, one ideally might hope for distinct features that are shared by many models in the string theory landscape. Most optimistically, these could lead to intrinsically stringy predictions in both particle physics and cosmology. Hence, a better understanding of the landscape as well as its statistics and dynamics, such as tunneling and the population mechanism, is very important. In some corners of the landscape, string theory already provides statistical preference for a small cosmological constant [148] or for the type of inflationary model [169]. Finally, the upcoming experimental data, e.g., from the LHC and CMB polarization data from Planck, might provide further guidance for model building in string theory. This includes, for instance, answers to the questions of what the energy scale of inflation is and whether low energy supersymmetry is realized in nature.

[1] For instance we find potentially de-stabilizing effects on moduli stabilization in the LVS and Kähler uplifting scenario in a study of the effect of certain α'^4 corrections [166] to the scalar potential [167]. However, to make a decisive statement on the relevance of these corrections one has to calculate all corrections at least to fourth order in α' to the scalar potential.

[2] For attempts in this direction see e.g., [168].

Acknowledgements

First of all, I would like to express my deep gratitude to Jan Louis for taking me as a PhD student and providing excellent guidance, as well as sharing his insights and intuition with me. I am equally grateful for Alexander Westphal's supervision, enthusiasm, encouragement and creative insight. I would like to thank Rhiannon Gwyn, Yang-Hui He, Danny Martínez-Pedrera, Dhagash Mehta, Matthew Niemerg, Francisco Pedro, Alexandru Valeanu and especially Roberto Valandro - I learned so much during our fruitful collaborations. Also, I would like to thank my office mates Thomas Danckaert, Manuel Hohmann, Christoph Horst, Reinke Sven Isermann, Martin Schasny, Luca Tripodi, and Lucila Zárate and all the people from the II. Institute for theoretical physics and the DESY theory group for creating such a lively and and stimulating atmosphere. I would like to thank Kristen Jorgenson and Lucila Zárate for proof-reading and Reinke Sven Isermann for printing and submitting this manuscript for me. Also, I want to thank the Hong Kong University of Science and Technology, where part of this work was completed, for their hospitality. Finally, I am deeply indebted to Christiane, Heinz, Silvia, Kristen and my friends for always supporting me.

Appendix A

F-term induced shifts of the moduli - details

We present details on the derivation of the F-term induced shifts presented in Section 6.2.2.

A.1 Deviation of s and u_a from the SUSY minimum

We will now estimate the correction $\delta\vec{\theta}$ for a general complex structure sector to be of the order $\hat{\xi}/\mathcal{V}$ multiplied with terms depending on $K_{c.s.}$, W_0 and derivatives of these expressions with respect to s and u_a. To analyze the scaling of $V^{(0)}_{\vec{\theta}_0\,\vec{\theta}_0}$ with respect to our expansion parameter $\hat{\xi}/\mathcal{V}$ only the overall factor e^K is relevant since there is otherwise no t dependence in $V^{(0)}$. Hence

$$V^{(0)}_{\vec{\theta}_0\,\vec{\theta}_0} \sim \mathcal{V}^{-2} \quad . \tag{A.1}$$

To analyze the scaling of $\delta V^{(1)}_{\vec{\theta}_0}$ with respect to $\hat{\xi}/\mathcal{V}$, we have to build the derivatives of $V^{(T)}$ and $V^{(T,\tau)}$ with respect to s and u_a respectively and evaluate at the supersymmetric minimum. A detailed calculation given in Section 4.1 of [21] yields

$$\delta V^{(1)}_{\vec{\theta}_0} \sim W_0\,|(W_0)_{\vec{\theta}_0}|\,\frac{\hat{\xi}}{\mathcal{V}^3}\,. \tag{A.2}$$

So finally going back to eq. (6.26) we indeed obtain

$$\delta\vec{\theta}_i \sim \frac{\hat{\xi}}{\mathcal{V}}\,, \tag{A.3}$$

to be a 1-st order perturbation of the supersymmetric minimum $\vec{\theta}_0$.

Note that our analysis does not take into account a possible dependence of $\delta\vec{\theta}$ on $h^{2,1}$. This implies the potential caveat that a perturbative expansion of the shift from the supersymmetric minimum in $\hat{\xi}/\mathcal{V}$ might not be consistent for large $h^{2,1}$, as we will now discuss. The parts of the scalar potential $V^{(T)}$ and $V^{(T,\tau)}$ depend on $U_1, \ldots, U_{h^{2,1}}$ via the flux superpotential W_0. Hence, when we calculate the deviation of the 0-th order supersymmetric VEV of the dilaton or a complex structure modulus to 1-st order we might expect the deviation to depend on the number of fields that are supersymmetrically stabilized. In the worst case, one could expect the deviation to grow with the number of fields included such that the 1-st order deviation would eventually become of the same order as the 0-th order VEV which would make our perturbative expansion valid only up to certain number of fields included. This is what one could expect naively, since a growing number of fields could 'pull away' the supersymmetrically stabilized fields from their VEVs via $\delta V^{(1)}$ the stronger the more fields are included.

However, we will give here a short argument why we expect no such deleterious dependence of the shifts $\delta\vec{\theta}$ on $h^{2,1}$ to arise. Upon inspection of eq. 6.26 concerning the $u_a = \mathrm{Im}\, U_a$ we see that we can approximate the mass matrix $V^{(0)}_{\vec{\theta}_0\vec{\theta}_0}$ entering there by two extreme cases within which we will typically find realistic examples. Consider first the non-generic case, where $V^{(0)}_{\vec{\theta}_0\vec{\theta}_0} \sim \langle\mu^2\rangle \mathrm{diag}(\mathcal{O}(1), \ldots, \mathcal{O}(1))$ is roughly diagonal, where μ denotes the common mass scale assumed for this non-generic case. Now we note that $\delta V^{(1)}_{\vec{\theta}_0} \sim |(W_0)_{\vec{\theta}_0}|$ and from the 3-cycle decomposition of the CY 3-fold we have eq. (5.21). At a generic point in the interior of moduli space of a generic CY we expect the periods $\mathcal{G}_i$, in being the dual complex structures, to have the same sizes as the U_a, and thus $\delta V^{(1)}_{\vec{\theta}_0} \sim |(W_0)_{\vec{\theta}_0}|$ will be roughly constant in $h^{2,1}$. For our first case of a roughly diagonal mass matrix this implies that the shifts $\delta\vec{\theta}$ are roughly constant in $h^{2,1}$. Now consider the 2nd generic case of a non-diagonal mass matrix which we approximate by $V^{(0)}_{\vec{\theta}_0\vec{\theta}_0} \sim \langle\mu^2\rangle\mathcal{O}(1)$ $\forall i,j = 1 \ldots h^{2,1}$. In this case, each row on the LHS of eq. (A.4), which is eq. (6.26) before inversion, contains a sum over all $\delta\vec{\theta}_i$ with roughly equally sized coefficients

$$V^{(0)}_{\vec{\theta}_0\,\vec{\theta}_0} \cdot \delta\vec{\theta} = -\delta V^{(1)}_{\vec{\theta}_0}\,. \tag{A.4}$$

Now as $V^{(0)}_{\vec{\theta}_0\vec{\theta}_0}$ has roughly equal sized entries everywhere, eq. (A.4) should have a solution

$$\delta\vec{\theta} \sim \left\langle \frac{1}{\mu^2} \right\rangle \frac{1}{h^{2,1}}\,, \tag{A.5}$$

for the shifts of the complex structure moduli, where μ denotes the mass scale of the eigenvalues of a mass matrix with roughly equal entries everywhere. As a given

tree-level mass matrix $V^{(0)}_{\vec{\theta}_0\vec{\theta}_0}$ for a given model will in general fall in between these two extreme cases, we expect no positive power of $h^{2,1}$ to appear in the shifts $\delta\vec{\theta}$.

A.2 Backreaction on the Kähler modulus

We will now derive an expression for the 1-st order shift in δt of the Kähler modulus due to 2-nd order terms in the scalar potential. δt will then be used to calculate the perturbance of the mass $m_t^2 \simeq K^{T\bar{T}} \cdot V^{(T)}_{tt}$ due to these 2-nd order terms. Splitting eq. (6.16) into 1-st order $V^{(T)}$ and 2-nd order $\delta V^{(2)} = V^{(T,\tau)} + V^{(\tau)} + V^{(U)}$ terms we can perform an expansion in δt along the lines of eq. (6.25) in δt and obtain [21]

$$\frac{\delta t}{t} = -\frac{(\delta V^{(2)})_t}{t\, V^{(T)}_{tt}} = \frac{\hat{\xi}\Delta}{\mathcal{V}} \ , \tag{A.6}$$

where Δ is a function which is $\mathcal{O}(1)$ in the fluxes, whose overall sign and dependence on $h^{2,1}$ and hence the smallness of $\delta t/t$ is in general unknown. We can expand the perturbed mass $\tilde{m}_t^2$

$$\begin{aligned}\tilde{m}_t^2 &= m_t^2 + (\partial_t m_t^2)\,\delta t + \frac{1}{2}(\partial_t^2 m_t^2)\,\delta t^2 + \dots \\ &= \frac{5W_0^2}{4s\,\mathcal{V}^2} \cdot \frac{\hat{\xi}}{\mathcal{V}}\, e^{K_{c.s.}} \left(1 - \frac{31}{2}\frac{\hat{\xi}\Delta}{\mathcal{V}} + \mathcal{O}\left(\frac{\hat{\xi}\Delta}{\mathcal{V}}\right)^2\right) \ .\end{aligned} \tag{A.7}$$

So if Δ is negative it cannot cause a tachyonic direction in t. However, if Δ is positive, only values of Δ that are smaller than roughly $\mathcal{O}(10)$ can be allowed to keep the spectrum tachyon free. Due to its constant scaling in the fluxes we typically expect $\Delta = \mathcal{O}(1)$.

Let us pause here again to discuss a possible dependence of the expansion on $h^{2,1}$. Once it is shown that the dilaton and complex structure moduli are stabilized supersymmetrically with a 1-st order deviation one expects this to induce a 2-nd order term in the potential. This is due to the quadratic dependence of $V^{(\tau)}$ and $V^{(U)}$ on the respective F-terms and the structure of $V^{(T,\tau)}$ which is a 1-st order term times F_τ. Since $V^{(T)}$ is a 1-st order term we expect an effective 1-st order correction on the stabilization of t. A correction of the VEV of t induces a correction in m_t^2 which could in the worst-case create a tachyonic direction in t.

Similar to the situation discussed above for the deviation of the dilaton and the complex structure moduli from the supersymmetric minimum, there is the danger that the correction to m_t^2 will be negative and scale with positive powers of $h^{2,1}$. Then, a non-tachyonic t direction would only be possible up to a certain upper

bound on $h^{2,1}$. Note, that in case the correction to m_t^2 is positive, a scaling with $h^{2,1}$ would even increase m_t^2 and make this direction more stable in the end.

Appendix B

The type IIB perspective of $\mathbb{CP}^4_{11169}[18]$ - details

B.1 D7-branes from the IIB perspective

It was found in [129] that for a single invariant D7-brane saturating the D7-tadpole cancellation condition, its world volume is given by the (non-generic) polynomial equation

$$\eta^2 - \xi^2 \chi = 0\,, \tag{B.1}$$

with η and χ sections of $\bar{K}^4$ and $\bar{K}^6$, respectively. (For practical purposes, η and χ can be seen as polynomials in the complex coordinates u_i of the resolved base manifold B_3.) This D7-brane is called in the literature 'Whitney brane', as it has the singular shape of the so called Whitney umbrella [129].

For non-generic forms of the polynomials η an χ, the Whitney brane can split into different stacks. In particular a stack of $2N_i$ branes wrapping the invariant toric divisor $D_i : \{u_i = 0\}$ manifests itself via the factorizations $\eta = u_i^{N_i}\tilde{\eta}$ and $\chi = u_i^{2N_i}\tilde{\chi}$ such that eq. (B.1) becomes

$$u_i^{2N_i}\left(\tilde{\eta}^2 - \xi^2\tilde{\chi}\right) = 0\,, \tag{B.2}$$

where on the invariant divisor at $u_i = 0$ there is an $Sp(N_i)$ stack and $\tilde{\eta}^2 - \xi^2\tilde{\chi}$ describes a Whitney brane of lower degree. Since the Whitney brane has always to be described by a holomorphic equation, N_i cannot be made arbitrarily large.

For $u_{i=1,\dots,4}$ we can be more specific. Eq. (B.2) becomes

$$u_i^{2N_i}\left(\tilde{\eta}^2_{(4n_\xi - n_i N_i,\dots)} - \xi^2\tilde{\chi}_{(6n_\xi - 2n_i N_i,\dots)}\right) = 0\,, \tag{B.3}$$

where the dots denote the degrees that are imposed via the weight system of the resolved ambient space X_4^{amb}. If the degree in the first scaling is the most restrictive we obtain the strongest bound from the holomorphicity of $\tilde{\chi}$, i.e.,

$$N_i \leq 3\frac{n_\xi}{n_i}\,. \tag{B.4}$$

B.2 Consistency constraints for D7-branes on $\mathbb{CP}^4_{11169}[18]$

We give more details on the constraints that have to be fulfilled in order to realize a consistent D7-brane configuration on $\mathbb{CP}^4_{11169}[18]$ as is summarized in Section 7.2.

B.2.1 D7-brane configuration

We discuss the inclusion of D7-branes, following the general procedure discussed in Appendix B.1. To cancel the D7-charge of the O7-planes at $\xi = 0$, the equation describing the D7-brane configuration is given by (see eq. (B.1))

$$\eta^2_{36,8} - \xi^2\chi_{54,12} = 0\,, \tag{B.5}$$

where the degrees of the η and χ polynomials are dictated by the degrees of ξ and by the requirement that $[D7] = -8[O7] = -8D_\xi$. It turns out [22] that for a maximal rank of $N_1 = N_{lg} = 27$ of the gauge group on the invariant divisor D_1, the Whitney brane in eq. (B.5) splits into a brane and an image brane. This generically induces a non-trivial flux on these split branes in order to cancel Freed-Witten anomalies which in turn could generated additional chiral zero-modes. This can be avoided by a lower degree gauge group $Sp(24)$ on D_1 such that the Whitney brane does not split. Furthermore, this gauge group on D_1 enforces a further factorization of eq. (B.5) in u_5 which induces an $SO(24)$ gauge group on D_5^{fix}.

B.2.2 Rigidifying D_1 by gauge flux

The equation describing D_1 is $u_1 = 0$, which can be deformed to $u_1 + \zeta_2 u_2 + \zeta_3 u_3 = 0$. We see that we have two deformation moduli, consistent with the fact that $h^{2,0}(D_1) = 2$. We need to lift such zero modes in order to avoid destroying gaugino condensation on the D7-brane stack wrapping D_1. In Section 3.3 of [22], an explicit gauge flux $\mathcal{F}_{D_1}$ wrapping D_1 is constructed that fixes these deformation moduli. This rigidifying flux is taken such that it is not a pull-back of a CY_3 2-form,

i.e., it will not generate additional chiral matter and will not enter in the D-term constraints. The flux constrains the holomorphic embedding of the D-brane by the F-term constraint $\mathcal{F}^{2,0} = 0$ as first suggested in [90] and introduced in [170]. Furthermore, the explicit flux constructed in [22] that rigidifies all the D7-branes in the $Sp(24)$ stack induces a D3-charge of

$$Q_{D3}^{\mathcal{F}_{D_1}} = 144\,, \tag{B.6}$$

and breaks the $Sp(24)$ gauge group to $SU(24)$.

B.2.3 Avoiding D-terms and zero-modes from matter fields

In Appendix B.2.1, we introduced D7-brane stacks on the divisors D_1 and D_5. If the branes carry non-zero flux, we have to worry about possible charged matter fields arising at the intersection of the two D7-brane stacks or from the D7-brane bulk spectrum. These zero modes might force the contribution to the superpotential from gaugino condensation to be zero. These problematic fluxes also generate Kähler moduli dependent Fayet-Iliopoulos (FI) terms ξ_i [89, 99, 171]. This would introduce a D-term potential for the Kähler moduli. However, the method of Kähler uplifting which we use requires a pure F-term potential.

In the following, we show that additional zero-modes and D-terms can be avoided for an appropriate choice of gauge flux F on the branes wrapping the divisors D_1 and D_5^{fix}. The gauge flux F combines with the pull-back of the bulk B-field on the wrapped 4-cycle to give the gauge invariant field strength

$$\mathcal{F} = F - B\,. \tag{B.7}$$

The number of additional zero modes and the Kähler moduli dependent Fayet-Iliopoulos terms appearing in D-terms are given by integrals of the form

$$\int_{D_i} \mathcal{F}_{D_i} \wedge D = \int_{X_3} D \wedge D_i \wedge \mathcal{F}_{D_i}\,, \tag{B.8}$$

where D is an arbitrary divisor in the 3-fold X_3. If it is possible to choose the fluxes $\mathcal{F}_{D_1}$ and $\mathcal{F}_{D_5^{\text{fix}}}$ such that eq. (B.8) vanishes for $i = 1, 5$ these fluxes do not have any problematic consequences. In particular, an integral such as (B.8) vanishes if the flux $\mathcal{F}_{D_i}$ is orthogonal to the 2-forms of D_i that are pull-backed from the CY 3-fold X_3.

When turning on gauge flux one has to make sure that the Freed-Witten anomaly [135, 136] is canceled, i.e., the gauge flux on a brane wrapping divisor D has to satisfy

$$F + \frac{c_1(D)}{2} \in H^2(X_3, \mathbb{Z})\,. \tag{B.9}$$

If the divisor D is non-spin, its first Chern class $c_1(D)$ is odd and F cannot be set to zero. On the other hand, the expression appearing in the physical quantities is the gauge invariant flux eq. (B.7). By choosing the B-field appropriately, one can make this invariant flux equal to zero. For a set of D7-brane stacks wrapping non-intersecting divisors, the global B-field can be chosen such that the pull-back on all such divisors make $\mathcal{F} = 0$ for all the stacks. However, for intersecting stacks this is not possible in general. In Section 3.4 of [22] we prove that our case is not generic in this respect: We can choose the B-field such that both $\mathcal{F}_{D_1}$ and $\mathcal{F}_{D_5^{\text{fix}}}$ are trivial, i.e., eq. (B.8) vanishes. Hence, additional zero-modes as well as D-terms can be avoided by tuning of the gauge flux.

B.2.4 D3-tadpole cancellation condition

The D3-tadpole has to cancel for consistency. The compactification ingredients that induce a D3-charge are the (fluxed) D7-branes, the O7-planes, the D3-branes, the O3-planes and the RR and NS field strengths F_3 and H_3. The RR and NS fluxes and the D3-branes have a positive contribution given by eq. (5.22) and $Q_{D3}(N_{D3} \times D3) = N_{D3}$, respectively. In our case we do not have O3-planes, while we have O7-planes. Each O7-plane contributes negatively by $Q_{D3}^{O7} = -\chi(O7)/6$. We have two O7-planes, whose D3-charge sum up to $Q_{D3}^{O7s} = -92$ where we used $\chi(O7_{u_5}) = 3$ and $\chi(O7_Q) = 549$.

A stack of N_i D7-branes and their N_i images wrapping a divisor D_i contributes to the total D3-charge positively via the gauge flux and negatively via a geometric contribution:

$$Q_{D3}^{D7}(D_i) = 2N_i \left(-\frac{1}{2} \int_{D_i} \mathcal{F}_{D_i} \wedge \mathcal{F}_{D_i} - \frac{\chi(D_i)}{24} \right) , \tag{B.10}$$

where the overall factor two comes from sum over the stack and its image stack which have the same D3-charge. For the brane-stacks on D_1 and D_5^{fix} described in Appendix B.2.1, we obtain the following D3-tadpole:

$$Q_{D3}^{\text{stacks}} = Q_{D3}^{\mathcal{F}_{D_1}} - 2N_1 \frac{\chi(D_1)}{24} - 2N_5 \frac{\chi(D_5^{\text{fix}})}{24} = 144 - 3 - 72 = 69 , \tag{B.11}$$

where we have used $N_1 = 24$, $N_5 = 12$, eq. (B.6) for the D3-charge of $\mathcal{F}_{D_1}$, $\chi(D_1) = 36$ and $\chi(D_5^{\text{fix}}) = 3$.

The Whitney brane, defined by the equation $\eta^2 - \xi^2\chi = 0$, has a singular world volume. Thus we have to compute its contribution to the D3-tadpole indirectly, see [134] and Section 3.5 of [22], taking into account the trivial flux on the

brane [129, 133]. One obtains two possible results for the charge of the Whitney brane, i.e., $Q^W_{D3} = -81$ and $Q^W_{D3} = -73$.

Taking into account the contribution from the O7-planes and the D7-brane stacks, and the negative contribution from the Whitney brane, we obtain the following total D3-brane charge from our brane configuration:

$$L = Q^{\text{O7s}}_{D3} + Q^{\text{stacks}}_{D3} + Q^W_{D3} = \begin{cases} -104 & \text{for } Q^W_{D3} = -81 \\ -96 & \text{for } Q^W_{D3} = -73\,. \end{cases} \tag{B.12}$$

Appendix C

The F-theory perspective of $\mathbb{CP}^4_{11169}[18]$

C.1 D7-branes from the F-theory perspective

Let us now discuss the constraints on the large gauge group rank in the perturbative limit of F-theory. This theory is physically equivalent to weakly coupled type IIB. However, the geometric F-theory picture provides a different perspective and a cross check of our results in the IIB picture presented in Appendix B.1.

Before we discuss the D7-brane setup in F-theory let us set the stage. To obtain an $\mathcal{N} = 1$ effective four dimensional effective theory starting from 12-dimensional F-theory we have to compactify on an elliptically fibered CY 4-fold. More specifically, the 4-fold can be described as a hypersurface in an ambient fivefold which is a $\mathbb{CP}^2_{123}$ fibration over a three dimensional base B_3, i.e. one introduces three additional complex coordinates coordinates and a scaling relation

$$(X, Y, Z) \sim (\lambda^2 X, \lambda^3 Y, \lambda Z)\,. \tag{C.1}$$

As far as the scaling in the classes of the base is concerned Z scales as a section of the canonical bundle K of B_3, in order to ensure the CY condition of the 4-fold. The elliptically fibered CY 4-fold can be defined by the Tate model [172, 173]:

$$Y^2 + a_1 XYZ + a_3 YZ^3 = X^3 + a_2 X^2 Z^2 + a_4 XZ^4 + a_6 Z^6\,, \tag{C.2}$$

where the Tate polynomials a_i are functions of the base coordinates u_i such that they are sections of $\bar{K}^i$.

In F-theory, D7-branes manifest themselves via singularities of the elliptic fibration. To engineer a singularity on a divisor $D_j : \{u_j = 0\}$ the Tate polynomials

have to factorize as

$$a_i = u_j^{w_i} a_{i,w_i} \,, \tag{C.3}$$

with positive integer numbers w_i encoding which kind of singularity is realized. Since a_{i,w_i} has to be holomorphic, w_i cannot be made arbitrarily large. For a tabular overview of the possible resolvable singularities that can arise in such a construction see [174] and Table 1 of [22]. The singularities with Coxeter number larger than 30 are either of the Sp, SU or SO type. We can again analyze the constraints on the maximal gauge group rank in more detail. The most severe constraints regarding holomorphicity of eq. (C.3) come from a_3 and a_6, leading to the same large gauge group indicator N_{lg} as in the IIB picture.

So far our F-theory discussion has been for generic values of the string coupling. However, we eventually want to obtain a stable de Sitter vacuum by using the leading α' correction to the Kähler potential [108] which is only known in perturbative type IIB. As long as this correction remains unknown in non-perturbative F-theory, we have to restrict our analysis to Sen's weak coupling limit $g_s \to 0$ [98]. It turns out,[1] that there is no restriction on the a_i in the Sen limit as long as the weak coupling limit exists. Hence, a singular configuration over a divisor D_j enforced via a factorization $a_i = u_j^{w_i} a_{i,w_i}$ remains intact in the weak coupling limit.

C.2 D7-branes on $\mathbb{CP}^4_{11169}[18]$

In this section, we revisit some results of Section 7.2 by using the F-theory language. We first discuss the D7-brane configuration in F-theory. We consider the CY 4-fold that is an elliptic fibration over the base manifold

$$B_3 : \begin{array}{c|ccccc} u_1 & u_2 & u_3 & u_4 & u_5 \\ \hline 1 & 1 & 1 & 6 & 0 \\ 0 & 0 & 0 & 1 & 1 \end{array} \,. \tag{C.4}$$

The toric divisors of B_3, defined by the equations $u_i = 0$ will be called $\hat{D}_i$, in order to distinguish them from their double covers D_i in X_3 (given by the complete intersection $\{u_i = 0\} \cap \{\xi^2 - P_{18,4} = 0\}$ in X_4^{amb}).

We find that enforcing an $Sp(24)$ singularity on the divisor $\hat{D}_1$ of B_3 forces us to impose an $SO(24)$ singularity on $\hat{D}_5$. This agrees with the type IIB perspective discussed in Appendix B.2.1. This can be seen in detail from the factorization of the Tate polynomials in u_1 and u_5, see Section 4 of [22].

[1] For a detailed discussion of the D7-brane configuration in the Sen limit see Section 2.2 of [22].

Now we consider the 4-fold where the $Sp(24)$ singularity is resolved along the lines described in [175, 176] and Appendix B.1 of [22]. The resolution introduces a set of new divisors, the exceptional divisors E_{2i-1} $(i = 1, ..., N)$, that are $\mathbb{P}^1$ fibrations over the surface in the base B_3 where the fiber degenerates. From the F-theory point of view, the gaugino condensation contribution to the superpotential is generated by M5-instantons wrapping the exceptional divisors that resolve the corresponding singularity [177]. In the presence of fluxes, the necessary condition for an M5-instanton wrapping a divisor D to contribute to the superpotential is that $\chi_0(D) \geq 1$, which is the known modification of the condition $\chi_0(D) = 1$ without fluxes [75, 178].

In Appendix B.1 of [22], we derive the following formula for the arithmetic genus of the exceptional divisors

$$\begin{aligned} \chi_0(E_{2i-1}) &= \chi_0(D);\ i = 1, .., N-1\,, \\ \chi_0(E_{2N-1}) &= \chi_0(\hat{D})\,, \end{aligned} \tag{C.5}$$

where $\hat{D}$ is the divisor $\{p_{\hat{D}} = 0\}$ on the base manifold B_3 where the singularity sits and D is its double cover in X_3.

In our example we imposed an $Sp(N_1 = 24)$ singularity on the divisor $\hat{D}_1$ which implies

$$\chi_0(E_{2i-1}) = 3 \text{ for } i = 1, \ldots, N_1 - 1 \qquad \text{and} \qquad \chi_0(E_{2N_1-1}) = 1\,, \tag{C.6}$$

using $\chi_0(D_1) = 3$. We see that all of them satisfy the necessary condition for an M5-instanton to contribute to the superpotential in the presence of fluxes. This agrees with what we found in type IIB language, where we have seen that this actually happens, i.e. switching on a proper gauge flux fixes the deformation on the wrapped divisor, leading to the possibility of having gaugino condensation.

Appendix D

Reducing the complex structure moduli space of $\mathbb{CP}^4_{11169}[18]$

Consider the two parameter ψ, ϕ-family of 3-folds $\mathbb{CP}^4_{11169}[18]$ given by the vanishing of the polynomials

$$x_1^{18} + x_2^{18} + x_3^{18} + x_4^3 + x_5^2 - 18\psi x_1 x_2 x_3 x_4 x_5 - 3\phi x_1^6 x_2^6 x_3^6 \,, \tag{D.1}$$

i.e., all except two of the 272 complex structure moduli which correspond to monomials in the general degree 18 CY hypersurface equation have been set to zero. As was discussed in [137], eq. (D.1) is invariant under a global $\Gamma = \mathbb{Z}_6 \times \mathbb{Z}_{18}$ symmetry. This symmetry is used in the Greene-Plesser construction [138] to construct the mirror CY which in this case has $h^{1,1} = 272$ and $h^{2,1} = 2$. Furthermore, the moduli ψ and ϕ in eq. (D.1) describe the two complex structure moduli of this mirror manifold. As was pointed out in [179], the periods of the mirror agree with those of $\mathbb{CP}^4_{11169}[18]$ at the Γ symmetric point. Also, [179] shows that the complete set of $h^{2,1}$ complex structure moduli can be divided into a Γ-invariant subspace and its complement. The moduli with trivial transformation are exactly those that do not vanish at the Γ symmetric point, in this case ψ and ϕ.

To make use of the agreement of the prepotential for the complex structure sector of $\mathbb{CP}^4_{11169}[18]$ and its mirror in the large complex structure limit, it is useful to introduce the complex coordinates U_1 and U_2 that are related to ψ and ϕ as [137]

$$\begin{aligned} X_1 = -\frac{1}{q_1}\big(&1 + 312q_1 + 2q_2 + 10260q_1^2 - 540q_1q_2 - q_2^2 \\ &- 901120q_1^3 + 120420q_1^2q_2 + 20q_2^3 + \dots\big) \,, \\ X_2 = -\frac{1}{q_2}\big(&1 + 180q_1 - 6q_2 + 11610q_1^2 + 180q_1q_2 + 27q_2^2 \\ &+ 514680q_1^3 - 150120q_1^2q_2 - 5040q_1q_2^2 - 164q_2^3 + \dots\big) \,, \end{aligned} \tag{D.2}$$

up to third order in the $q_j \equiv e^{2\pi i U_j}$ with the large complex structure coordinates

$$X_1 = \frac{(18\psi)^6}{3\phi} \qquad \text{and} \qquad X_2 = (3\phi)^3 \,. \tag{D.3}$$

The large complex structure limit corresponds to $X_j \to \infty$ which is equivalent to $\mathrm{Im}(U_j) \to \infty$ as can be seen from eq. (D.2).

There are two conifold singularities given by the equations [137]

$$\begin{aligned} \mathrm{CF}_1 &: \ (26244\psi^6 + \phi)^3 = 1 \qquad \Leftrightarrow \qquad \frac{X_2}{27}\left(\frac{X_1}{432} + 1\right)^3 = 1 \,, \\ \mathrm{CF}_2 &: \ \phi^3 = 1 \qquad \Leftrightarrow \qquad \frac{X_2}{27} = 1 \,. \end{aligned} \tag{D.4}$$

Let us come back to the problem of finding supersymmetric extrema by solving eq. (5.23). As was noted in [140, 180], to find an extremum it is sufficient to turn on fluxes only along the six Γ-invariant 3-cycles, i.e.,

$$f = (f_{1_1}, f_{1_2}, f_{1_3}, f_{2_1}, f_{2_2}, f_{2_3}, 0, ..., 0) \quad \text{and} \quad h = (h_{1_1}, h_{1_2}, h_{1_3}, h_{2_1}, h_{2_2}, h_{2_3}, 0, ..., 0) \,, \tag{D.5}$$

having set to zero all the components along the $b_3 - 6$ non-invariant 3-cycles. It is then possible to achieve $D_a W = 0$ for *all* 272 complex structure moduli,[1] and hence to find a minimum of the positive definite tree-level no-scale scalar potential eq. (5.13). This is due to the fact that, for this Γ invariant flux, the symmetry Γ is realized at the level of the four-dimensional effective action. Note that the restriction to flux on the Γ invariant cycles is purely for simplicity, as the analysis of the complete 272 dimensional complex structure moduli space is practically extremely challenging.

Let us explain more detailed why the flux vector in eq. (D.5) generically provides a stable minimum of *all* 272 complex structure moduli [140, 180]. We first consider $D_{\tilde{U}_a} W_0 = 0$, where $\tilde{U}_a$ for $a = 3, \ldots, 272$ denote the non-trivially transforming moduli under $\Gamma = \mathbb{Z}_6 \times \mathbb{Z}_{18}$. In the large complex structure limit, the prepotential $\mathcal{G}$ is a polynomial function of all $h^{2,1}$ complex structure moduli that has to transform trivially under Γ, since if it would not, Γ could be used to fix the non-trivially transforming moduli.[2] Hence, the non-trivially transforming $\tilde{U}_a$ have to appear at least quadratic in $\mathcal{G}$ in order to represent a Γ invariant contribution

[1] Note that orientifolding will project out some of the 272 complex structure moduli. Since the exact number of projected out directions depends on the position of the O-plane we stick to the upper bound of 272 for a general treatment.

[2] $\mathcal{G}$ completely determines the moduli space of the (before orientifolding) $\mathcal{N} = 2$ moduli space. If it would not be invariant the complex structure moduli space would have been reduced, i.e., some flat directions lifted but this does not happen just because there exists a Γ symmetric point.

to $\mathcal{G}$. This information, together with having switched on flux only along the Γ invariant directions, is sufficient to show

$$W_{0,\tilde{U}_a} = K_{\tilde{U}_a} = 0 \quad \text{at} \quad \tilde{U}_a = 0 \quad \text{for} \quad a = 3, \ldots, 272\,, \tag{D.6}$$

since $W_{0,\tilde{U}_a}$ is a polynomial function which is at least linear in the $\tilde{U}_a$, see eq. (5.21) and $K_{\tilde{U}_a}$ is a rational function which is at least linear in the numerator in the $\tilde{U}_a$, see eq. (5.16). Hence, $D_{\tilde{U}_a} W_0 = W_{0,\tilde{U}_a} + K_{\tilde{U}_a} W_0 = 0$ at $\tilde{U}_a = 0$ for $a = 3, \ldots, 272$. This reduces the full set of conditions $D_a W = 0\ \forall a$ to the three equations

$$D_I W|_{\tilde{U}_a = 0} = 0 \qquad \text{for} \quad I = \tau, U_1, U_2\,. \tag{D.7}$$

This is equivalent to set $\tilde{U}_a = 0$ from the beginning and study the stabilization problem for the reduced case with two complex structure moduli.

Finally, we mention that in order to have a valid description of the complex structure moduli by a polynomial prepotential $\mathcal{G}$ we have to ensure that we are not in the vicinity of the conifold points eq. (D.4), i.e.,

$$\left| \frac{X_2}{27} \left(\frac{X_1}{432} + 1 \right)^3 - 1 \right| \geq \epsilon_{CF} \qquad \text{and} \qquad \left| \frac{X_2}{27} - 1 \right| \geq \epsilon_{CF}\,, \tag{D.8}$$

with small ϵ_{CF}.

Bibliography

[1] A. G. Riess *et. al.* [Supernova Search Team], *Observational evidence from supernovae for an accelerating universe and a cosmological constant*, *Astron.J.* **116** (1998) 1009–1038 [astro-ph/9805201].

[2] S. Perlmutter *et. al.* [Supernova Cosmology Project], *Measurements of Omega and Lambda from 42 high redshift supernovae*, *Astrophys.J.* **517** (1999) 565–586 [astro-ph/9812133]. The Supernova Cosmology Project.

[3] G. Hinshaw, D. Larson, E. Komatsu, D. Spergel, C. Bennett *et. al.*, *Nine-Year Wilkinson Microwave Anisotropy Probe (WMAP) Observations: Cosmological Parameter Results*, 1212.5226.

[4] P. Ade *et. al.* [Planck Collaboration], *Planck 2013 results. XVI. Cosmological parameters*, 1303.5076.

[5] K. Story, C. Reichardt, Z. Hou, R. Keisler, K. Aird *et. al.*, *A Measurement of the Cosmic Microwave Background Damping Tail from the 2500-square-degree SPT-SZ survey*, 1210.7231.

[6] Z. Hou, C. Reichardt, K. Story, B. Follin, R. Keisler *et. al.*, *Constraints on Cosmology from the Cosmic Microwave Background Power Spectrum of the 2500-square degree SPT-SZ Survey*, 1212.6267.

[7] J. L. Sievers, R. A. Hlozek, M. R. Nolta, V. Acquaviva, G. E. Addison *et. al.*, *The Atacama Cosmology Telescope: Cosmological parameters from three seasons of data*, 1301.0824.

[8] S. Kachru, R. Kallosh, A. D. Linde, J. M. Maldacena, L. P. McAllister *et. al.*, *Towards inflation in string theory*, *JCAP* **0310** (2003) 013 [hep-th/0308055].

[9] D. Baumann, A. Dymarsky, I. R. Klebanov, J. M. Maldacena, L. P. McAllister *et. al.*, *On D3-brane Potentials in Compactifications with Fluxes and Wrapped D-branes*, *JHEP* **0611** (2006) 031 [hep-th/0607050].

[10] D. Baumann, A. Dymarsky, I. R. Klebanov and L. McAllister, *Towards an Explicit Model of D-brane Inflation*, *JCAP* **0801** (2008) 024 [0706.0360].

[11] C. Cheung, P. Creminelli, A. L. Fitzpatrick, J. Kaplan and L. Senatore, *The Effective Field Theory of Inflation*, *JHEP* **0803** (2008) 014 [0709.0293].

[12] R. Gwyn, M. Rummel and A. Westphal, *Relations between canonical and non-canonical inflation*, 1212.4135.

[13] R. Gwyn, M. Rummel and A. Westphal, *Resonant non-Gaussianity with equilateral properties*, 1211.0070.

[14] S. B. Giddings, S. Kachru and J. Polchinski, *Hierarchies from fluxes in string compactifications*, *Phys.Rev.* **D66** (2002) 106006 [hep-th/0105097].

[15] K. Dasgupta, G. Rajesh and S. Sethi, *M theory, orientifolds and G - flux*, *JHEP* **9908** (1999) 023 [hep-th/9908088].

[16] S. Kachru, R. Kallosh, A. D. Linde and S. P. Trivedi, *De Sitter vacua in string theory*, *Phys.Rev.* **D68** (2003) 046005 [hep-th/0301240].

[17] R. Bousso and J. Polchinski, *Quantization of four form fluxes and dynamical neutralization of the cosmological constant*, *JHEP* **0006** (2000) 006 [hep-th/0004134].

[18] J. L. Feng, J. March-Russell, S. Sethi and F. Wilczek, *Saltatory relaxation of the cosmological constant*, *Nucl.Phys.* **B602** (2001) 307–328 [hep-th/0005276].

[19] L. Susskind, *The Anthropic landscape of string theory*, hep-th/0302219.

[20] S. Weinberg, *The Cosmological Constant Problem*, *Rev.Mod.Phys.* **61** (1989) 1–23.

[21] M. Rummel and A. Westphal, *A sufficient condition for de Sitter vacua in type IIB string theory*, *JHEP* **1201** (2012) 020 [1107.2115].

[22] J. Louis, M. Rummel, R. Valandro and A. Westphal, *Building an explicit de Sitter*, *JHEP* **1210** (2012) 163 [1208.3208].

[23] S. Ashok and M. R. Douglas, *Counting flux vacua*, *JHEP* **0401** (2004) 060 [hep-th/0307049].

[24] F. Denef and M. R. Douglas, *Distributions of flux vacua*, *JHEP* **0405** (2004) 072 [hep-th/0404116].

[25] D. Martinez-Pedrera, D. Mehta, M. Rummel and A. Westphal, *Finding all flux vacua in an explicit example*, 1212.4530.

[26] Y.-H. He, D. Mehta, M. Niemerg, M. Rummel and A. Valeanu, *Exploring the Potential Energy Landscape Over a Large Parameter-Space*, 1301.0946.

[27] B. Freivogel, M. Kleban, M. Rodriguez Martinez and L. Susskind, *Observational consequences of a landscape*, *JHEP* **0603** (2006) 039

[hep-th/0505232].

[28] V. Mukhanov, *Physical foundations of cosmology*, *Cambridge, UK: Univ. Pr.* (2005).

[29] S. Weinberg, *Cosmology*, *Oxford, UK: Oxford Univ. Pr.* (2008).

[30] L. Bergstrom and A. Goobar, *Cosmology and particle astrophysics*, *Second edition, Springer* (2003).

[31] A. D. Linde, *Prospects of inflation*, *Phys.Scripta* **T117** (2005) 40–48 [hep-th/0402051].

[32] C. Burgess, *Lectures on Cosmic Inflation and its Potential Stringy Realizations*, *Class.Quant.Grav.* **24** (2007) S795 [0708.2865].

[33] D. Baumann, *TASI Lectures on Inflation*, 0907.5424.

[34] H. Aihara *et. al.* [SDSS Collaboration], *The Eighth Data Release of the Sloan Digital Sky Survey: First Data from SDSS-III*, *Astrophys.J.Suppl.* **193** (2011) 29 [1101.1559].

[35] A. H. Guth, *The Inflationary Universe: A Possible Solution to the Horizon and Flatness Problems*, *Phys.Rev.* **D23** (1981) 347–356.

[36] A. D. Linde, *Decay of the False Vacuum at Finite Temperature*, *Nucl. Phys.* **B216** (1983) 421.

[37] A. Albrecht and P. J. Steinhardt, *Cosmology for Grand Unified Theories with Radiatively Induced Symmetry Breaking*, *Phys.Rev.Lett.* **48** (1982) 1220–1223.

[38] M. Gasperini and G. Veneziano, *Pre - big bang in string cosmology*, *Astropart.Phys.* **1** (1993) 317–339 [hep-th/9211021].

[39] J. Khoury, B. A. Ovrut, P. J. Steinhardt and N. Turok, *The Ekpyrotic universe: Colliding branes and the origin of the hot big bang*, *Phys.Rev.* **D64** (2001) 123522 [hep-th/0103239].

[40] A. A. Starobinsky, *A New Type of Isotropic Cosmological Models Without Singularity*, *Phys.Lett.* **B91** (1980) 99–102.

[41] F. Bezrukov and M. Shaposhnikov, *The Standard Model Higgs boson as the inflaton*, *Phys.Lett.* **B659** (2008) 703–706 [0710.3755].

[42] A. Golovnev, V. Mukhanov and V. Vanchurin, *Vector Inflation*, *JCAP* **0806** (2008) 009 [0802.2068].

[43] G. W. Hordenski *Int. J. Theor. Phys.* **10** (1974) 363–384.

[44] C. Deffayet, X. Gao, D. Steer and G. Zahariade, *From k-essence to generalised Galileons*, *Phys.Rev.* **D84** (2011) 064039 [1103.3260].

[45] T. Kobayashi, M. Yamaguchi and J. Yokoyama, *Generalized G-inflation:*

Inflation with the most general second-order field equations, *Prog.Theor.Phys.* **126** (2011) 511–529 [1105.5723].

[46] J. Garriga and V. F. Mukhanov, *Perturbations in k-inflation*, *Phys.Lett.* **B458** (1999) 219–225 [hep-th/9904176].

[47] X. Chen, M.-x. Huang, S. Kachru and G. Shiu, *Observational signatures and non-Gaussianities of general single field inflation*, *JCAP* **0701** (2007) 002 [hep-th/0605045].

[48] P. Franche, R. Gwyn, B. Underwood and A. Wissanji, *Attractive Lagrangians for Non-Canonical Inflation*, *Phys.Rev.* **D81** (2010) 123526 [0912.1857].

[49] E. Silverstein and D. Tong, *Scalar speed limits and cosmology: Acceleration from D-cceleration*, *Phys.Rev.* **D70** (2004) 103505 [hep-th/0310221].

[50] M. Alishahiha, E. Silverstein and D. Tong, *DBI in the sky*, *Phys.Rev.* **D70** (2004) 123505 [hep-th/0404084].

[51] J. M. Maldacena, *Non-Gaussian features of primordial fluctuations in single field inflationary models*, *JHEP* **0305** (2003) 013 [astro-ph/0210603].

[52] X. Chen, R. Easther and E. A. Lim, *Generation and Characterization of Large Non-Gaussianities in Single Field Inflation*, *JCAP* **0804** (2008) 010 [0801.3295].

[53] R. Flauger, L. McAllister, E. Pajer, A. Westphal and G. Xu, *Oscillations in the CMB from Axion Monodromy Inflation*, *JCAP* **1006** (2010) 009 [0907.2916].

[54] R. Flauger and E. Pajer, *Resonant Non-Gaussianity*, *JCAP* **1101** (2011) 017 [1002.0833].

[55] N. Barnaby and M. Peloso, *Large Nongaussianity in Axion Inflation*, *Phys.Rev.Lett.* **106** (2011) 181301 [1011.1500].

[56] N. Barnaby, E. Pajer and M. Peloso, *Gauge Field Production in Axion Inflation: Consequences for Monodromy, non-Gaussianity in the CMB, and Gravitational Waves at Interferometers*, *Phys.Rev.* **D85** (2012) 023525 [1110.3327].

[57] L. Leblond and S. Shandera, *Simple Bounds from the Perturbative Regime of Inflation*, *JCAP* **0808** (2008) 007 [0802.2290].

[58] S. Shandera, *The structure of correlation functions in single field inflation*, *Phys.Rev.* **D79** (2009) 123518 [0812.0818].

[59] J. Fergusson and E. Shellard, *The shape of primordial non-Gaussianity and the CMB bispectrum*, *Phys.Rev.* **D80** (2009) 043510 [0812.3413].

[60] P. Creminelli and M. Zaldarriaga, *Single field consistency relation for the 3-point function*, *JCAP* **0410** (2004) 006 [astro-ph/0407059].

[61] C. Pahud, M. Kamionkowski and A. R. Liddle, *Oscillations in the inflaton potential?*, *Phys.Rev.* **D79** (2009) 083503 [0807.0322].

[62] S. R. Behbahani and D. Green, *Collective Symmetry Breaking and Resonant Non-Gaussianity*, 1207.2779.

[63] X. Chen, *Primordial Non-Gaussianities from Inflation Models*, *Adv.Astron.* **2010** (2010) 638979 [1002.1416].

[64] J. Fergusson, M. Liguori and E. Shellard, *The CMB Bispectrum*, *JCAP* **1212** (2012) 032 [1006.1642].

[65] S. R. Behbahani, A. Dymarsky, M. Mirbabayi and L. Senatore, *(Small) Resonant non-Gaussianities: Signatures of a Discrete Shift Symmetry in the Effective Field Theory of Inflation*, 1111.3373.

[66] L. McAllister, E. Silverstein and A. Westphal, *Gravity Waves and Linear Inflation from Axion Monodromy*, *Phys.Rev.* **D82** (2010) 046003 [0808.0706].

[67] C. Blake, E. Kazin, F. Beutler, T. Davis, D. Parkinson *et. al.*, *The WiggleZ Dark Energy Survey: mapping the distance-redshift relation with baryon acoustic oscillations*, *Mon.Not.Roy.Astron.Soc.* **418** (2011) 1707–1724 [1108.2635].

[68] T. Abbott *et. al.* [Dark Energy Survey Collaboration], *The dark energy survey*, astro-ph/0510346.

[69] M. B. Green, J. Schwarz and E. Witten, *Superstring Theory. Vol. 1: Introduction. Vol. 2: Loop Amplitudes, Anomalies and Phenomenology*, *Cambridge, Uk: Univ. Pr.* (1987).

[70] J. Polchinski, *String theory. Vol. 1: An introduction to the bosonic string. Vol. 2: Superstring theory and beyond*, *Cambridge, Uk: Univ. Pr.* (1998).

[71] K. Becker, M. Becker and J. Schwarz, *String theory and M-theory: A modern introduction*, *Cambridge, Uk: Univ. Pr.* (2007).

[72] R. Blumenhagen, D. Lust and S. Theisen, *Basic concepts of string theory*, *Heidelberg, Germany: Springer* (2013).

[73] E. Witten, *String theory dynamics in various dimensions*, *Nucl.Phys.* **B443** (1995) 85–126 [hep-th/9503124].

[74] M. Henneaux and C. Teitelboim, *DYNAMICS OF CHIRAL (SELFDUAL) P FORMS*, *Phys.Lett.* **B206** (1988) 650.

[75] F. Denef, *Les Houches Lectures on Constructing String Vacua*, 0803.1194.

[76] T. Kaluza, *On the Problem of Unity in Physics*, *Sitzungsber.Preuss.Akad.Wiss.Berlin (Math.Phys.)* **1921** (1921) 966–972.

[77] O. Klein, *Quantum Theory and Five-Dimensional Theory of Relativity. (In German and English)*, *Z.Phys.* **37** (1926) 895–906.

[78] J. M. Lindert, F. D. Steffen and M. K. Trenkel, *Direct stau production at hadron colliders in cosmologically motivated scenarios*, *JHEP* **1108** (2011) 151 [1106.4005].

[79] P. Candelas, G. T. Horowitz, A. Strominger and E. Witten, *Vacuum Configurations for Superstrings*, *Nucl.Phys.* **B258** (1985) 46–74.

[80] B. R. Greene, *String theory on Calabi-Yau manifolds*, hep-th/9702155.

[81] L. Abbott and P. Sikivie, *A Cosmological Bound on the Invisible Axion*, *Phys.Lett.* **B120** (1983) 133–136.

[82] J. Preskill, M. B. Wise and F. Wilczek, *Cosmology of the Invisible Axion*, *Phys.Lett.* **B120** (1983) 127–132.

[83] M. Dine and W. Fischler, *The Not So Harmless Axion*, *Phys.Lett.* **B120** (1983) 137–141.

[84] S. R. Coleman and F. De Luccia, *Gravitational Effects on and of Vacuum Decay*, *Phys. Rev.* **D21** (1980) 3305.

[85] A. D. Linde, *Eternally Existing Selfreproducing Chaotic Inflationary Universe*, *Phys.Lett.* **B175** (1986) 395–400.

[86] V. Balasubramanian and P. Berglund, *Stringy corrections to Kahler potentials, SUSY breaking, and the cosmological constant problem*, *JHEP* **0411** (2004) 085 [hep-th/0408054].

[87] V. Balasubramanian, P. Berglund, J. P. Conlon and F. Quevedo, *Systematics of moduli stabilisation in Calabi-Yau flux compactifications*, *JHEP* **0503** (2005) 007 [hep-th/0502058].

[88] C. Burgess, R. Kallosh and F. Quevedo, *De Sitter string vacua from supersymmetric D terms*, *JHEP* **0310** (2003) 056 [hep-th/0309187].

[89] M. Haack, D. Krefl, D. Lust, A. Van Proeyen and M. Zagermann, *Gaugino Condensates and D-terms from D7-branes*, *JHEP* **0701** (2007) 078 [hep-th/0609211].

[90] M. Cicoli, S. Krippendorf, C. Mayrhofer, F. Quevedo and R. Valandro, *D-Branes at del Pezzo Singularities: Global Embedding and Moduli Stabilisation*, *JHEP* **1209** (2012) 019 [1206.5237].

[91] O. Lebedev, H. P. Nilles and M. Ratz, *De Sitter vacua from matter superpotentials*, *Phys.Lett.* **B636** (2006) 126–131 [hep-th/0603047].

[92] K. A. Intriligator, N. Seiberg and D. Shih, *Dynamical SUSY breaking in meta-stable vacua*, *JHEP* **0604** (2006) 021 [hep-th/0602239].

[93] M. Cicoli, A. Maharana, F. Quevedo and C. Burgess, *De Sitter String Vacua from Dilaton-dependent Non-perturbative Effects*, *JHEP* **1206** (2012) 011 [1203.1750].

[94] A. Westphal, *de Sitter string vacua from Kahler uplifting*, *JHEP* **0703** (2007) 102 [hep-th/0611332].

[95] C. Vafa, *Evidence for F theory*, *Nucl.Phys.* **B469** (1996) 403–418 [hep-th/9602022].

[96] T. Weigand, *Lectures on F-theory compactifications and model building*, *Class.Quant.Grav.* **27** (2010) 214004 [1009.3497].

[97] A. Maharana and E. Palti, *Models of Particle Physics from Type IIB String Theory and F-theory: A Review*, 1212.0555.

[98] A. Sen, *Orientifold limit of F theory vacua*, *Phys.Rev.* **D55** (1997) 7345–7349 [hep-th/9702165].

[99] H. Jockers and J. Louis, *D-terms and F-terms from D7-brane fluxes*, *Nucl.Phys.* **B718** (2005) 203–246 [hep-th/0502059].

[100] T. W. Grimm and J. Louis, *The Effective action of N = 1 Calabi-Yau orientifolds*, *Nucl.Phys.* **B699** (2004) 387–426 [hep-th/0403067].

[101] E. Cremmer, S. Ferrara, C. Kounnas and D. V. Nanopoulos, *Naturally Vanishing Cosmological Constant in N=1 Supergravity*, *Phys.Lett.* **B133** (1983) 61.

[102] J. R. Ellis, A. Lahanas, D. V. Nanopoulos and K. Tamvakis, *No-Scale Supersymmetric Standard Model*, *Phys.Lett.* **B134** (1984) 429.

[103] M. R. Douglas and S. Kachru, *Flux compactification*, *Rev.Mod.Phys.* **79** (2007) 733–796 [hep-th/0610102].

[104] M. Grana, *Flux compactifications in string theory: A Comprehensive review*, *Phys.Rept.* **423** (2006) 91–158 [hep-th/0509003].

[105] R. Blumenhagen, B. Kors, D. Lust and S. Stieberger, *Four-dimensional String Compactifications with D-Branes, Orientifolds and Fluxes*, *Phys.Rept.* **445** (2007) 1–193 [hep-th/0610327].

[106] S. Gukov, C. Vafa and E. Witten, *CFT's from Calabi-Yau four folds*, *Nucl.Phys.* **B584** (2000) 69–108 [hep-th/9906070].

[107] J. M. Maldacena and C. Nunez, *Supergravity description of field theories on curved manifolds and a no go theorem*, *Int.J.Mod.Phys.* **A16** (2001) 822–855 [hep-th/0007018].

[108] K. Becker, M. Becker, M. Haack and J. Louis, *Supersymmetry breaking and alpha-prime corrections to flux induced potentials*, *JHEP* **0206** (2002) 060 [hep-th/0204254].

[109] M. Berg, M. Haack and B. Kors, *String loop corrections to Kahler potentials in orientifolds*, *JHEP* **0511** (2005) 030 [hep-th/0508043].

[110] L. E. Ibanez and A. M. Uranga, *String theory and particle physics: An introduction to string phenomenology, p.458*, *Cambridge, UK: Univ. Pr.* (2012).

[111] G. Veneziano and S. Yankielowicz, *An Effective Lagrangian for the Pure N=1 Supersymmetric Yang-Mills Theory*, *Phys.Lett.* **B113** (1982) 231.

[112] M. Cicoli, J. P. Conlon and F. Quevedo, *Systematics of String Loop Corrections in Type IIB Calabi-Yau Flux Compactifications*, *JHEP* **0801** (2008) 052 [0708.1873].

[113] J. P. Conlon, F. Quevedo and K. Suruliz, *Large-volume flux compactifications: Moduli spectrum and D3/D7 soft supersymmetry breaking*, *JHEP* **0508** (2005) 007 [hep-th/0505076].

[114] K. Bobkov, V. Braun, P. Kumar and S. Raby, *Stabilizing All Kahler Moduli in Type IIB Orientifolds*, *JHEP* **1012** (2010) 056 [1003.1982].

[115] K. Choi, A. Falkowski, H. P. Nilles, M. Olechowski and S. Pokorski, *Stability of flux compactifications and the pattern of supersymmetry breaking*, *JHEP* **0411** (2004) 076 [hep-th/0411066].

[116] P. Breitenlohner and D. Z. Freedman, *Positive Energy in anti-De Sitter Backgrounds and Gauged Extended Supergravity*, *Phys.Lett.* **B115** (1982) 197.

[117] P. Candelas and H. Skarke, *F theory, SO(32) and toric geometry*, *Phys.Lett.* **B413** (1997) 63–69 [hep-th/9706226].

[118] L. Covi, M. Gomez-Reino, C. Gross, J. Louis, G. A. Palma *et. al.*, *de Sitter vacua in no-scale supergravities and Calabi-Yau string models*, *JHEP* **0806** (2008) 057 [0804.1073].

[119] S. R. Coleman, *The Fate of the False Vacuum. 1. Semiclassical Theory*, *Phys. Rev.* **D15** (1977) 2929–2936.

[120] C. G. Callan Jr. and S. R. Coleman, *The Fate of the False Vacuum. 2. First Quantum Corrections*, *Phys. Rev.* **D16** (1977) 1762–1768.

[121] S. W. Hawking and I. G. Moss, *Supercooled Phase Transitions in the Very Early Universe*, *Phys. Lett.* **B110** (1982) 35.

[122] D. Lust, S. Reffert, W. Schulgin and S. Stieberger, *Moduli stabilization in*

type IIB orientifolds (I): Orbifold limits, *Nucl.Phys.* **B766** (2007) 68–149 [hep-th/0506090].

[123] S. S. AbdusSalam, J. P. Conlon, F. Quevedo and K. Suruliz, *Scanning the Landscape of Flux Compactifications: Vacuum Structure and Soft Supersymmetry Breaking*, *JHEP* **0712** (2007) 036 [0709.0221].

[124] P. Candelas, X. C. De La Ossa, P. S. Green and L. Parkes, *A Pair of Calabi-Yau manifolds as an exactly soluble superconformal theory*, *Nucl.Phys.* **B359** (1991) 21–74.

[125] D. Gallego and M. Serone, *An Effective Description of the Landscape - I*, *JHEP* **01** (2009) 056 [0812.0369].

[126] D. Gallego, *On the Effective Description of Large Volume Compactifications*, *JHEP* **06** (2011) 087 [1103.5469].

[127] Y. Sumitomo, S. H. H. Tye and S. S. C. Wong, *Statistical Distribution of the Vacuum Energy Density in Racetrack Kähler Uplift Models in String Theory*, 1305.0753.

[128] M. Kreuzer and H. Skarke, *Complete classification of reflexive polyhedra in four-dimensions*, *Adv.Theor.Math.Phys.* **4** (2002) 1209–1230 [hep-th/0002240].

[129] A. Collinucci, F. Denef and M. Esole, *D-brane Deconstructions in IIB Orientifolds*, *JHEP* **0902** (2009) 005 [0805.1573].

[130] J. Gray, Y.-H. He, V. Jejjala, B. Jurke, B. D. Nelson *et. al.*, *Calabi-Yau Manifolds with Large Volume Vacua*, *Phys.Rev.* **D86** (2012) 101901 [1207.5801].

[131] R. Blumenhagen, S. Moster and E. Plauschinn, *Moduli Stabilisation versus Chirality for MSSM like Type IIB Orientifolds*, *JHEP* **0801** (2008) 058 [0711.3389].

[132] R. Blumenhagen, V. Braun, T. W. Grimm and T. Weigand, *GUTs in Type IIB Orientifold Compactifications*, *Nucl.Phys.* **B815** (2009) 1–94 [0811.2936].

[133] A. Collinucci, M. Kreuzer, C. Mayrhofer and N.-O. Walliser, *Four-modulus 'Swiss Cheese' chiral models*, *JHEP* **0907** (2009) 074 [0811.4599].

[134] M. Cicoli, C. Mayrhofer and R. Valandro, *Moduli Stabilisation for Chiral Global Models*, *JHEP* **1202** (2012) 062 [1110.3333].

[135] R. Minasian and G. W. Moore, *K theory and Ramond-Ramond charge*, *JHEP* **9711** (1997) 002 [hep-th/9710230].

[136] D. S. Freed and E. Witten, *Anomalies in string theory with D-branes*,

Asian J.Math **3** (1999) 819 [hep-th/9907189].

[137] P. Candelas, A. Font, S. H. Katz and D. R. Morrison, *Mirror symmetry for two parameter models. 2.*, *Nucl.Phys.* **B429** (1994) 626–674 [hep-th/9403187].

[138] B. R. Greene and M. Plesser, *Duality in Calabi-Yau Moduli Space*, *Nucl.Phys.* **B338** (1990) 15–37.

[139] O. DeWolfe, A. Giryavets, S. Kachru and W. Taylor, *Type IIA moduli stabilization*, *JHEP* **0507** (2005) 066 [hep-th/0505160].

[140] F. Denef, M. R. Douglas and B. Florea, *Building a better racetrack*, *JHEP* **0406** (2004) 034 [hep-th/0404257].

[141] A. J. Sommese and C. W. Wampler, *The numerical solution of systems of polynomials arising in Engineering and Science*. World Scientific Publishing Company, 2005.

[142] J. P. Conlon and F. Quevedo, *On the explicit construction and statistics of Calabi-Yau flux vacua*, *JHEP* **0410** (2004) 039 [hep-th/0409215].

[143] A. D. Linde and A. Westphal, *Accidental Inflation in String Theory*, *JCAP* **0803** (2008) 005 [0712.1610].

[144] J. J. Blanco-Pillado, M. Gomez-Reino and K. Metallinos, *Accidental Inflation in the Landscape*, *JCAP* **1302** (2013) 034 [1209.0796].

[145] D. Marsh, L. McAllister and T. Wrase, *The Wasteland of Random Supergravities*, *JHEP* **1203** (2012) 102 [1112.3034].

[146] X. Chen, G. Shiu, Y. Sumitomo and S. H. Tye, *A Global View on The Search for de-Sitter Vacua in (type IIA) String Theory*, *JHEP* **1204** (2012) 026 [1112.3338].

[147] T. C. Bachlechner, D. Marsh, L. McAllister and T. Wrase, *Supersymmetric Vacua in Random Supergravity*, *JHEP* **1301** (2013) 136 [1207.2763].

[148] Y. Sumitomo and S.-H. H. Tye, *A Stringy Mechanism for A Small Cosmological Constant*, *JCAP* **1208** (2012) 032 [1204.5177].

[149] Y. Sumitomo and S. H. Tye, *A Stringy Mechanism for A Small Cosmological Constant - Multi-Moduli Cases -*, *JCAP* **1302** (2013) 006 [1209.5086].

[150] Y. Sumitomo and S.-H. H. Tye, *Preference for a Vanishingly Small Cosmological Constant in Supersymmetric Vacua in a Type IIB String Theory Model*, 1211.6858.

[151] D. Mehta, *Lattice vs. Continuum: Landau Gauge Fixing and 't Hooft-Polyakov Monopoles*, *Ph.D. Thesis, The Uni. of Adelaide,*

Australasian Digital Theses Program (2009).

[152] D. Mehta, A. Sternbeck, L. von Smekal and A. G. Williams, *Lattice Landau Gauge and Algebraic Geometry*, *PoS* **QCD-TNT09** (2009) 025 [0912.0450].

[153] D. Mehta, *Finding All the Stationary Points of a Potential Energy Landscape via Numerical Polynomial Homotopy Continuation Method*, *Phys.Rev.* **E (R) 84** (2011) 025702 [1104.5497].

[154] D. Mehta, *Numerical Polynomial Homotopy Continuation Method and String Vacua*, *Adv.High Energy Phys.* **2011** (2011) 263937 [1108.1201].

[155] M. Kastner and D. Mehta, *Phase Transitions Detached from Stationary Points of the Energy Landscape*, *Phys.Rev.Lett.* **107** (2011) 160602 [1108.2345].

[156] R. Nerattini, M. Kastner, D. Mehta and L. Casetti, *Exploring the energy landscape of XY models*, *Physical Review E 87,* **032140** (2013) [1211.4800].

[157] M. Maniatis and D. Mehta, *Minimizing Higgs Potentials via Numerical Polynomial Homotopy Continuation*, *Eur.Phys.J.Plus* **127** (2012) 91 [1203.0409].

[158] D. Mehta, Y.-H. He and J. D. Hauenstein, *Numerical Algebraic Geometry: A New Perspective on String and Gauge Theories*, *JHEP* **1207** (2012) 018 [1203.4235].

[159] C. Hughes, D. Mehta and J.-I. Skullerud, *Enumerating Gribov copies on the lattice*, *Annals Phys.* **331** (2013) 188–215 [1203.4847].

[160] D. Mehta, J. D. Hauenstein and M. Kastner, *Energy landscape analysis of the two-dimensional nearest-neighbor ϕ^4 model*, *Phys.Rev.* **E85** (2012) 061103 [1202.3320].

[161] J. Hauenstein, Y.-H. He and D. Mehta, *Numerical Analyses on Moduli Space of Vacua*, 1210.6038.

[162] T. Y. Li, *Solving polynomial systems by the homotopy continuation method*, *Handbook of numerical analysis* **XI** (2003) 209–304.

[163] T. Li, T. Sauer and J. Yorke, *The cheater's homotopy: an efficient procedure for solving systems of polynomial equations*, *SIAM Journal on Numerical Analysis* **26** (1989), no. 5 1241–1251.

[164] T. Li and X. Wang, *Nonlinear homotopies for solving deficient polynomial systems with parameters*, *SIAM journal on numerical analysis* **29** (1992), no. 4 1104–1118.

[165] H. Cohen, *A Course in Computational Algebraic Number Theory*, *Springer* (1993).

[166] T. W. Grimm, R. Savelli and M. Weissenbacher, *On α' corrections in N=1 F-theory compactifications*, 1303.3317.

[167] F. Pedro, M. Rummel and A. Westphal, *α'^2 corrections and the extended no-scale structure* , *To appear.*

[168] M. Cicoli, S. Krippendorf, C. Mayrhofer, F. Quevedo and R. Valandro, *D3/D7 Branes at Singularities: Constraints from Global Embedding and Moduli Stabilisation*, 1304.0022.

[169] F. G. Pedro and A. Westphal, *The Scale of Inflation in the Landscape*, 1303.3224.

[170] M. Bianchi, A. Collinucci and L. Martucci, *Magnetized E3-brane instantons in F-theory*, *JHEP* **1112** (2011) 045 [1107.3732].

[171] M. Dine, N. Seiberg and E. Witten, *Fayet-Iliopoulos Terms in String Theory*, *Nucl.Phys.* **B289** (1987) 589.

[172] J. Tate, *"Algorithm for determining the type of a singular fiber in an elliptic pencil"*, *Modular Functions of One Variable IV, Lecture Notes in Mathematics* **vol. 476** (1975) pp. 33–52, Berlin / Heidelberg: Springer.

[173] M. Bershadsky, K. A. Intriligator, S. Kachru, D. R. Morrison, V. Sadov and C. Vafa, *Geometric singularities and enhanced gauge symmetries*, *Nucl.Phys.* **B481** (1996) 215–252 [hep-th/9605200].

[174] R. Donagi and M. Wijnholt, *Higgs Bundles and UV Completion in F-Theory*, 0904.1218.

[175] A. Collinucci and R. Savelli, *On Flux Quantization in F-Theory*, *JHEP* **1202** (2012) 015 [1011.6388].

[176] A. Collinucci and R. Savelli, *On Flux Quantization in F-Theory II: Unitary and Symplectic Gauge Groups*, *JHEP* **1208** (2012) 094 [1203.4542].

[177] S. H. Katz and C. Vafa, *Geometric engineering of N=1 quantum field theories*, *Nucl.Phys.* **B497** (1997) 196–204 [hep-th/9611090].

[178] R. Kallosh, A.-K. Kashani-Poor and A. Tomasiello, *Counting fermionic zero modes on M5 with fluxes*, *JHEP* **0506** (2005) 069 [hep-th/0503138].

[179] P. Candelas, X. de la Ossa and F. Rodriguez-Villegas, *Calabi-Yau manifolds over finite fields. 1.*, hep-th/0012233.

[180] A. Giryavets, S. Kachru, P. K. Tripathy and S. P. Trivedi, *Flux compactifications on Calabi-Yau threefolds*, *JHEP* **0404** (2004) 003 [hep-th/0312104].